POLITECNICO DI TORINO

Corso di Laurea Magistrale
in Ingegneria Biomedica

Master Thesis

Design and validation of a workbench for knee joint biomechanical analysis

Relator
Prof.ssa Cristina Bignardi

Supervisor
Prof. Bernardo Innocenti

Student
Nicola Armillotta

March 2020

alla mia famiglia
che mi ha permesso di seguire i miei sogni

Abstract

The knee joint is one of the most complex articulations in human body.

Its structure has been investigated for decades with several techniques such as clinic imaging, finite element analysis and robot simulations.

The huge quantity of soft tissues of this joint provide stability during everyday tasks. However, the knee is constantly subjected to forces so high that can easily reach up to four times the total weight of our body. For this reason, knee joint is the one that gets damaged the most in human being.

Kinematic and kinetic strongly depend on boundary condition such as load history, soft tissue properties and anatomy of the subject. All these elements can be very different for each person and make difficult to generalize results achieved in studies. TC and MR images provide anatomical information without describing any kinetic and kinematic behaviour of the joint and because of the difficulties of acquiring in-vivo data, new methods of investigation are developing thanks to new technologies. Motion parameters like speed, forces and position can be easily recorded with non-invasive techniques and they can be evaluated by a proper model that enable to investigate internal forces and reactions.

In order build reliable models to be referred, it is necessary to own specific instrumentation to emulate different daily tasks while acquiring and elaborating motion parameters. Several devices are required to obtain all movement features, and price sure plays an important role for the optimization of the system.

For the project it was aimed to arrange a proper structure that allowed the kinematic analysis of an open-chain leg extension, carried out by femoral quadriceps contraction. Department's laboratory didn't own such build to perform active motions. For this reason, it was first necessary to design a suitable structure for keeping and sustaining the movement, achieved using a CAD software.

The leg ride must be visible to the motion capture cameras already installed in the lab, which means that the frame must enable macro-adjustment of sample position in order to enhance the quality of the record. To achieve this, the structure was designed to rotate and regulate its position according to camera view field. Also, it had to be the most general possible, that means that it must be able to allow quantitative investigation independently on leg properties such as length and weight.

Once the first prototype was sketched, enabling frame rotation and modularity, a second phase of design followed to improve its feasibility. The optimization of the design was considered to reduce the costs of the manufacturing and to make the structure the most versatile possible. The final prototype is composed by three main structures that can be assembled according to the operator will. The total cost of the aluminium holding system was lower than 80 eur, and the rotating mechanism was around 600 eur.

Muscle force has been realized by a linear actuator rightly linked to the tibial tuberosity by a thread. The contraction was performed according to the anatomical axis of the femur. The patella's role of optimizing the quadriceps work was emulated too cause its absolute non negligibility. Also, a primary calibration of the motor was necessary to ensure the measurement reliability, followed by a statistical evaluation of system reliability.

Data related to the contraction of skeletal muscle were acquired by an electronic system that was able to process information in real time. That mean that the workbench was able to elaborate different parameters and quickly provide outputs related on them. For this reason, it also had the duty of modulating leg extension according to the investigated task. The communication between different hardware and software was performed and checked to ensure coherence between supply and acquired parameters.

Two main different function were implemented to perform different actuation: constant speed and force ramp leg extension, providing detailed description of muscle force request for both tasks.

Lot of attention was paid for safety of the workbench. First the human operator must operate without any risks. Pieces and frame components like gearhead reducer were also evaluated under this point of view. Furthermore, specimen and devices such as cameras, motor and prosthesis, must work without any risk of being damaged. Thus, it was guaranteed by controlling internal temperature of the motor and ensuring a torque limitation once the total extension position has been reached by the specimen.
An important investigation on temperature required a deep investigation, and several meetings took place with expert technicians, also from the very motor company, to argue about some issues shown by the heating models provided by motor documentation.

An issue about the speed rotation was shown by the motor, requiring a new adjustment for the workbench by using a motor gearhead to reduce initial speed burst and to perform the movement slower while providing the proper supply.

Once the set-up is over, it'll be interesting to perform a first cadaver test and compare muscle activity in different work conditions.

The actual mass plays an active role on force demand, but of course other parameters such as joint friction, soft tissue laxity and anatomical conformation influence kinetic and kinematic of the knee. Forces read by the system were comparable to the ones that are findable in literature in similar boundary condition, which means that the final system is safe, modular, reliable and provides a good model to emulate physiological knee extension to analyse joint behaviour.

Prefazione

L'articolazione del ginocchio è una delle più complesse individuabili nel corpo umano.

La sua struttura è stata studiata negli ultimi decenni usando diverse tecniche tra cui imaging clinico, analisi agli elementi finiti e simulazioni robotiche.

La gran quantità di tessuti molli che la compongono le forniscono grande stabilità durante le comuni attività quotidiane. Ad ogni modo, il ginocchio è costantemente sottoposto a forze tanto elevate da poter facilmente raggiungere fino a quattro volte il peso corporeo del soggetto. Per questo motivo, risulta essere l'articolazione che si danneggia più frequentemente nell'uomo.

Cinematica e cinetica sono fortemente influenzate da una serie di condizioni al contorno quali storia di carico, proprietà dei tessuti molli e dalla stessa anatomia del soggetto. Questi fattori possono essere molto diversi in ciascuno di noi e ciò rende difficile generalizzare i risultati degli studi. Immagini TC e MR forniscono informazioni anatomiche dell'articolazione, senza tuttavia procurare indicazioni sulla sua cinematica e cinetica e, viste le difficoltà di acquisire dati biomedici in vivo, nuovi metodi di analisi sono stati sviluppati sfruttando le nuove tecnologie. I parametri cinematici come velocità, forza e posizione nello spazio possono essere facilmente acquisiti con tecniche non invasive e forniscono un'analisi accurata delle forze interarticolari sviluppate durante l'attività, se convogliate in un modello di calcolo corretto.
Per poter costituire una risorsa affidabile è importante possedere una strumentazione specifica, che possa emulare il task di interesse consentendone un'indagine quantitativa. Diversi dispositivi sono necessari per acquisire i parametri caratteristici del moto e un'attenta valutazione dei costi-benefici deve sempre essere effettuata quando si costituisce un nuovo sistema.

L'obiettivo del progetto era quello di costituire una struttura adatta all'analisi biomeccanica dell' estensione in open chain della gamba, condotta mediante contrazione del quadricipite femorale. Il laboratorio del dipartimento non possedeva una struttura che consentisse l'analisi del movimento attivo della gamba. Per questo motivo, prima di tutto è stato necessario progettare un frame adatto allo scopo di mantenere in posizione il sample e di sostenerne l'estensione. Gli elementi sono stati progettati usando un software CAD.

La corsa della gamba doveva essere visibile alle camere per analisi del movimento, già installate nel laboratorio. Per questo, il frame doveva consentire macro-spostamenti per poter rendere lo specimen meglio visibile. Per garantire questa capacità, la struttura fu pensata per essere in grado di ruotare su se stessa, così da essere posizionata a seconda del campo di osservazione del sistema di motion capture. Inoltre, questo frame doveva essere il più generale possibile, e in particolare doveva permettere analisi coerenti e affidabili senza dipendere dalla gamba utilizzata per i test, la quale può variare ad esempio in dimensioni e peso.

Una volta che il primo prototipo fu ideato garantendo rotazione e modularità, si entrò in

una seconda fase di design volta ad ottimizzare la fattibilità delle sue componenti. La riduzione dei costi di produzione è stato il punto cardine del processo, assieme al renderne la lavorazione il più facile possibile seppur garantendone alta versatilità di montaggio. Il prodotto finale è composto da tre strutture principali che possono essere assemblate in qualunque momento del set up a scelta dell'operatore. Il costo totale dell sistema di supporto in alluminio è stato inferiore agli 80 euro mentre la base rotante si è aggirata nell'intorno dei 600 euro.

La forza muscolare è stata realizzata con un attuazione lineare, collegata tramite apposito filo alla tuberosità tibiale. La direzione del cavo segue l'asse anatomico del femore, come il quadricipite nelle condizioni fisiologiche. Il ruolo di ottimizzazione del lavoro muscolare dovuto alla rotula non è trascurabile ed è stato opportunamente simulato. Prima di poter acquisire dati, è stata necessaria una calibrazione del motore per valutarne affidabilità e ripetibilità.

I dati relativi alla contrazione del muscolo scheletrico sono stati acquisiti da un sistema elettronico in grado di monitorare diversi parametri in tempo reale. Questa caratteristica è stata sfruttata per elaborare dati durante il task ed ottenere velocemente degli output in loro funzione. Così facendo è stato possibile controllare l'estensione della gamba a seconda dell'attività investigata. La comunicazione tra le differenti componenti hardware e software è stata controllata più volte per accertarsi della coerenza tra i valori applicati e quelli letti. Sono state implementate due funzioni distinte per analizzare casi di estensione differenti: a

velocità costante e a rampa di forza, ed è stata ottenuta una descrizione dettagliata della forza muscolare esercitata in entrambi i casi.

La sicurezza del progetto ha richiesto molta attenzione: l'operatore deve lavorare in condizioni di totale sicurezza. Componenti e moduli del frame sono stati progettati anche tenendo conto di questo aspetto. I samples e i diversi dispositivi quali motore e protesi devono lavorare senza alcun rischio di danneggiarsi. Questo grado di sicurezza è stato garantito attraverso un costante monitoraggio limitando la coppia muscolare, una volta che la posizione di massima estensione viene raggiunta, e della temperatura interna al motore. Riguardo quest'ultimo, è stato necessario uno studio approfondito organizzando diversi meeting con tecnici e ingegneri del dipartimento nonché dell'azienda produttrice stessa, per discutere di alcune problematiche relative al modello termico fornito nei data sheet.

Durante le fasi finali della tesi si è inoltre presentato un problema relativo alla velocità di rotazione del motore. Questo ha richiesto un'indagine che ha portato alla necessità di utilizzare un riduttore, in modo da ridurre il burst iniziale e ottenere un'estensione sufficientemente lenta mentre viene erogata la corrente voluta.

Una volta concluso il progetto, sarebbe interessante effettuare un test su cadavere e investigare diversi elementi, con proprietà diverse, in termini di attività muscolare necessaria a compiere lo stesso task. Inoltre, numerosi sviluppi futuri si prestano emulare nuove attività e a raccogliere un maggior numero di informazioni.

La massa del campione gioca un ruolo determinante per questi test, così come altri fattori

come la frizione sviluppata durante il moto, la lassità dei tessuti molli nonché la conformazione anatomica influenzano fortemente cinetica e cinematica del ginocchio. Le forze acquisite dal sistema si sono dimostrate coerenti e dimostrano che il prototipo risulta sicuro, modulare, affidabile e assimilabile a un buon modello per poter analizzare l'estensione del ginocchio e investigarne le proprietà.

Contents

1 Background

1.1 Native knee joint

1.1.1 Anatomy

The knee is a peculiar and complex hinge joint that combine four different bones: the distal part of the femur, the proximal region of the tibia, the proximal fibula and the patella. For this reason, the knee joint is considered as three distinct joints: the patella-femoral articulation and the two tibia-condylar articulation [1, 2].

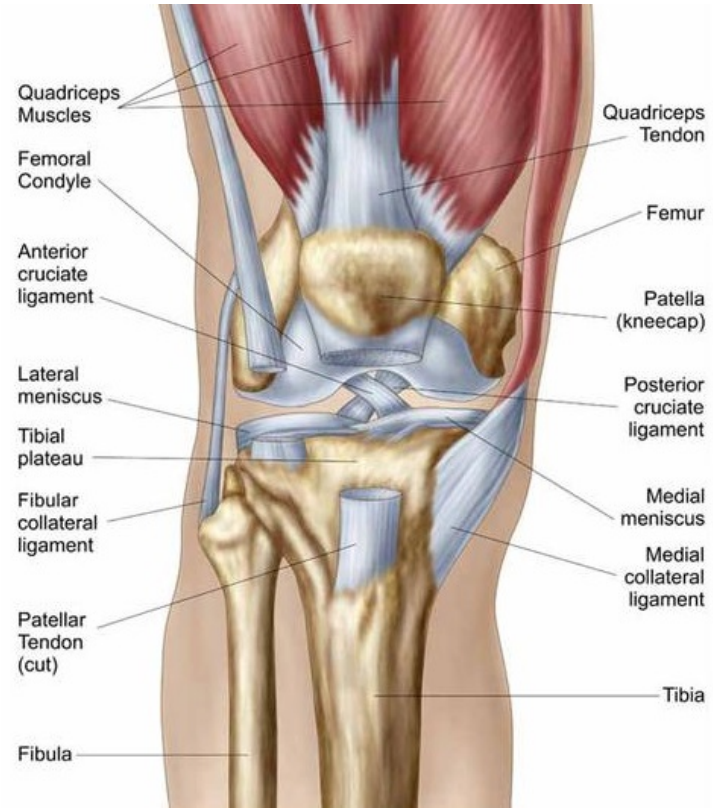

Figure 1.1: Knee anatomy (verywellhealth.com)

The patella is placed in front of the femoral condyles and it's commonly defined as "floating" because its position is kept only by tendons.

There are several soft tissues in knee joint, that are useful to stabilize the articulation during the physiologic movement and to spread forces developed during daily activities.

- ligaments are tissues that provides high stability to the joint. There are lot of ligaments, but it's possible to identify two main groups:

  (a) Tibiofemoral ligaments, which belong to the tibiofemoral joint. Some of them can be distinguished and are the ACL and PCL, respectively anterior and

posterior cruciate ligament. They are probably the most famous ligaments cause their common break for stressful sports like football and tennis. Cruciate ligaments provide antero-posterior stability and steadiness in full extension by twisting together. Two other important ligaments are the MCL and LCL, respectively medial and lateral collateral ligament, that link the tibia and the femur. They increase knee stability, guide its movement and limit the medio-lateral translation;

(b) Patellofemoral ligaments instead link the patella to the femur. MPFL medial patellofemoral ligament provide mediolateral stability of the kneecap, that would go lateral due to the direction of the quadriceps contraction. The patellar tendon allows the leg extension while the lateral retinaculum supply high stability to the knee joint.

- meniscus is a cartilage tissue placed on the top on the tibia plateau. The two condyles lay on this film that make forces distribute on a bigger surface, reducing pressure and stress for bones. These forces can reach a magnitude up to four time the body weight during everyday tasks and, without a proper spreading system, the joint would suffer such important solicitation. Furthermore, it reduces the impact between the two bones, acting as dumping system.

- the capsule is a fibrous membrane that provide lubrication to the joint, decreasing significantly the friction between surfaces.

- muscles are fibrous tissues that allow bones to move by contracting themselves.

1.1.2 Kinematics and kinetics

In the past, this articulation was thought as simple hinge joint. Thus, after several failures, the knee was deeply studied and its complexity was investigated. [3, 4, 5].

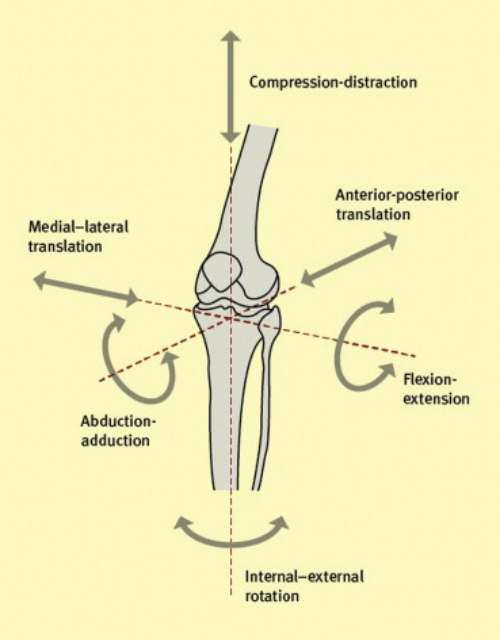

Figure 1.2: Actual degreed of freedom of the knee joint

A hinge joint is a mechanical structure that allows rotation in one plane and around a single axis, such as the hinge of the door. This simple movement is totally inappropriate for deep studies on knee joint. Picture 1.2 shows the actual movements that the joint is able to perform. There are six degrees of freedom (three translation and three rotation) around the three mechanical axes, that are named according to the anatomical references. The flexion-extension is the widest movement allowed by the articulation. It occurs on sagittal plane and describes an angular pattern from $/0°$ to $/120 - 140°$, where $/0°$ is the maximum extension phase. The movement is paired with anterior-posterior translation and is enhanced by a little offset of the posterior condyle by $12°$ for each $2mm$.

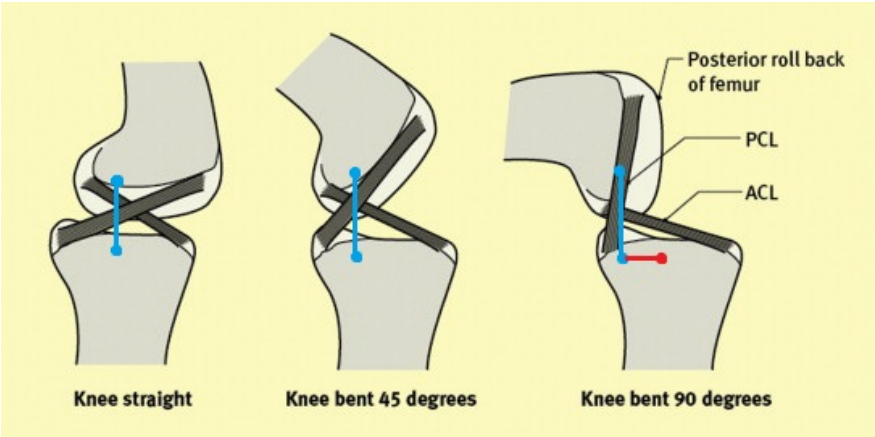

Figure 1.3: Knee roll-back (Orthopaedicsandtraumajournal.com)

The phenomenon called "roll-back" makes the joint even more different from a simple hinge. The projection on tibial plateau of the instant center of rotation of condyles is

different along the movement and the lever arm of the quadriceps muscles (related to insertion point of the tibia) is enhanced, lowering the effort required to the exercise [6]. Also, the patella optimizes muscle's activity by sliding on the femur during the task.
All these features must be preserved after prosthesis implant, that occur when patient is no longer able to perform physiologically his daily activities.

Knee joint open chain
Links are individual rigid bodies, connected by joints such as hinges. A kinematic chain refers to a series of articulated segments, such as the connected pelvis, thigh, leg and foot, which can move relatively and the movement of the proximal one had effects on all the other distal segments. In biomedical field, all limbs are comparable to a kinematic chain, where each segment is basically a long bone and the joints are the corresponding articulations, defined as the correct joint type.
An open kinematic chain is a structure where the distal segment of the chain moves in space while the proximal segment is fixed or stable at least.

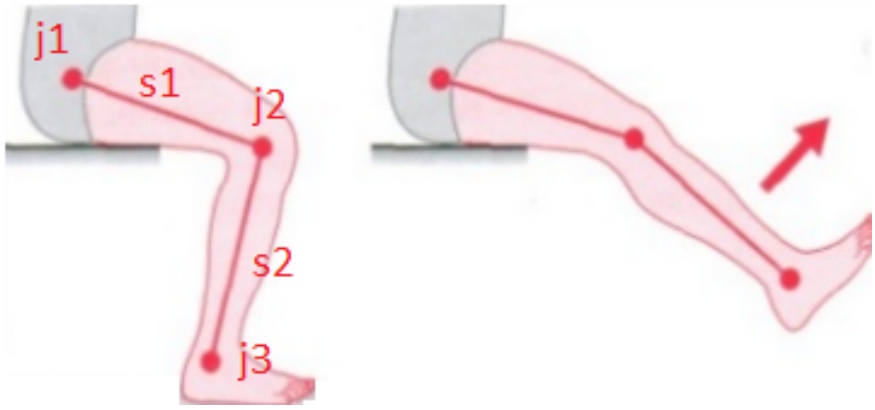

Figure 1.4: Leg curl as open chain (sciencecapsules.blogspot.com)

The picture shows that the lower limb can be studied as open chain, where s1 is the femur, s2 is the tibia, and j1 j2 j3 are respectively the hip-joint, the knee-joint and the ankle joint. On the other hand, a closed kinematic chain is a structure where the distal segment is fixed and the proximal part can move.

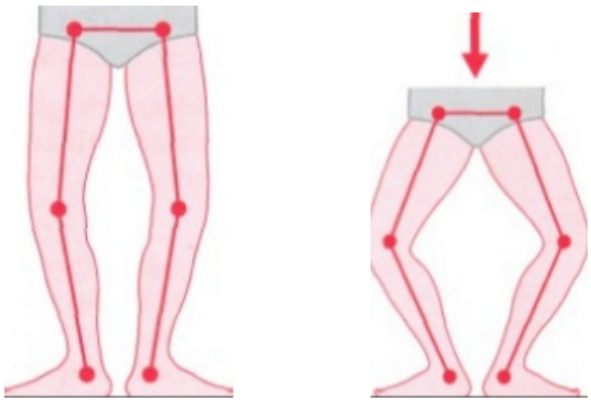

Figure 1.5: Squat as closed chain

The wanted knee extension is an open chain with two segments, the femur and the tibia, and their joint. The foot isn't considered because in human specimen is removed, and eventually its weight can be added to the leg to reproduce the natural situation.

1.2 Total replaced knee joint

1.2.1 Structure

The TKA total knee arthroplasty is a prosthesis that is implanted in patients who have important knee joint issues, like pathologies or traumas, that alter the physiologic mechanic of the joint.

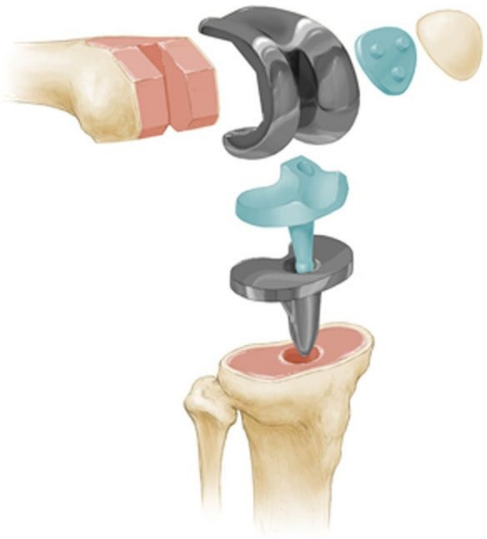

Figure 1.6: TKA prosthesis components (umhealthcare.net)

TKA insertion requires to cut the distal epiphysis of the femur and the tibial plateau to be replaced by two metal components, named according to the bone they are inserted into [7]. The back surface of the patella is cut too, and a plastic convex element is insert in order to slide on the femur and achieve the physiological kinematic.
Another plastic surface is placed instead of the menisci, emulating the natural interface between the two long bones. Because of the complete substitution of the native knee joint, these implants are implanted when all joint system of the patient is compromise. In fact, surgery should keep safe natural tissues when it's possible.

In general, TKA are divided in four main groups [6, 8, 9]:

1. CR cruciate retaining: this kind of prosthesis is implanted preserving the cruciate ligaments. In fact, if the tissues are healthy, they can work as if in the native joint.

2. PS posterior stabilized: the cruciate ligaments are removed during surgery cause their lack on usefulness. The plastic menisci have a protrusion that make an interaction with the femoral component called "cam and post", allowing the emulation of PCL functions.

Figure 1.7: CR and PS TKA prosthesis (orthobullet.com)

3. Fixed bearing: it's referred to the plastic tibial insert. The range of motion is limited because the internal-external rotation and the roll-back phenomena are more restricted than native joint.

4. Mobile bearing: this prosthesis allows greater freedom, but strong and healthy ligaments are necessary to avoid implant failure, and not all patient are able to bear this solution.

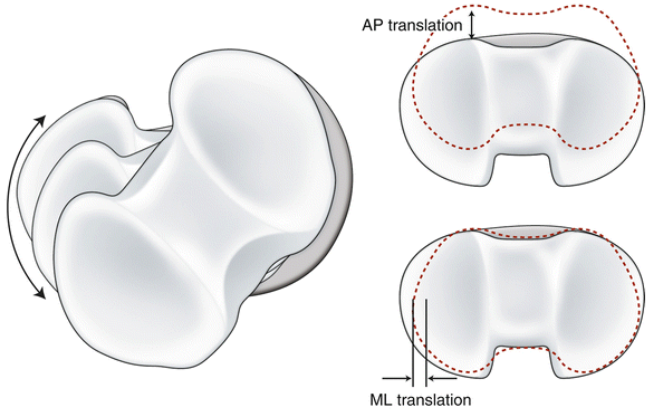

Figure 1.8: Mobile bearing prosthesis

Femoral component can be fixed by bone cement or cementless [10]. The two condyles can be asymmetric and the femoral element can replicate both the situation or even assume specific shapes called "j-curved" or "single-radius", depending to the patient's anatomy and requiring an accurate pre-surgery planning. [11].

1.2.2 Kinematics and kinetics

The movement of the joint follow the surface of the elements.
TKA's geometry is close to the native joint, but it guarantees functional geometry and allow daily movements. For example, the roll back must be preserved to keep the center of rotation changing according to physiological trail. The post-cam or natural PCL (ACL is usually sacrificed in TKA implants) let the prosthesis control the roll back. The physiologic posterior condylar offset also is maintained. Several fluoroscopic follow up showed however a high presence of abnormal kinematic patterns, which leads to a worse recovery for the patient. That's why the research is focused on patient specific prosthesis and surgery, obtaining a proper operation designed for the very patient [5].

2 Aim of the project

2.1 Aim and scheme of the activity

An old frame was available in the laboratory of the department. It was a simple structure, made by steel, composed by:

- a stuck base, screwed in the worktable;
- a vertical support;

- a cubic housing, shaped to be close to the resin cube used to incorporate the proximal part of the femur and to keep it fixed.

This build allowed to perform the wanted open chain tests, holding the femur to its apex and letting the tibia free to move. Unfortunately, the frame had three important limitations:

1. its base couldn't rotate;
2. the shape of the housing limited the kinds of analyzable specimen;
3. it only allowed to perform passive exercise.

The first part of the project involved the design of a new frame to overcome these issues. Once the structure was ready, it was necessary to implement an actuation system to perform the knee joint active extension and acquire related data.

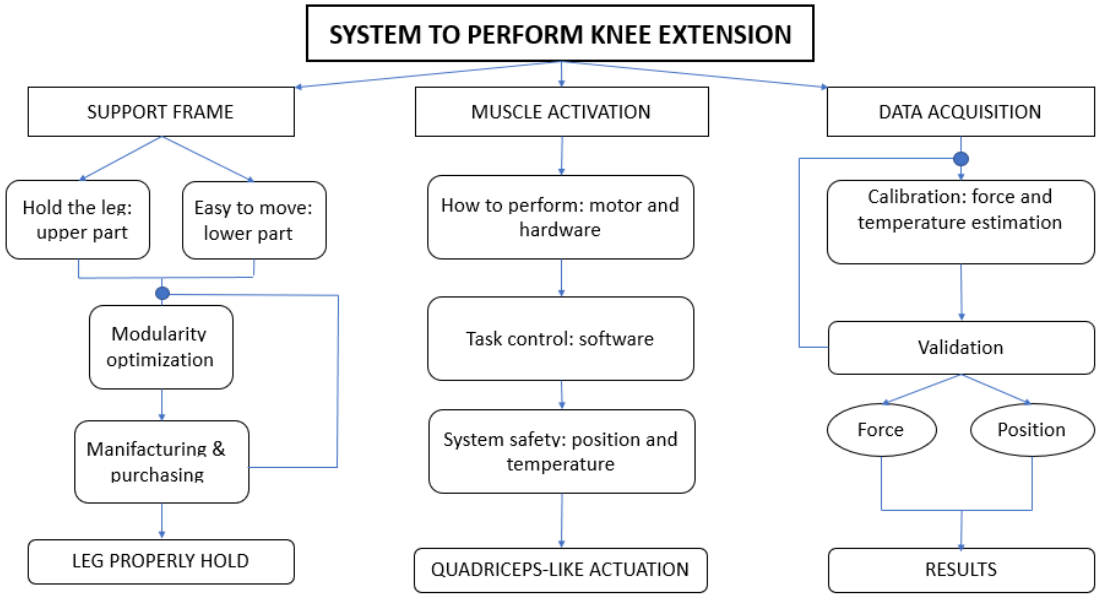

Figure 2.1: Activity flow chart

Thus, the thesis was structured as three main topics to be followed sequentially. All of them shared some common points: the system had to be comfortable to use and move, safe and the cheaper possible. Most important, the system had to be the most general possible. That means that the it can support, drive and provide coherent results independently on used specimen.

2.2 Requirements

The thesis had the main topic of obtaining a structure that allowed the wanted open chain analysis.

Holding frame
The purpose of this building was to keep the leg steady in a proper configuration.
As said before, the old frame lacked in versatility, so the new one had to surpass these limitations. Furthermore, it had to be the most modular possible, in order to obtain a structure that was stable, fast to assemble and handy even for just a single operator.
The starting point was the old steel-made frame, on which new features were added step by step, changing shapes and elements to got what needed. After the main sketch was settled, a new phase of optimization followed to make the elements easier and cheaper to be produced. All the pieces for this structure were designed with a CAD software called SolidWorks 2018.

Quadriceps contraction
One of the most important topics was the muscle actuation that lead the leg extension. In the human body, this task is achieved by the quadriceps, placed on the front of the thigh and covering all the bone as the biggest muscle on the entire body.

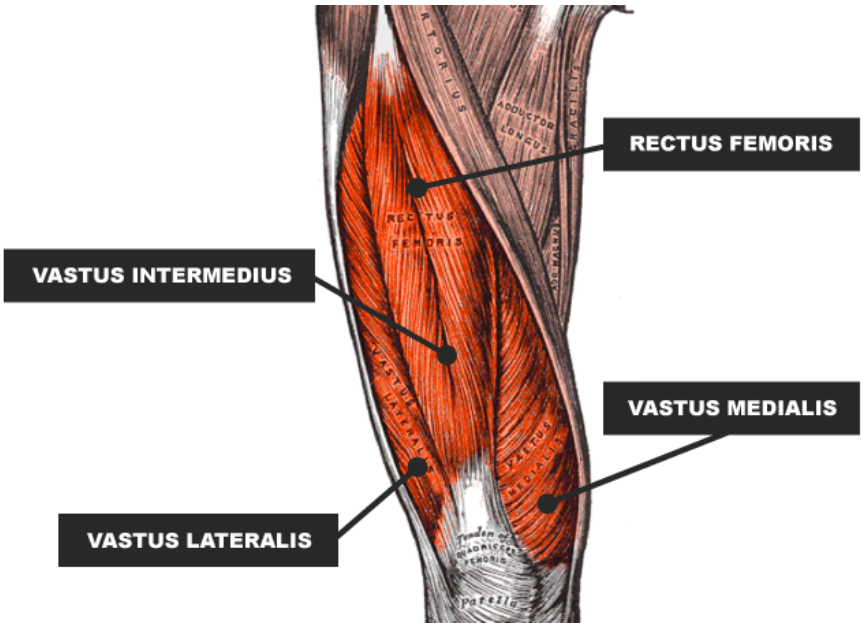

Figure 2.2: Main quadriceps muscles (e993.com)

This huge muscle is composed by 4 smaller muscles, so named because of their shape and related to the anatomical position terms. All of them ultimately insert into the tuberosity of the tibia exploiting the patellar tendon that, crossing the patella, allows the extension. [12].
The role of the patella deserves a deeper discussion, that will be done in chapter 6.2.7.

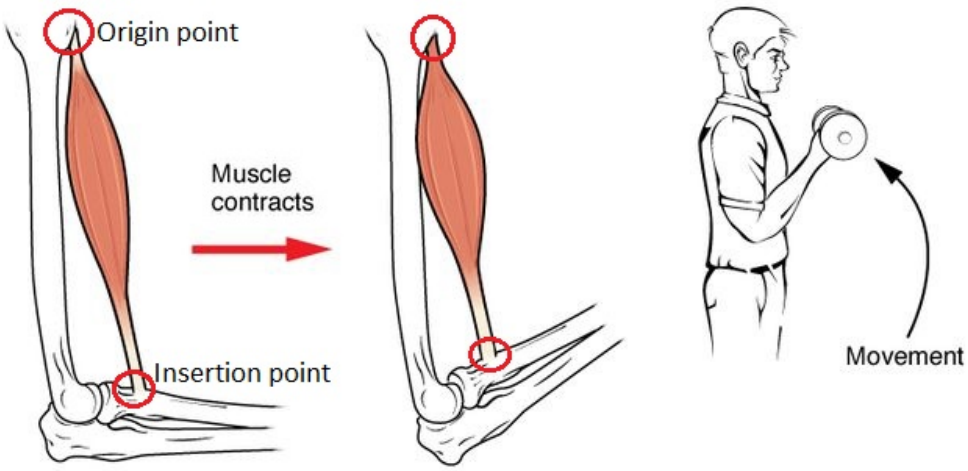

Figure 2.3: Biceps activation (shutterstock.com)

Skeletal muscles are attached by both their ends by tendons, which create a link between two different bones. These two points can be distinguished as the origin point and the insertion point.
It's well known that muscles can only actively contract their fibers, making them work only by pulling, and never pushing. When a muscle contracts, the origin pulls the insertion closer, using the bone as a lever, as shown in figure 2.4. The purpose is to find a way to emulate the action of quadriceps, following the anatomical axis and performing the extension as closest as possible to the physiological movement [13].
A handy way is to reproduce muscles as linear actuators, and a motor was useful for the purpose. The motor set-up, the controlling software and system safety will cover the most part of the job, because tests had to be reproducible in order to get useful data. That said, it was necessary that the applied forces could be controlled each time precisely.

Data acquisition
Once both the structure and the motor were consistent, the last step was the acquisition of the data.
First result was to record current data, supplied by the system to make spin the motor. These allowed to estimate the force of quadriceps applied to perform the movement, that was compared to the physiologic one described in literature. A comparison between each acquisition was necessary in order to discuss reliability and solidity of the system.
Furthermore, it was useful to analyze the movement of specific main points during the task with a motion capture system.

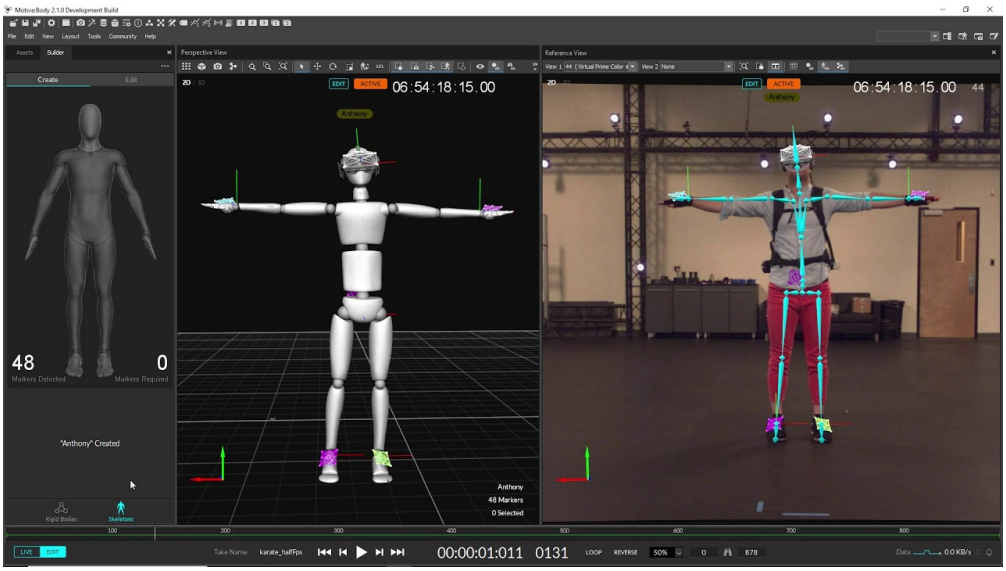

Figure 2.4: Example of camera utilization and dedicated software

Following with cameras the change of position of that points, called markers, it was possible to reconstruct an accurate 3D model of the episode. That way, it was possible to relate the reached position to the applied force.
This technology is widely used in gait analysis, but it's possible to take advantage of it also for smaller tasks such the knee extension.

3 Holding frame

3.1 Lower part

3.1.1 Main requirements

The lower part of the frame must be different from the previous model.
The old one was in fact screwed on a fixed support on the worktable, that didn't allow to move the vertical support at all.
This could be a problem once it's needed to move the specimen to get a better acquisition from infra-red cameras, where the pieces must be unscrewed and then re-screwed once the wanted position was reached.
To avoid this process, the idea was to build the base as two separated elements to obtain a relative motion of one related to the other. An easy way to achieve this can be to make one component able to rotate according to a common axis, so the two pieces were so thought:

1. Lower seat:
   This part had to be fixed on the table, allowing the other element to rotate on it by using a guide system;

2. Upper disk:
   This second piece was supposed to rotate on the lower seat in order to achieve the wanted exposition of the specimen.
   After the position was decided, the upper disk had to be fixed on the lower seat in order to prevent any other movement. Each test has to be reproducible, and it's necessary to not let this kind of artifacts happen during the acquisition because that will produce useless results.

3.1.2 Optimization

The lower part had to be the negative of the upper one, so the disk is free to rotate in its proper seat.

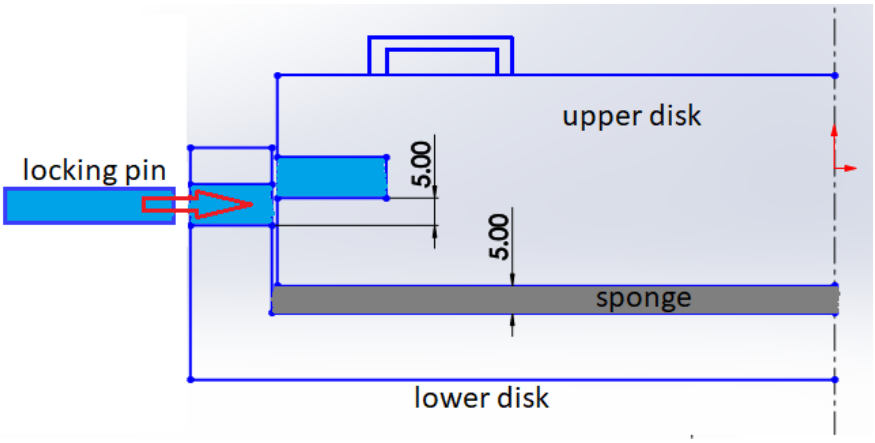

Figure 3.1: Lift-and-press system: sketch

The first idea was to get that movement by using two apposite handles to lift the upper disk, put it on the wanted position, and then return it to its place. After that, it'd be locked by four lateral pins that reach the internal pocket. A sponge layer of 5-10mm could be added between the internal surfaces to prevent movements of the upper disk. Finally, the disk had to be pushed down to let the pin reach the internal pocket, obtaining a steady configuration.
However, this solution was not good for several reason, in particular the set up wasn't very comfortable. The disk has to be lifted up, positioned, inlaid, pushed and only while it was kept pulled, the four pins could be inserted.
It's important to keep in mind that during all these steps, it's possible to have the upper part of the frame with the specimen attached on. All of this make the structure uneasy to lift, that can even fall during the whole process. To overcome the issue, it was clear that a sliding system could be the solution.
This way was decided to work with continuous rotation instead of discrete rotation.
Several solutions were investigated, such as ball bearings. Lateral bearings were subject to high shear stress by the very guidelines, so it was thought about a vertical system.
The solution worked out, but the structure would be heavy and complex, with a huge number of spheres to purchase and insert into the upper disk, making it very difficult to

manufacture. A new solution, close to the last one but easier to achieve, is to perform the rotation by friction and it was definitely the best solution. That upper element should slide on the lower by a linear interface which escorts the rotation while bearing the weight of the structure.
It was clear that the interface must not be horizontal, in order to prevent lateral sliding.

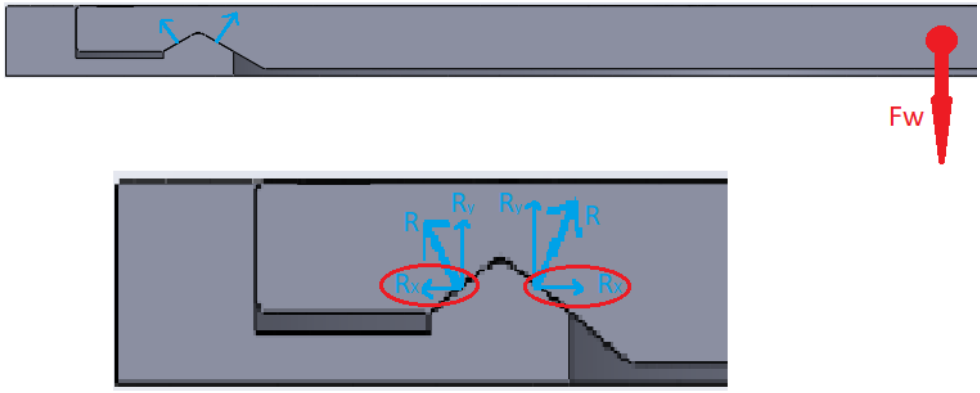

Figure 3.2: Self-centering concept

The interface was designed as self-centering, that is a structure that prevents any movements but the rotation thanks to how the two surfaces are oriented. As shown in picture 3.2, the weight (red) generates two opposite forces by reaction. The two horizontal components of both the resultants cause the self-centering of the upper disk, preventing any misalignment of the two elements.

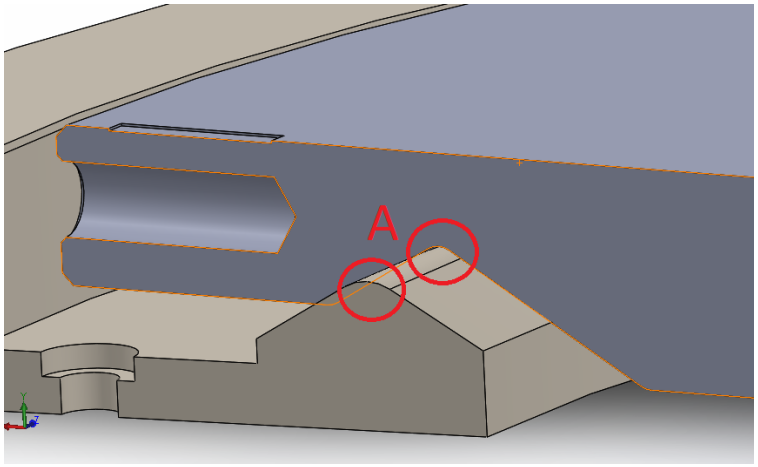

Figure 3.3: Self-centering sliding system

The A edges were smoothed to avoid stress concentration in a critical region, that could break the upper element.
The final result is a structure that allows an easy rotation taking advantage to the self centering drive, even with the specimen mounted on it.

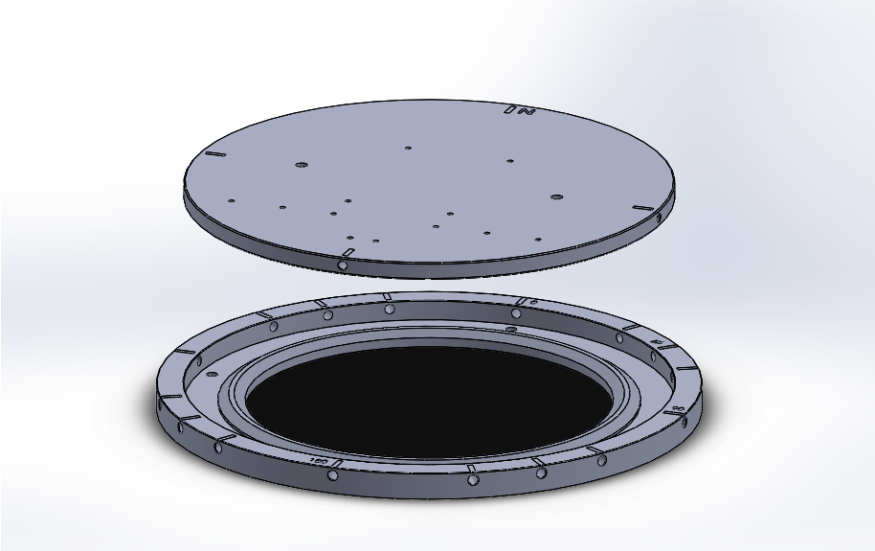

Figure 3.4: Completed base

3.2 Upper part: Blocking system

The femur must be steady during all the test. To achieve this, it's necessary that a stable blocking system able to prevent any displacement of the fixed bone. Detected macro-movements can be seen as actual movements during camera recording ruining the acquisition. In order to keep the correct positioning of the femur, two different solution were thought.

3.2.1 Resin

The old frame worked out for goat legs, taking advantage of a resin cube to fix the specimen on the frame. The first idea was to incorporate the proximal femur in a cubic cement as well.
Once the block is fixed to the bone, it should be put into a proper housing made by aluminium. That way, it was possible to change rapidly two different specimens by only removing the cube from its seat. To obtain this kind of system, it was necessary to use always the same housing so all the resin cubes must have the same dimensions. In that way, the structure is the most generic possible and allows to have a plenty of specimens ready for test while the housing stand still on the frame, with a quick change of leg performed by just one operator. Two bars pass through the apposite holes to prevent any slide of the cube.

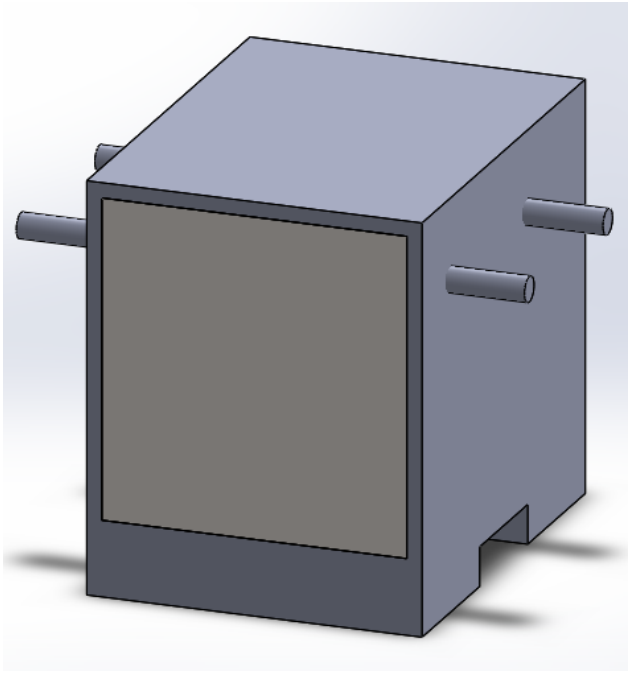

Figure 3.5: Resin-housing system

It was necessary that the operator could prepare everything in loco, which means that a proper system to produce the resin cube and wrap it around the proximal femur was needed.
To achieve this a new housing, almost identical to the previous, was sketched to contain the polymeric solution and the end of the femur. However, another holding frame was necessary to keep the leg steady for hours, to let the resin getting harder and fixing itself to the femur.
The building should hold the tibia (because it's the femur that needs to be immersed in the liquid resin), making this way necessary to have two different frames.

pros

1. Highly steady holding of the specimen
2. No pins are required on the bone
3. Fast and easy to assemble on the frame

cons

1. Requires another structure for the resin solidification
2. The same system clearly requires a different holding system
3. The preparation of the cube is time-consuming and cannot be properly stable for human legs

3.2.2 Clamping

The other idea was to use directly a clamping system to bear femur, because a similar system was needed anyway to prepare the resin cube. This solution required a way to make the grip reach the bone by linear.
A possible way to achieve this was to use a threaded bar into a threaded hole.

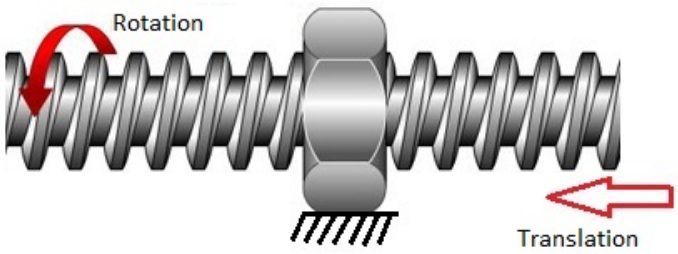

Figure 3.6: Screw rotating into threaded hole

Let's think about a fixed nut and a simple screw (picture 3.5). If the screw rotates inside the nut, it will proceed following the direction of the spin. If the screw rotates in the opposite direction, it is going to move to the new direction as well. The same result is achieved by making a threaded hole on the housing surface.
This way, the rotation of the bar became a linear movement in both directions that allow the screw to get closer or farther to the bone, clamping it during the set-up phase and making it free when necessary. After found out the way to make the grips move and grab the bone, a proper clamping system was designed as four elements, two steady and two floating.

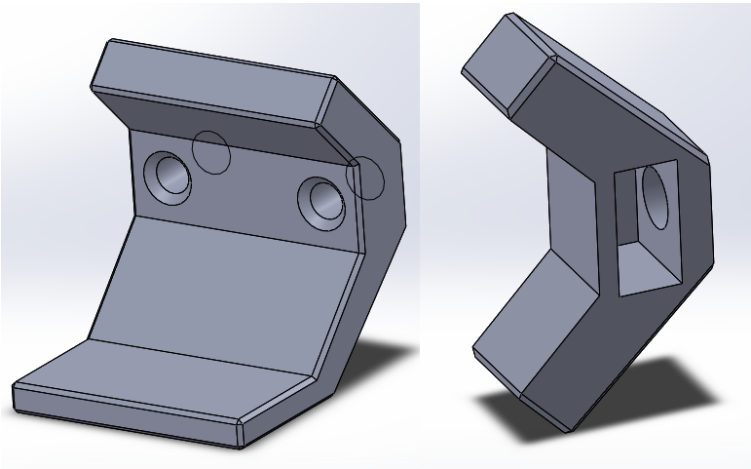

Figure 3.7: Steady clamp on the left, moving clamp on the right

The floating clamp was designed to reach the bone, pushing it until the other-side clamp and fixing the current position of the femur. Two pair of them were required to prevent bone rotation.
In order to increase the stability of the system and preventing back-sliding in extension phase, a back wall was added to support the proximal part of the femur. Furthermore, the

bone had to be wrapped with bandages to obtain a better distribution of the applied pressure, increasing specimen steadiness.

pros

1. Don't requires any preparation other a simple bandage around the femur
2. No pins are required on the bone
3. Fast and easy to assemble on the frame
4. Absolutely insignificant cost

cons

1. The system isn't so steady as the resin one
2. The clamping phase can be a little more troublesome than the other one

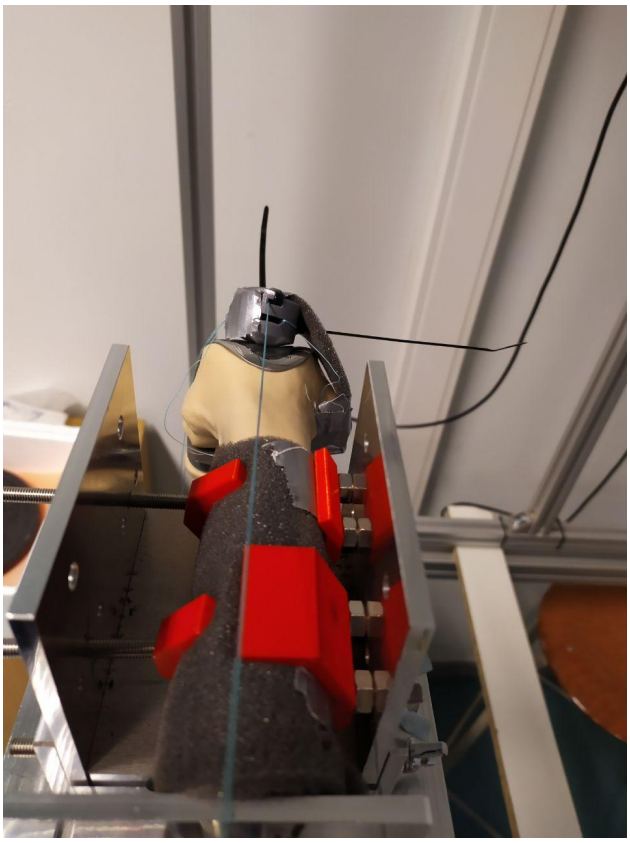

Figure 3.8: Clamping system at work

The final frame was focused on this second solution but, thanks to its high modularity and generality, it is possible to take advantage of resin cube method too.

3.3 Upper part: Horizontal seat

3.3.1 Main requirements

This upper element is the region composed by the higher number of separated pieces in all the frame.
It has to be available for different kind of limbs, also coming from different species like goat and pig. To achieve this, it was necessary to compose the seat using different simple elements, that could be easily swapped to get a stable holding structure for samples.

3.3.2 Optimization

The upper part of the frame is composed by several different pieces, that can be grouped in three main categories.

1. Seat

   This element is the shape where the resin cube fits into. On the other hands, it must allow clamps to move and grip the femur.

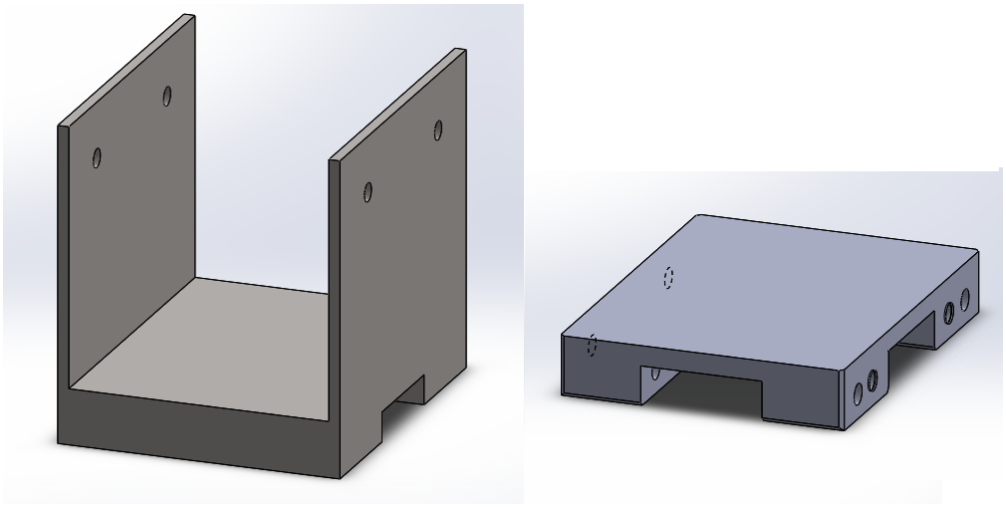

Figure 3.9: Seat before and after

At the beginning, it was designed to be a single element where the resin cube had to fit into. The two holes permitted to fix the resin cube with aluminium shaft or to fix the bone with the horizontal clamp.
Once the main requirements were successfully obtained, the design of the element was optimized to be the most general and cheaper as possible, reducing waste of material by adjust its shape. In picture 3.9 the left seat would be manufactured by milling machine. In this process about the 80% of the material would be wasted to obtain the basin. Because it's important designing elements also considering to minimizing

the manufacturing costs, the geometry was revisited and optimized by separating the lower part of the seat from its walls, making it a composition of smaller pieces. This way the price for its production was widely reduced. The picture 3.9 better show the obtained lighter seat and provide an idea of how much material was saved with this adjustment.
The two kind of holes in the final seat allow respectively to fix the seat on its inferior support (point 2) and to the lateral walls (point 3). The shape of the lower part was designed to have a crossing hole that is shorter than the total length of the edge.

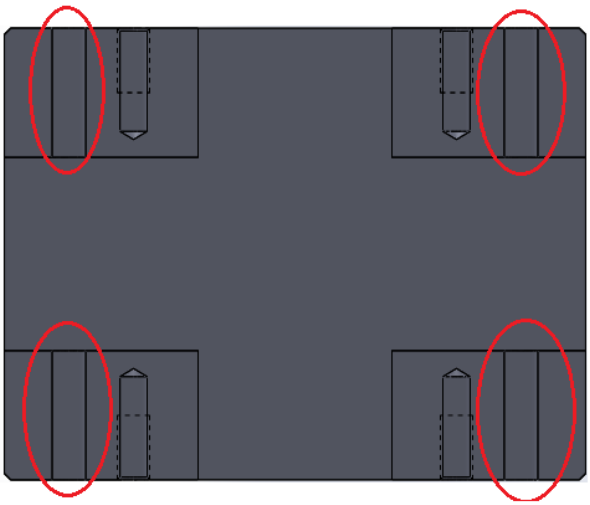

Figure 3.10: Hole deepness magnification

So shaped, the holes are deep around $20mm$ instead of $70mm$. The more the drill bit is long, the more does it costs (order of hundreds of euros), and that way it's possible to use a shorter bit two times by rotating the seat during the manufacturing, obtaining the same result.

2. Seat's support

This element is the link between the vertical support and the upper seat. Its purpose is to keep the seat as steady as possible, allowing an easy and quick set up of the upper elements.

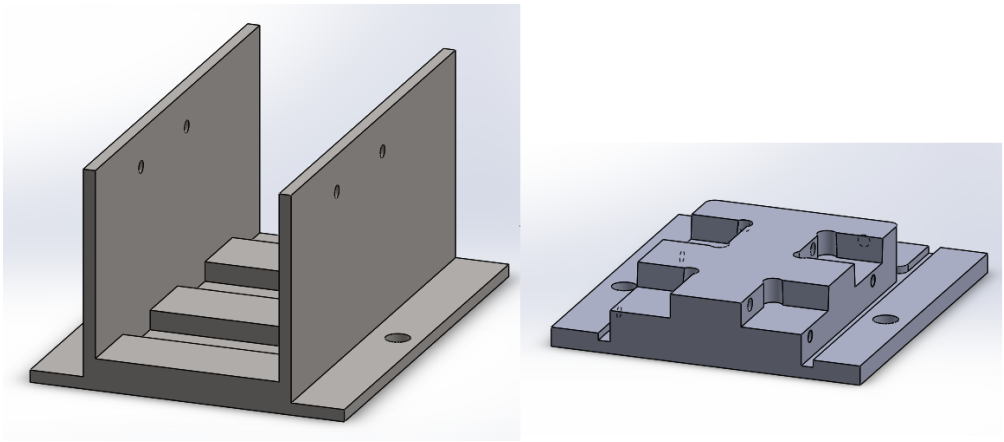

Figure 3.11: Support before and after

Like the previous piece, it was designed to be the negative of the element that is going to receive. In this case, it was shaped to receive the seat, and the step pattern on the floor matches with the lower part of the bench, less than a small tolerance. For the same reason as before, once the main requirements were achieved, it was important to optimize the shape to be less expensive and less difficult to produce. The two walls were removed as well and could be attached when by the two lateral holes, while the medial holes let the seat be quickly fixed to its support.

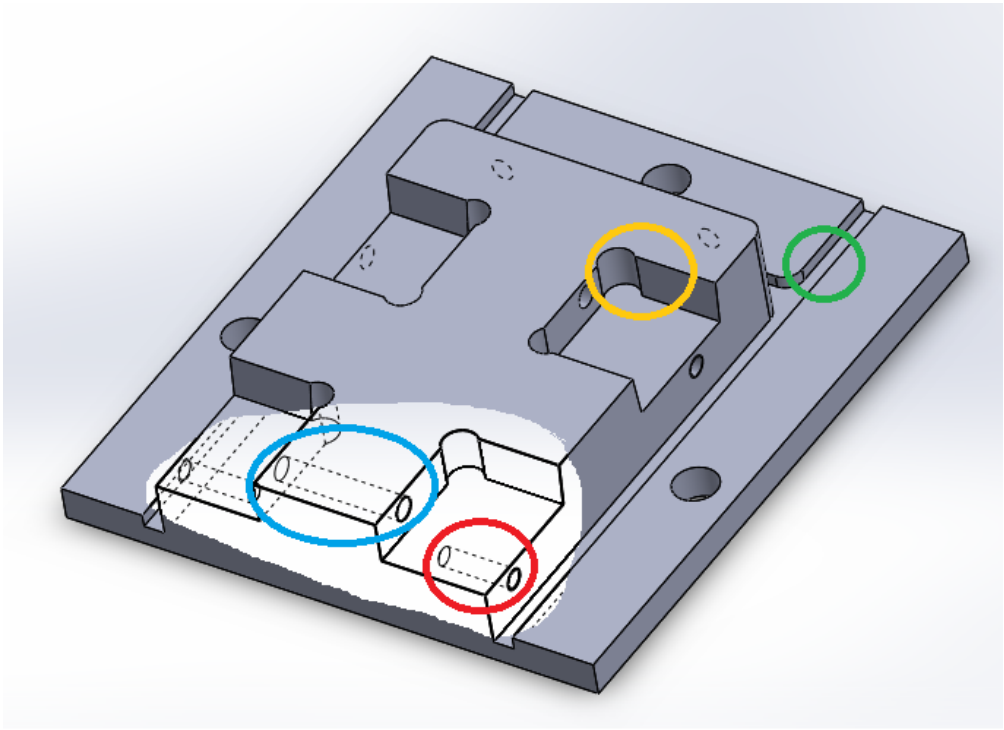

Figure 3.12: Top view of the support

After a meeting with the workshop technician, the shape of the upper region was re-designed.

* Green circle: thin ruts were added to better hold the walls during the set up. A third wall can be insert in the back region to prevent bone sliding during the pull.

  Orange circle: the milling machine couldn't perform perfect 90° angles because it works using circular tools with a specific diameter. For this reason, all right angles were replaced by round-type corners. Furthermore, lateral surfaces were slightly inclined to escort the seat insertion.

* Blue circle: this hole fixes the seat to its support. The hole making machine requires different drill bits to make different depth and, as for the previous element, the more is the length of the hole, the more the price increases (50 euros for $30mm$ against over 300 euros for $90mm$). A new shape was designed to avoid through holes with depths over $30mm$ without altering the negative shape of the upper surface.

* Red circle: the holes for attach the walls weren't through all, for the same reasons discussed in the previous point.

3. Walls

The separated walls were available to be attached during the set-up phase.

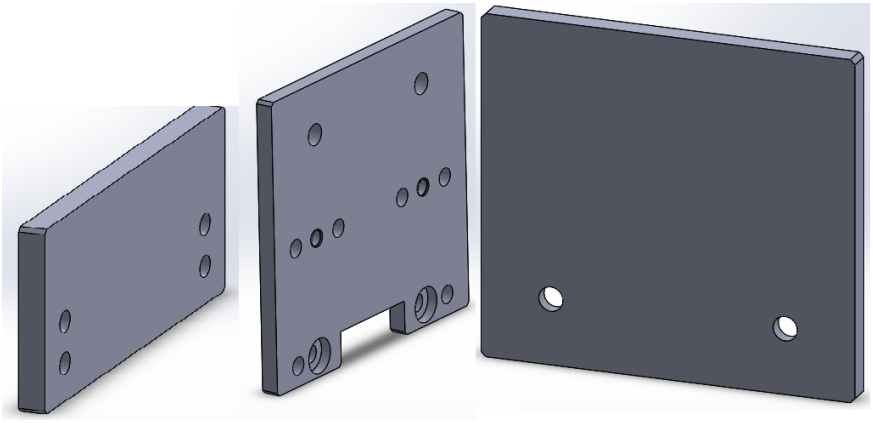

Figure 3.13: Respectively, support's wall, seat's wall and back wall

These pieces were designed to be screwed to the corresponding element. They can be fixed before or during the set-up phase, leaving to the operator the complete freedom to act.
Several holes can be noticed: the lowers are used to attach walls to the corresponding element while the higher holes on seat's wall allow to fix the leg in the two discussed way.

The support's lateral walls are lower than the seat's ones to enable an easy assembly of the two elements, especially if the seat has clamps and threaded bars already attached.
The result of the optimization is here shown by the picture below.

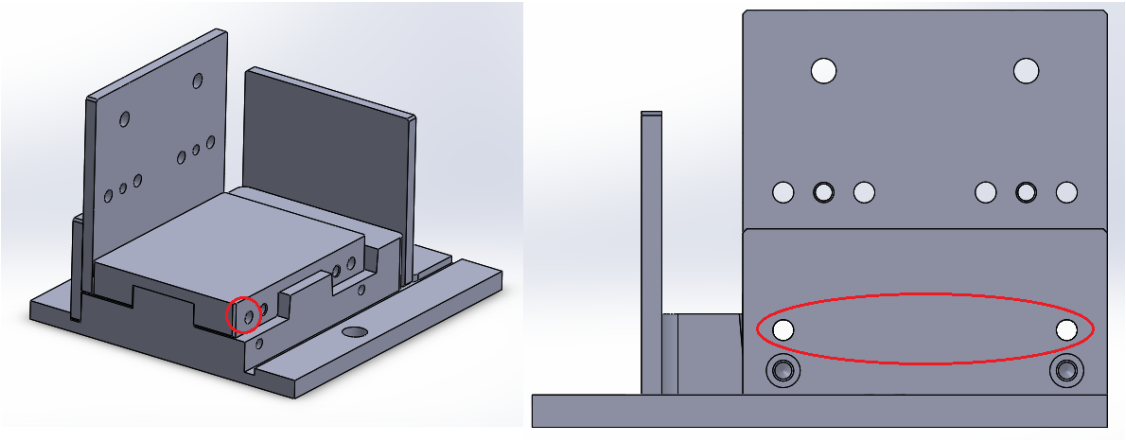

Figure 3.14: Partial assembly of the upper part of the holding frame

It can be noted how the modularity plays an important role during the optimization phase, obtained by different small elements that can be attached previously or when it's more suitable for the operator.
The red circles identify the not-threaded holes that, once all pieces are assembled, create a through hole where will be insert the threaded bar. That bar can be eventually locked by nuts, obtaining a fast and easy system to keep the seat steady to its support.

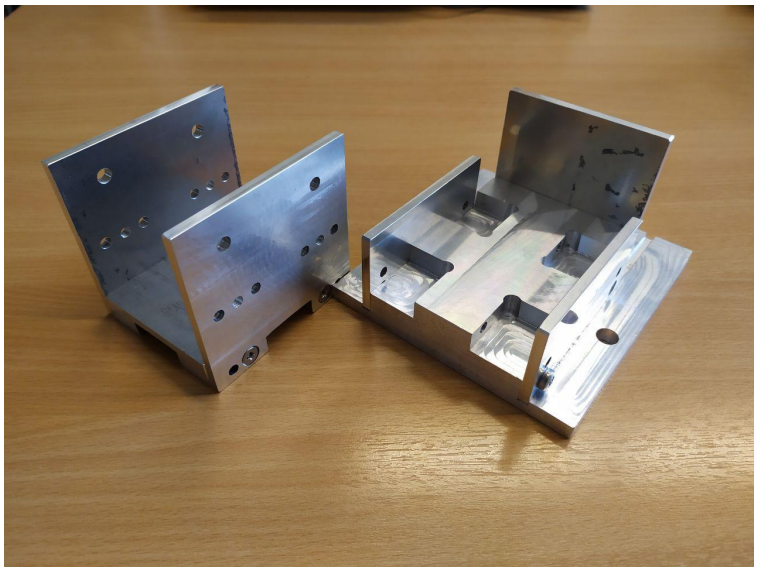

Figure 3.15: Manufactured prototype of the holding system

3.4 Vertical support

Both the lower part and the upper part were designed anew. The vertical support found on the old frame works perfectly for the purpose. This part was composed by steel, and it was safe from any of the possible stress issues.
Also, the attachment used to fix the lower part to the upper part were taken from the same old frame, as they were simple steel-made support bracket. A rough simulation performed on Solidworks revealed, as expected, that the maximum displacement is located on the top of the vertical support, and the maximum stress at its bottom. The value is not far from the theoretical one, evaluated as displacement of two beams in series, and it's about $0.123mm$ which is negligible for the analysis. Note that the applied force is very high compared to the common quadriceps forces findable in literature, that is about $300N$ [19]. This value was also verified by imposing a 2D mechanical equilibrium in maximum extension, which is the worst-case scenario, and will be discussed in chapter 6.

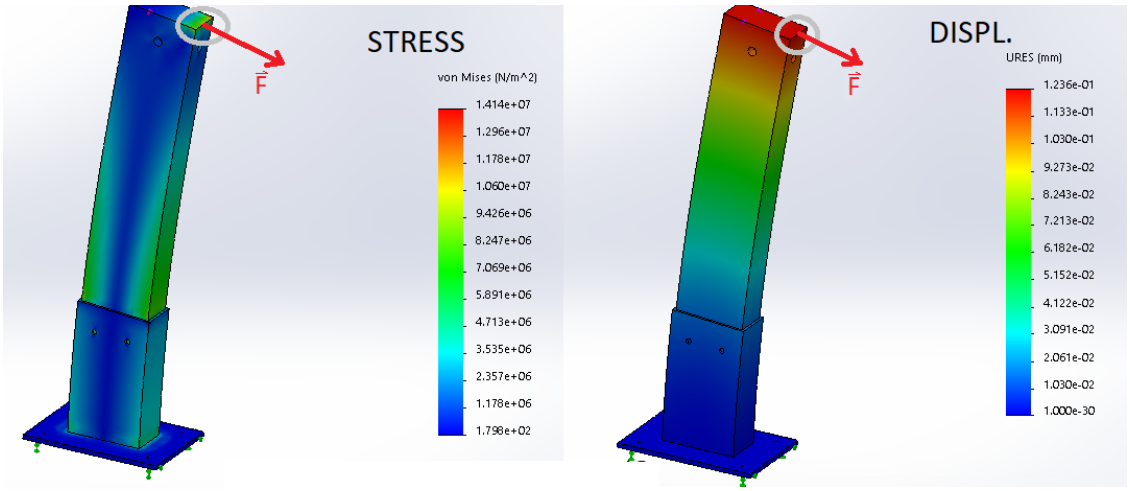

Figure 3.16: Vertical frame stress and displacement evaluation applying $100kgf$ on the highlighted edge

This one was steel made, so the structure is safe for the application supposed to bear. The other pieces were settled made by Aluminium, that is lighter and easier to move during assembly, because their stress is lower than the one acting on the vertical support.

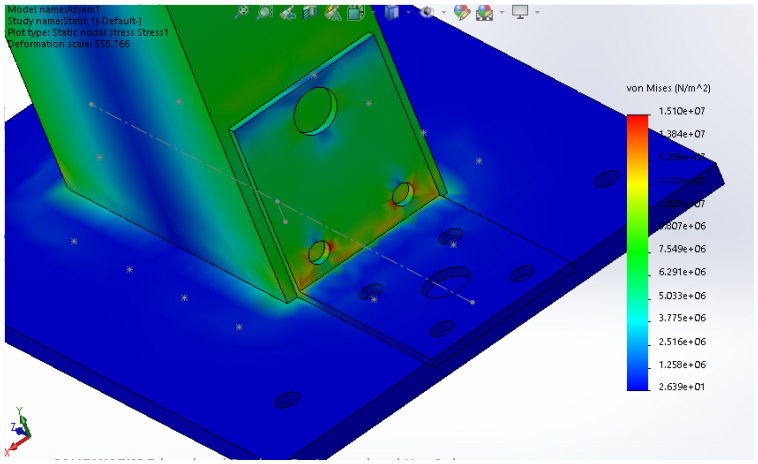

Figure 3.17: Support bracket solution evaluation

It was decided to attach the vertical support to the lower disk by two steel brackets at least. Figure 3.17 shows stress applied to the brackets when a force of $1000N$ acts on the top of the vertical frame. They were able to bear the stress without bending. This force won't be reached for this project, but this demonstrate that the frame can bear more stressful tests.

3.5 Final solution

During a meeting with the technician, two companies appeared to be handy for the purchase of raw material.
Several other societies were contacted in order to collect the more price quotation possible, but most of them never answered. Hemimex is a manufacturing company placed in Brussels, near the very university, while Blockenstock.fr is a french society with a huge on-line shop that allowed to evaluate prices without waiting for answers.
This factor was determinant: after too long waiting for Hemimex's answers, and their very low availability to receive me by person, it was decided to purchase the raw material directly from Blockenstock.fr's website to complete the manufacturing as soon as possible.

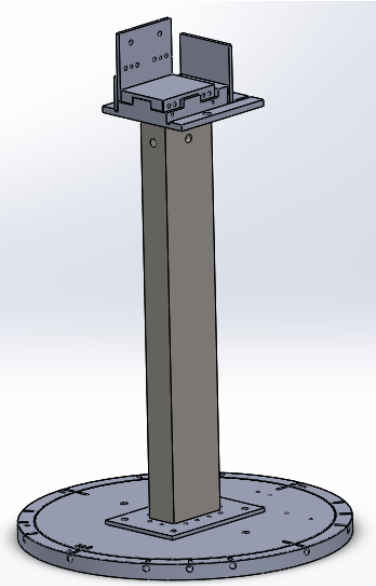

Figure 3.18: Final frame prototype

4 Quadriceps simulation

4.1 Maxon Motor

The extension of the knee is physiologically carried out by quadriceps muscles, which works is always by pulling (as discussed in chapter 2). In order to emulate the natural muscle activation, a DC motor was chosen before the very beginning of the thesis.

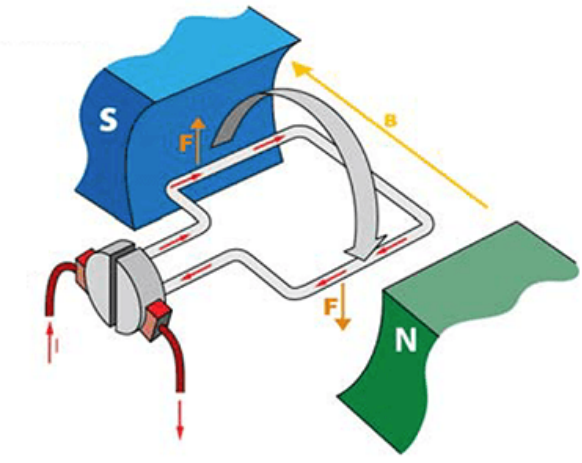

Figure 4.1: DC motor work (quora.com)

A DC motor is a rotary electrical machine able to convert a current flow into mechanical energy exploiting magnetic fields. In picture 4.1 can be distinguished two permanent

magnets, a wire and a stator [14].
The wire, that is placed between the two magnetic poles N and S, is absorbed in a magnetic field B and it is crossed by a certain current I, where electrons flow at a certain speed V with electrical charge q. According to Lorentz law, when the flow expresses a certain angle to the B field, the wire receives a force $F = q * V * B * cos\alpha$ that is proportional to electrons speed and electric charge. The force is the maximum when the plane of the wire is parallel to the magnetic field lines.
The two forces generate a couple that makes the coil rotate. The stator supply current to the wire and it's split in two parts, inverting the current flow during the rotation of the coil in order to keep it rotating by granting the two forces to push in the same verse. The contact between supply and stator is achieved by brushes in brushed motors.

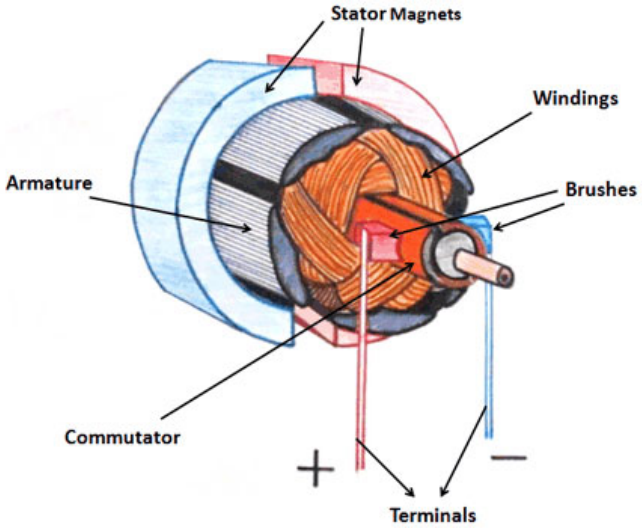

Figure 4.2: Usual DC motor (instrumentationforum.com)

DC motor takes advantage from this phenomenon and normally uses a huge number of coils to maximize the effect. Most of the DC motor are composed like this, with the advantages of low production costs, high reliability and easy to control [15].
The motor chosen for the quadriceps emulation is the RE65 DC brushed motor, provided by Maxon company.

Figure 4.3: Maxon motor, RE 65 graphite brushed

The RE65 can deal with high performance with a nominal current is $6.8A$ and speed up to $3500rpm$. The motor works with $48V$ as nominal voltage, that means a huge power supply is needed to supply that amount of electric tension.

The torque provided by the motor is related to the current with a proportional coefficient:

$$M = I * k_m \tag{4.1}$$

where

- I is the current provided to the motor;
- k_m is the torque constant;
- M is the output torque;

k_m is a constant own by the very motor, and it's findable on its data sheet as 123 $\frac{mNm}{A}$ for RE65 model.
In order to apply higher torque, it's necessary to increase the provided current: for each amps added, the torque will increase by $0.123N * m$.
It's also important to underline that the more torque is wanted, the less velocity can be reached.

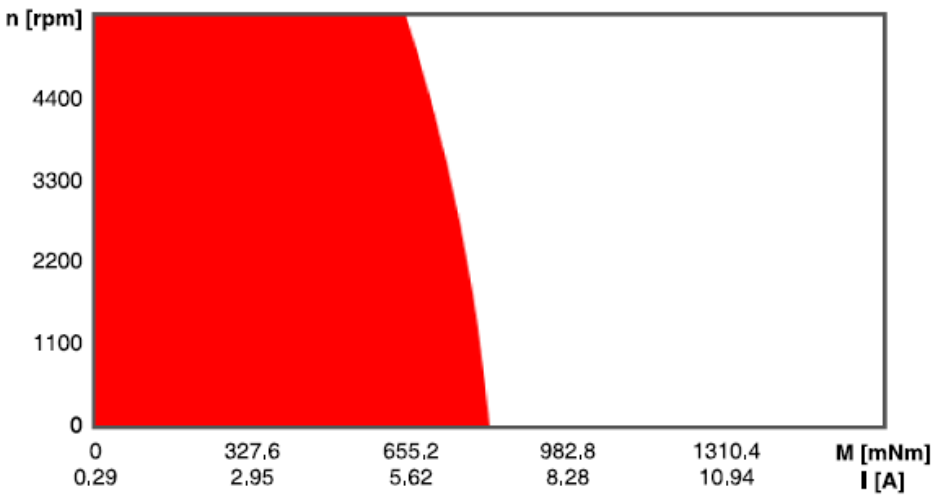

Figure 4.4: RE65 Operating range

The red region shows the condition for which the motor can work without any issues even for long periods of time, while the white region identify dangerous work condition, bearable only for short working time.
It's significant to notice that, over the $6.8A$, RE65 suffers also very low velocity. However, low speed shows several other issues, that will be widely discussed in chapter 7.

4.2 Encoder

The back side of the motor has a pocket to insert the encoder, that is an electronic component allowing to control motor positioning and its rotation velocity by a combination of logical levels.

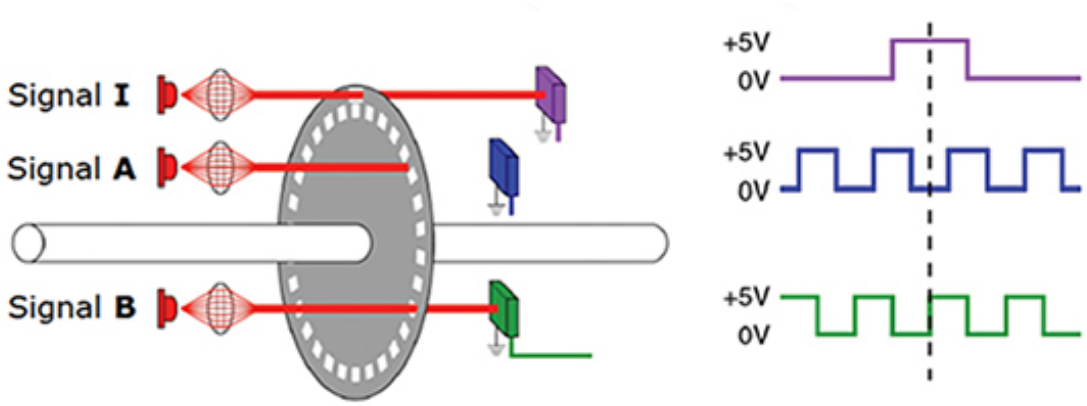

Figure 4.5: Encoder for pulse counting

The encoder is composed by a pierced opaque disk, a led light and a photo-detector, as shown in the picture. When light goes on the disk, it cannot pass through and the relative

detector isn't able to acquire the signal [16]. In this case, the logic level is "low". When the light passes through one of the holes, the signal reaches the photo-detector and the logic level switches to "high". A common encoder has two output signals, A and B, which produce a square waves in quadrature when the encoder shaft rotates. The square wave frequency indicates the speed of shaft rotation, whereas the A-B phase relationship indicates the direction of rotation. The encoder already inserted in RE65 owns a third channel (signal I) that is a reference signal, with just one pulse per revolution.
The encoder used in this project has 500 count per turn to discriminate the angular position of the motor, that means a sensitivity of 0.72 degrees.

4.3 Servo-controller

In order to achieve an accurate controlling of the motor, it's necessary to avoid a direct connection to the power supplier. A servo-controller is an electronic amplifier that allow a fine driving of the motor, and Escon 70/10 was purchased for the purpose.

Figure 4.6: Escon 70/10 servo-controller

This element is able to work with a nominal operating voltage of $70V$ and can provide $10A$ without any issue, reaching up to $30A$ but for short time.
The servo-controller is composed by several connections where cables can be screwed into.

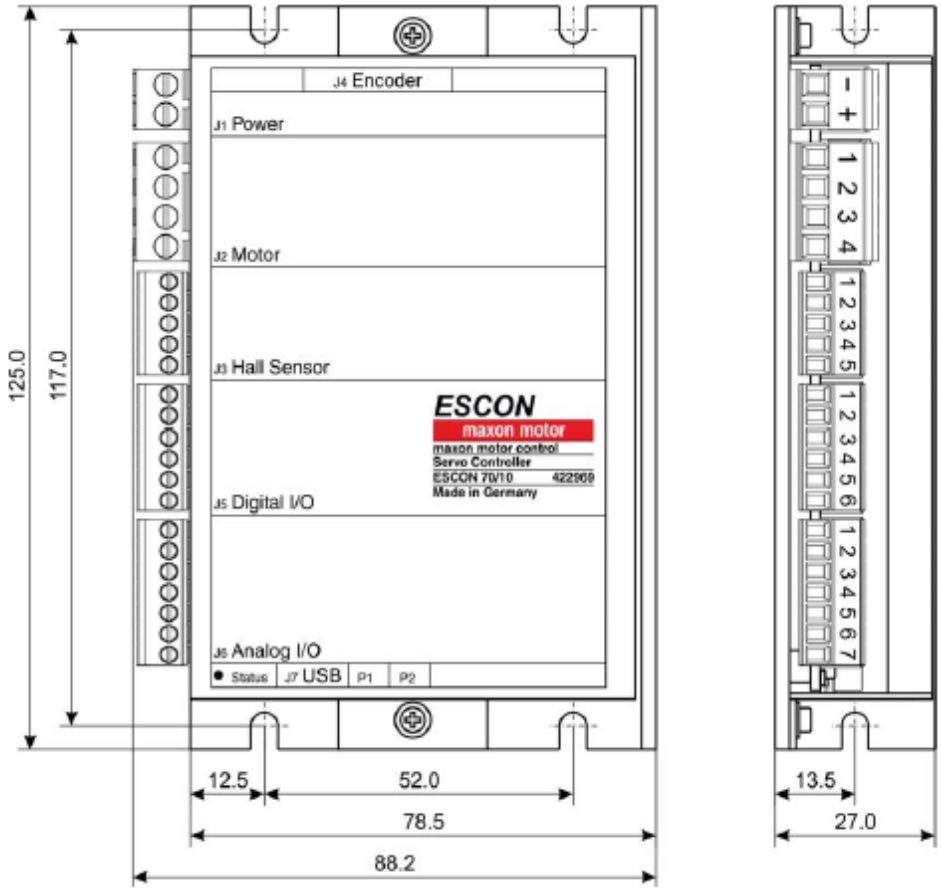

Figure 4.7: Escon 70/10 connections

- The first two pins (J1) are directly connected to the power supply, from which the Escon is going to get the firing. Once the servo is linked with the power supply, a led glows red.
- The second cluster (J2) provides current to the motor, that is modulated by the Escon: higher output from its port means higher input received by the motor.
- The third series of pins (J3) is dedicated at the supply of a Hall sensor. A Hall effect sensor is a device that is used to measure the magnitude of a magnetic field. Its output voltage is directly proportional to the magnetic field strength through it. Hall effect sensors are used for proximity sensing, positioning, speed detection, and current sensing applications. This component wasn't necessary for the main project and J3 wasn't used.
- In the upper side of the servo driver there's an ingress (J4) that is separated from the others and allow the servo to be directly connected to the encoder placed on the back of the motor. This way, the very servo can obtain a feedback of motor rotation, that can be displayed with a dedicated monitor.

- The fourth group of ports is used to connect digital input or output. A classic element linked to J5 is the logical switch, that receive supply from the controller and return a Boolean output which can be 0 or 1.

- The last series of pins (J6) is linked to an analog element like a potentiometer. This device provides a certain value to the Escon according to its internal resistance, that will be interpreted and used to modulate the supply sent to the motor.

4.3.1 Escon studio

The Maxon company provided a dedicated software to its customers.
This program, named "Escon studio", allow an easy controlling of the motor once the laptop is linked to the Escon servo driver.
As soon as Escon studio is launched, it will appear like this:

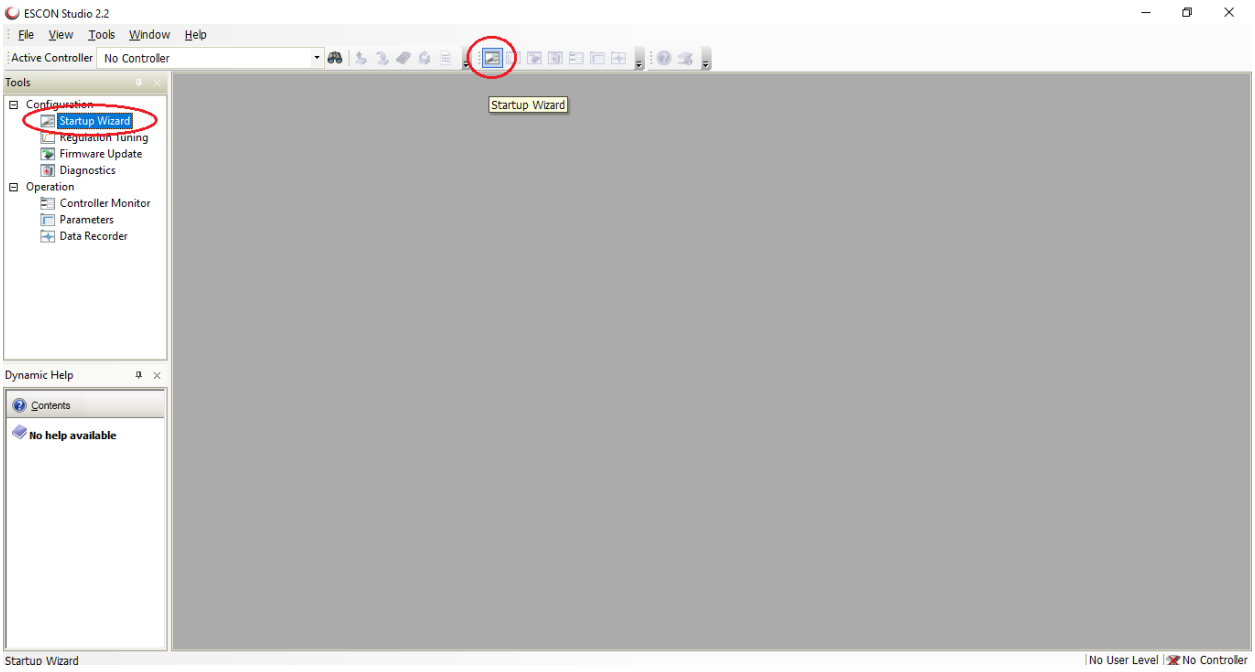

Figure 4.8: Escon studio layout

It was necessary to properly setting up the software for the purpose, giving information about the system directly to the software.
The first step was to open "Startup Wizard", highlighted in red in picture 4.8. The new window asked for the information used by the software to rightly control the motor input and output. This set up was essential to control the motor and each step described below refers to a different dialogue box.

1. Controller selection: choose here which kind of servo controller is going to be used for the application. It was selected the Escon 70/10.

2. Motor type: choose in this box if it's a DC or an EC Maxon motor that was decided to use. It was a DC motor for this project.

3. Motor data: define the motor's speed constant and its winding's thermal time constant, which are both written in its data sheet. Their values are respectively $77.8\frac{rpm}{V}$ and $123s$.

4. System data: specify the max permissible speed, nominal current and max output current limit, which are $3000rpm$, $10A$ and $30A$, again from the data sheet of servo driver and motor.

5. Speed sensor: the software needs to know if there was a position detector directly connected at the Escon servo, such as the encoder. In that case, more info must be provided to the software, like the number of pulse per turn.

6. Mode of operation: depending from the purpose of the test, it could be chosen between speed controller and current controller depending how the servo has to operate on the motor supplies. If the motor is supposed to work by controlling its speed, the servo works to keep the velocity as settled without controlling directly the given current. In the other hand, current control mean that the motor applies the chosen current to the motor, and its rotation speed is a consequence.
   It's important to remember that working with currents means working with the torque applied by the motor (4.1).

7. Enable: it was needed to select the enable functionality, the direction of rotation (clockwise CW or counterclockwise CCW) and the digital input that enable the spin.

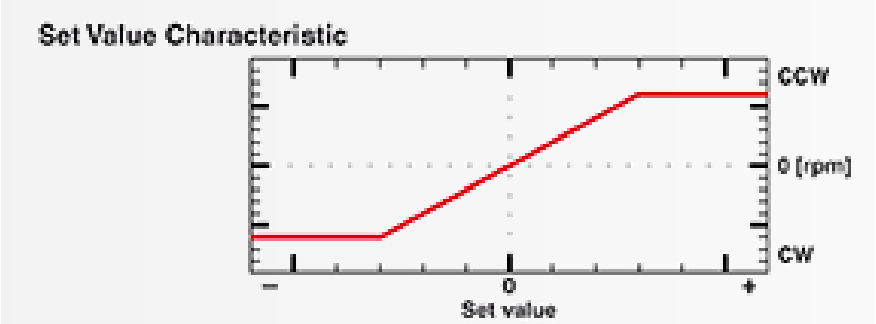

Figure 4.9: Enable function: high active

It could be chosen between high active or low active. The logical state was given by the corresponding digital input linked to the Escon servo, such as a simple switch. It was obvious that, for a simple switch with only two different configuration, there was only two possible situation: CCW or steady. In order to allow the motor to perform a CW rotation, a more complicated switch was required. Anyway, the purpose of the study was to focus on the quadriceps contraction, that means that one direction was enough to replicate muscle contraction. In the future, it's possible to add a new feature for studying the hamstrings work.

8. Set value: this data are probably the most important data required in order to perform a well-controlled movement of the leg.

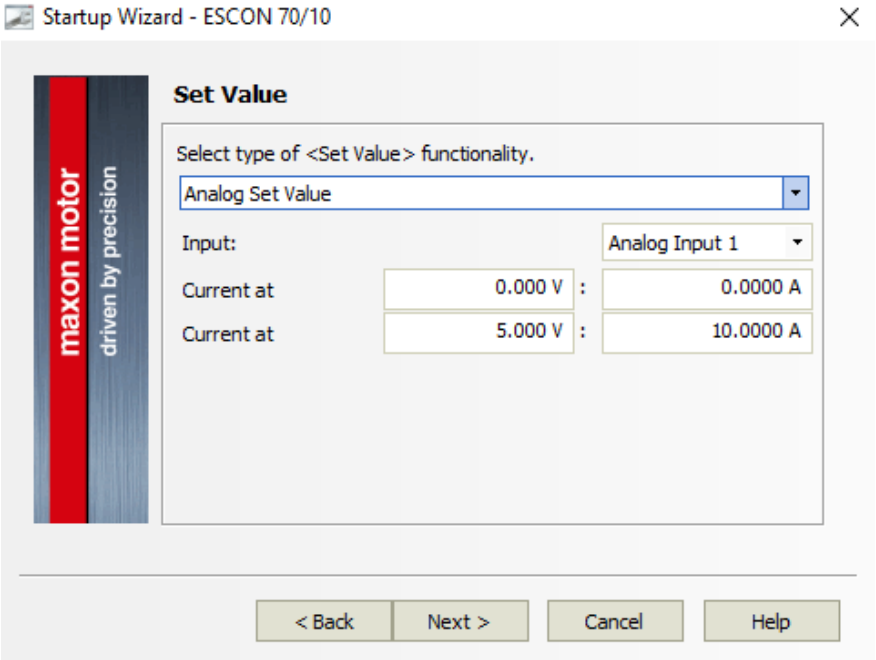

Figure 4.10: Set value example for current controlled motor

It was said in the previous chapter that the analog pins (J6) allow the servo controller to modulate the input given to the motor.
The servo is able to read the voltage input in the appropriate pin of the cluster. Depending of what acquires, Escon driver provides a certain input to the motor according to the operation mode chosen.
At this point, both the lowest and highest value of voltage are detailed to make the software build a supply scale, with the related values of current/velocity that's supposed to provide to the motor.

9. Offset: it could be useful to set a proper offset, depending on what is needed for the test. There was no need to use this feature.

10. Digital inputs and outputs: sometimes more than one single digital value is required. In this window was possible to set if it's needed to connect more digital devices or ask for more data acquisition.
In the described situation, only "digital input 1: enable" was decided on step 7.

11. Analog inputs: as the previous point, it could be useful to use more than one potentiometer, or maybe other different analog devices. Here is possible to add more of these elements, but only for input data.
For the purpose, only "analog input1 : set value" was previously settled on step 8.

12. Analog outputs: it was very important to set what kind of analog output the Escon driver must return.

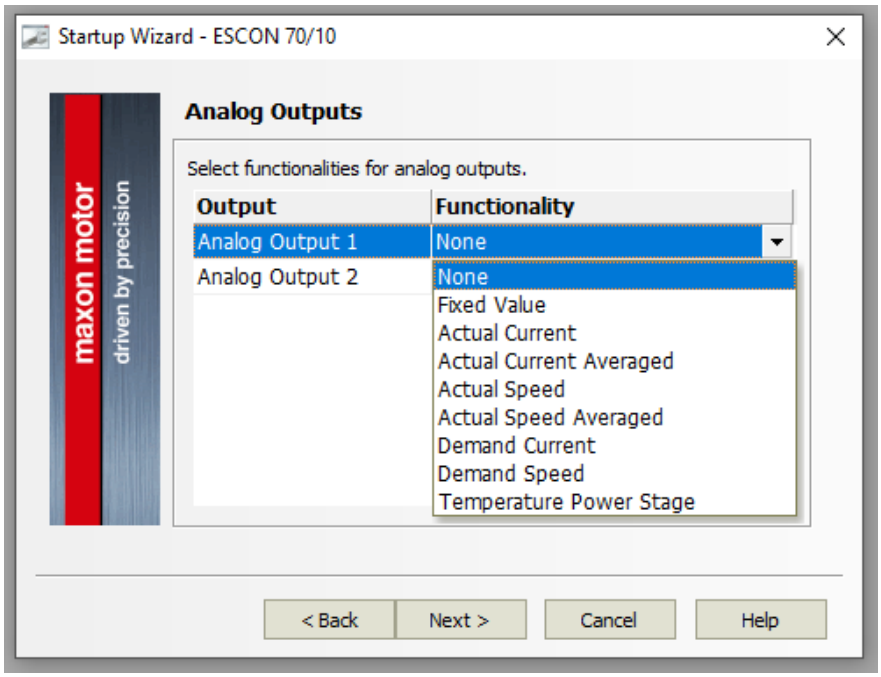

Figure 4.11: Analog output parameters

By choosing one of the previous options, it was possible to set a specific pin, enabling to communicate with another device. This meant that the software was able to give information about the motor controlling to other tools. This feature allowed to program a sophisticated feedback-based controlling of the motor, and will be exploited as described in chapter 5.

4.4 First support

The motor had to be steady in its position during all the working time, allowing only the shaft to rotate. If its housing wasn't kept fixed while applying the torque, it could be the motor itself to get closer to the insertion point instead obtaining the wanted extension cause of the difference between their weight. As shown in picture 4.3 the DC was cylindrical-shaped and the upper base, the one with the shaft, shows several threaded holes and a minor cylinder (further information on annex 2). These three features were useful to fix the case and a proper support was designed to achieve the wanted blockage.
It's important to underline that this element was made by 3D printed PLA, which means no manufacturing process will be performed on metal and the prototype could be planned taking care of 3D printing considerations like avoiding threaded holes and guarantee a continuity for layers.

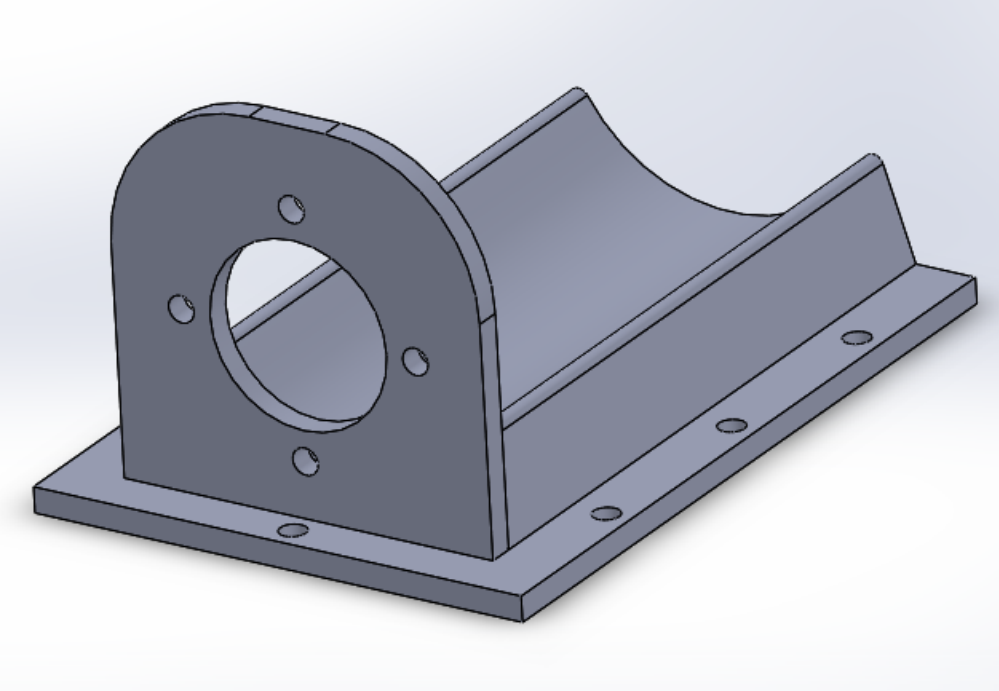

Figure 4.12: Motor support

The picture allows to better visualize how the support was conceived:

- The vertical surface has a central hole and four smaller ones.
  The motor small cylinder was supposed to pass through the bigger hole and slide until its upper surface touch the support. Once the shift ends, the four holes permitted the motor to be screwed to the support, fixing its position without altering the wanted shaft rotation.

- The cylindrical shape of the case leant against the horizontal backing, that was shaped as emi-circumference with a diameter shortly bigger than the motor's. That's because the purpose of this part was only to bear the weight of the motor, that was two kilos, making all the system steady. The housing was also designed to be longer than the case in order to prevent any kind of damage that could occur during the set-up phase, where the motor can got hit for accident .

- The lower base had not-threaded holes, with the same pattern of used in the rotating disk. This way, both the motor and its support move together with the frame, avoiding any issues about their relative position.
  This structure was good enough for the purpose but showed several features that could be optimized. After the motor's temperature behavior study in chapter 6, a new improved support will be produced to increase heat dissipation.

4.5 Shaft's cap

When the DC motor receives supply, it started to make the shaft rotating, as described in chapter 4.1. The matter was that, in order to produce quadriceps contraction, the motor should act as a linear actuator.
Actuators are a different kind of motor that provides a linear sliding of its shaft instead of a rotation.

Figure 4.13: Electric linear actuator (RS pro brochure)

Once the current starts flowing in this electronic device, the shaft starts to run forward or backward, applying the wanted displacement or pulling a wire properly attached to the element.
In order to obtain this kind of movement, it was necessary to add a cap to the motor shaft and convert the rotation to a linear actuation.
Also for this case, the piece was made by 3D printing.

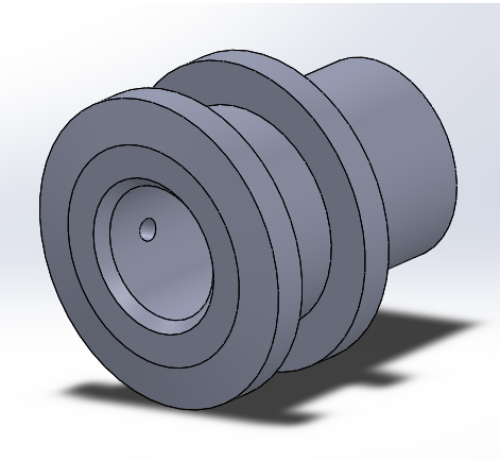

Figure 4.14: First cap

The first sketch was simple but functional: the shaft entered in the cap loop and fixed by an external hydraulic clamp. A wire, attached to the tibia, passes through two holes and

get blocked with a proper node to made its end thicker than the very hole. The top surface of the shaft had to be fixed before the through-all hole to let the wire cross the structure. The most important part of the cap was the external diameter of the surface where are placed the holes, because it is directly related to the force applied by the motor.
It is discussed in 4.1 that

$$M = I * k_m \tag{4.1 bis}$$

the force applied by using the cap could be evaluated according the moment of a force equation:

$$F = M/r \tag{4.2}$$

where:

- F is the pulling force;
- M is the torque applied by the motor by rotating;
- r is the radius of the shaft;

By simply substitution:

$$F = (I * k_m)/r \tag{4.3}$$

The more the radius is, the more current is required to obtain the same force.
First it was important to focus on the thickness of the cylindrical surface to avoid the cap breaking. The PLA is a polymeric material which owns mechanical properties lower than aluminium or steel, and it was important to keep this in mind while printing a 3D piece. Furthermore, 3D printing makes the piece not homogeneous and it was difficult to evaluate the mechanical properties of a 3D-made element. It was decided to use a trial-and-error approach, in safe conditions such as a dead-weight calibration (described in chapter 6). After the test, it was possible to reduce cap's diameter to enhance the forces obtained, allowing to reach higher torques with the same amount of current. The design was then improved until a good result was obtained:

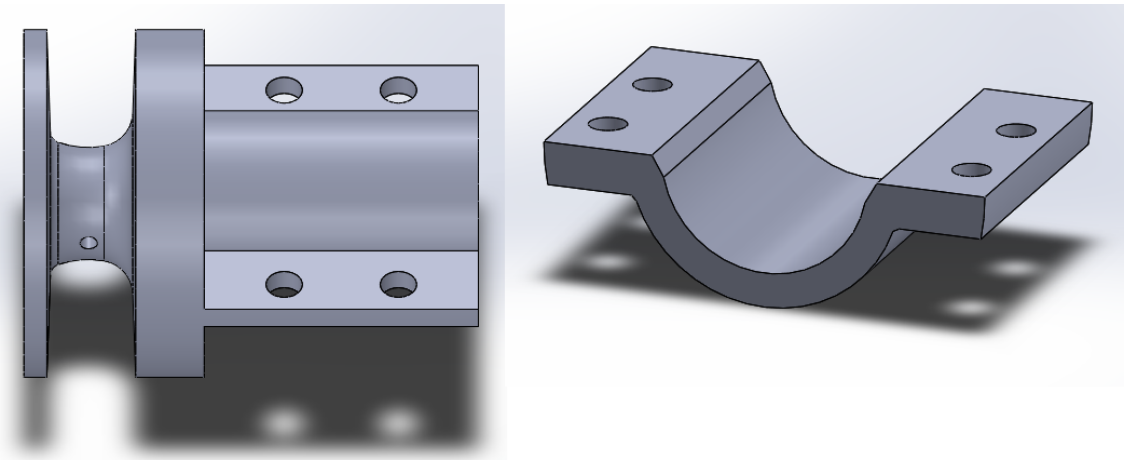

Figure 4.15: Final cap: respectively cap element and fixing element

This solution has two bigger changes:

1. The structure was now composed by two separate pieces;
   The shaft enters a specific-made housing inside the cap elements, obtaining a first steadiness by friction. The groove didn't reach the distal region where there is the hole, so this part was basically full of PLA now and so its mechanical resistance is increased related to the first cap. Once the cap element was placed, the fixing element was added as negative of the missing part, locking the position thanks to four nuts and bolts. A thin film of sponge was placed around the shaft to increase friction and distribute equally the compression force between cap and shaft surfaces.

2. The radius where the wire wraps was lowered than before.
   The diameter was reduced from $20mm$ to $10mm$, that meant that the current required to get a certain torque was halved. The thickness was enough to guarantee the cap safety. Further information about the relation between current and force obtained are detailed in chapter 6.
   Once the cap was fixed and steady, the motor was able to achieve the linear actuation as the quadriceps does in natural leg extension.

4.6 Baseplate

There are several element that compose the first prototype of the motor-controlling system:

- The motor with its PLA support;
- The servo-driver;
- A switch;
- A potentiometer;
- Electrical wires;

- A power supply;
- An electronic platform (ArduinoUno).

All this elements made the whole system hard to move and dispersive.
To guarantee a tidy system, a baseplate was designed as following.

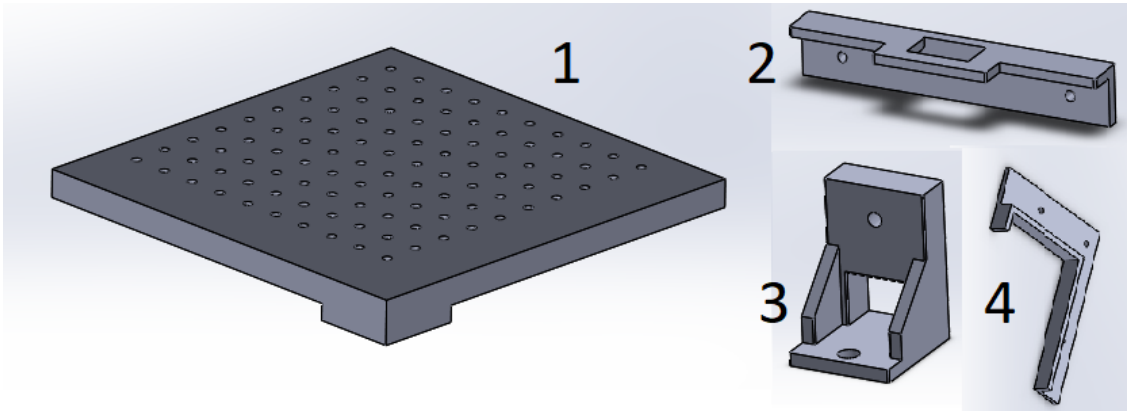

Figure 4.16: plate individual elements, in order: the square, the bench, the seat and the bracket.

The purpose was always to get a modular solution to be arranged according the situations:

1. A square panel, with a pattern of pierces studied to be the most general possible and to allow other pieces to be fixed where they are needed. Four plates were thought to compose the final structure;
2. A bench, that had to hold the switch and keep it steady;
3. The seats, where the bench was attached. These were not directly related to the bench and in the future, it will be possible to design a different bench (for example, to hold a display) and using them as well. Furthermore, there's a passage that allowed wires easily pass through;
4. The brackets, that could be used to protect bigger elements from sliding. They were thought to keep still a breadboard, that was used to improve the control of the rotation.
   All of them were printed in PLA because they weren't supposed to bear any kind of forces. The result was a light modular baseplate that could be assembled previously and brought later at the laboratory. The four-square bases formed a tidy assembly, where the elements were placed opportunely and could eventually be moved if required.

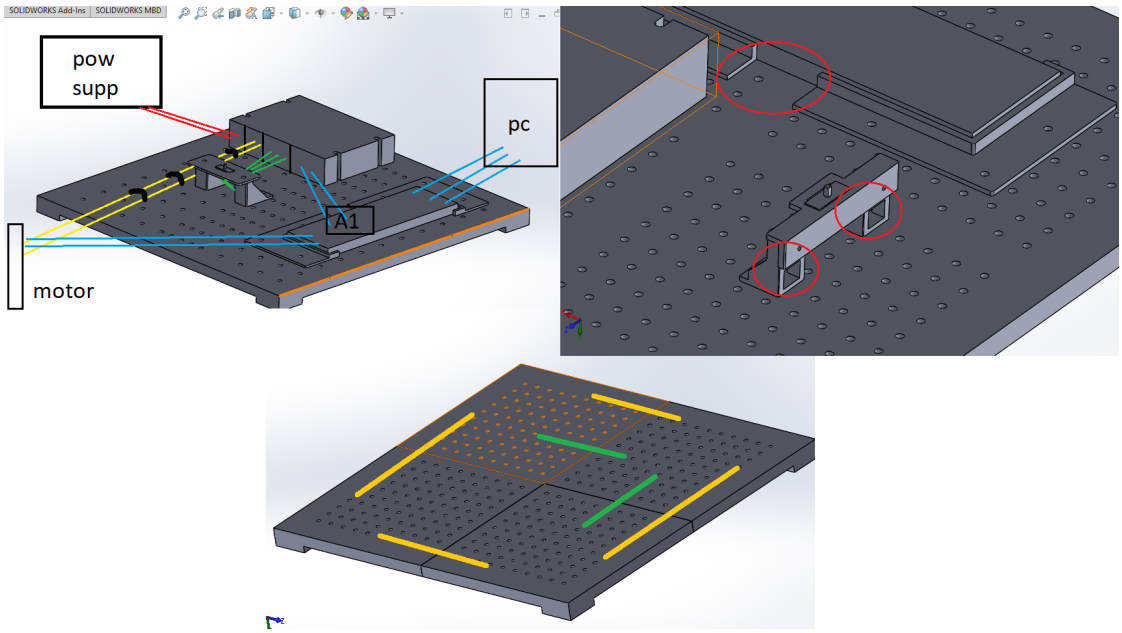

Figure 4.17: Assembled modular baseplate

It can be seen how the first prototype was arranged, with all cables properly connected. ArduinoUno was an additional hardware exploited to control the motor rotation, and will be discussed in chapter 5. The breadboard was steady but easy to remove if necessary, thanks to a little distance between the two brackets.
Finally, the four plates had to be fixed together by small metal joints (yellow lines), and the attached elements were exploited to keep the squares too (green lines).

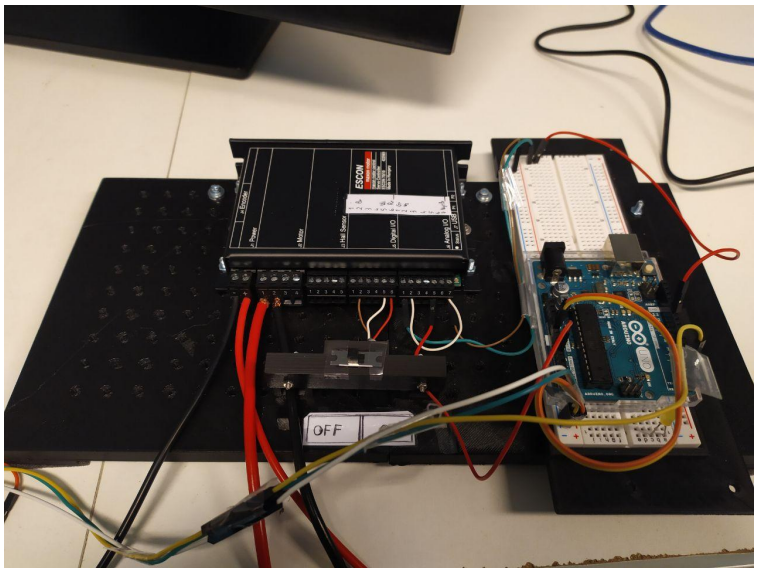

Figure 4.18: Final baseplate

At the end, it was decided to use only two of the original four plates. That was because there wasn't an excessive number of elements to be attached on, so a little cleanness was

lost to reduce printed material and encumbrance. If other elements will be required, for instance an LCD monitor, it can be added just by printing other plates.

5 Motor controlling

5.1 Purposes

The purpose of the thesis requires to perform a controlled extension of the knee. The movement had to be the closest possible to the physiological one by using a proper system to modulate the input while monitoring data.
In particular, there were two main features that would be interesting to acquire: the applied force in function of the position, and the position reached in function of the force applied. Both of tests could be filmed with the optical system in order to obtain more detailed data.

5.1.1 Constant speed

A first task required to perform a constant speed extension by imposing the motor velocity. In the meanwhile, it was necessary to constantly acquire the current supplied to the motor to evaluate the quadriceps activity.
The movement had to be as slow as possible to neglect the inertia of the tibia. Furthermore, this allows the reduction of the visco-elasticity effect of tendons in cadaver tests, that depends on the velocity of the performed task.

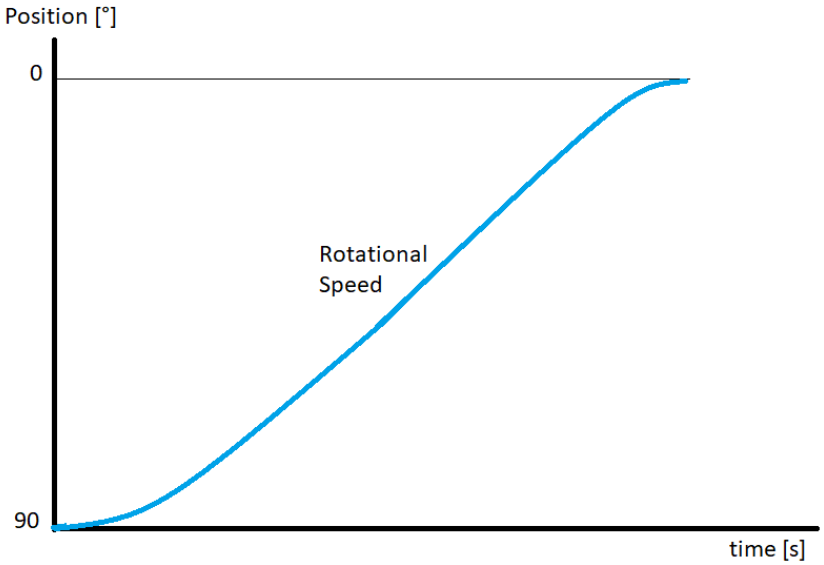

Figure 5.1: Angular position. It can be considered as linear function of the time, where the slope is the speed rotation

Once the system was properly calibrated, it was possible to acquire the force values by simply monitoring the current provided to the motor. The calibration phase is described in chapter 6.

5.1.2 Step force

The second task chosen was to perform the movement following a ramp of current.

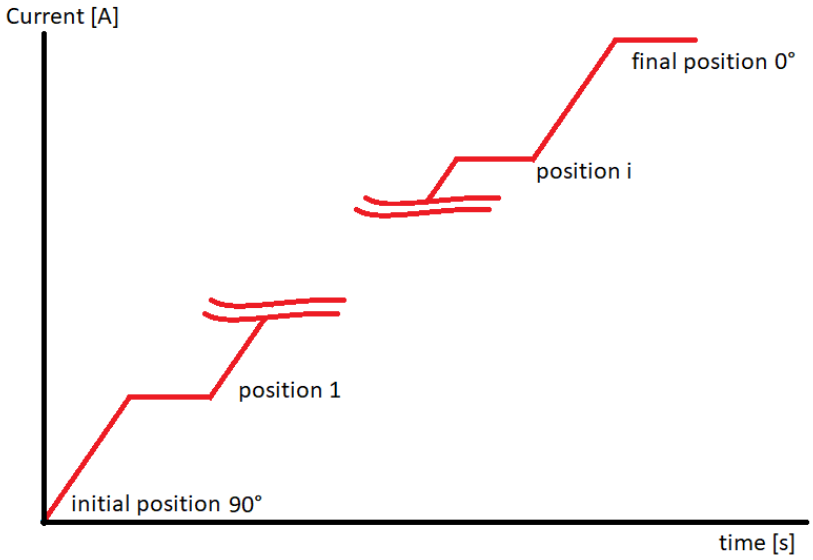

Figure 5.2: Current pattern

The idea was to apply a certain force to the tibia, waiting until the motion stops, then increase the force and wait again for the leg to stop. These steps were repeated until the full extension was reached. The important data to be collected were the supply provided and the angular position of the tibia, achievable by reading the encoder pulse counter.
In the meanwhile, optical system allows to record the complete ride and to obtain a comparison of the acquired data.
The current wasn't supposed to follow a pattern that is the same for all the tests: because the servo was supposed to wait for the leg to stop before increasing the supplies, it was necessary to develop a system able to observe the leg and acting according the requirements. It was pointless using the same pattern of activation to acquire position data because it strongly depends on investigated specimen. The result doesn't depend only from the weight of the tibia, but involves patella features, tissue laxity, insertion point of the quadriceps, friction between surfaces and so on.
The function must change its behaviour by its own and not depending on pre-planning parameters, that are also hard to estimate in some cases (like for the characterization of soft tissues). It was chosen to lead the function with a feedback system.

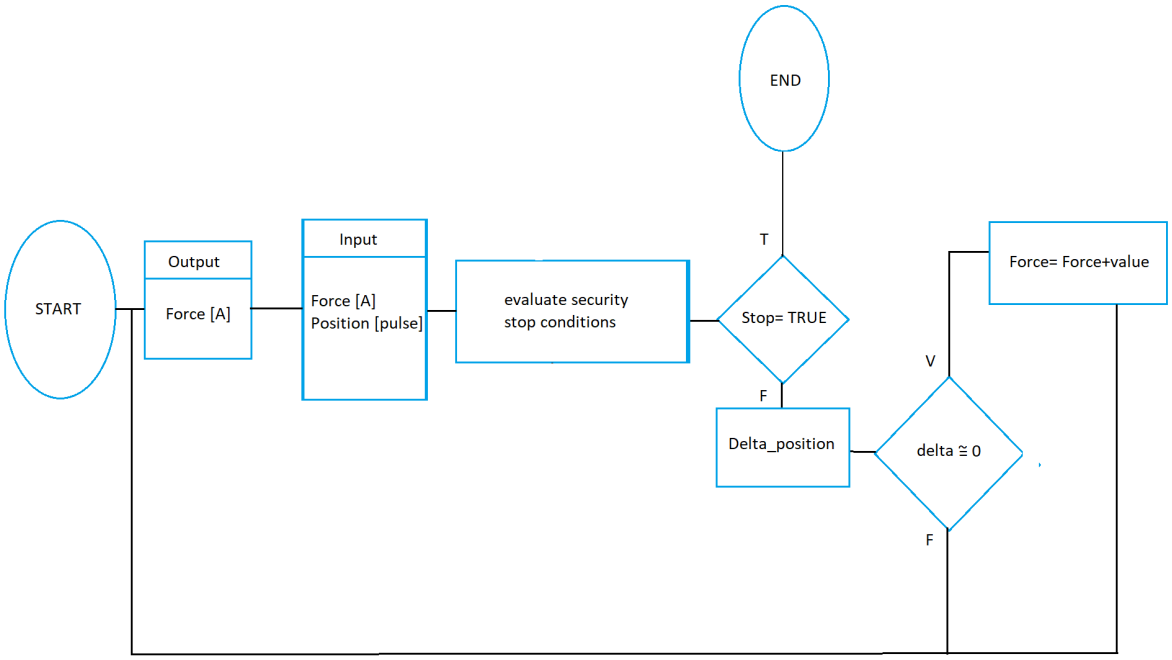

Figure 5.3: Flow-chart of the controlling system

To obtain this kind of current controlling, it was sketched the logic pattern shown in picture 5.3. It could be resumed in the following macro-steps:

1. An initial force was applied with a certain current as output. This force had to be enough to perform a little displacement at least, but in general a small amount of current was already sufficient;

2. The system acquires data about the test while it was running. In particular, it had to read the actual current applied and the number of pulse of the encoder;

3. Before continuing, it was necessary to check for stop conditions such as position and temperature. Once one of these parameters exceeded a certain threshold, the test had to be ended. Further information will follow in chapter 6;

4. Then, a delta position was calculated as difference between the previous and the current position;

5. The system checked if the position hasn't been changed for a while. If the motor was still moving, then it's $FALSE$, and the system restart from the initial block, supplying the same current as before and always monitoring the actual current and position.
   If the motor had stopped its rotation, then it was TRUE, and the system increased the torque. In that way, when the process restarted, a higher force was applied and the tibia continued its movement until the next steady phase, when the applied force balances the torque caused by the gravity force, reaching the mechanical equilibrium.

This logic pattern allowed the wanted step function, and it was possible to acquire position reached related to the current given.
This is a feedback controlling system, that decided how to act depending on the actual situation of the test and not on boundary conditions.

5.2 Escon Studio limitation

The software provided by Maxon company for the controlling of the motor allowed to perform the rotation and, in the meanwhile, collect data such as actual current, speed rotation and so on, like explained in the previous chapter.
It was possible to impose a constant velocity for the shaft rotation, perform the test and save data simply by asking for this information during the start-up wizard phase.
However, the software showed a huge limitation: it couldn't acts depending on acquired data. It wasn't able to read the collected data in real time, that were only displayed by a monitor and could eventually be saved at the end of the test. For this reason, it wasn't possible to apply the logic pattern showed in picture 5.3 to control the current.
Furthermore, Escon studio wasn't even able to follow a specific function for the supply. It could only work by a single step of current based on the input received by the analog cluster.
The only way to achieve the wanted current controlling was to follow this pattern:

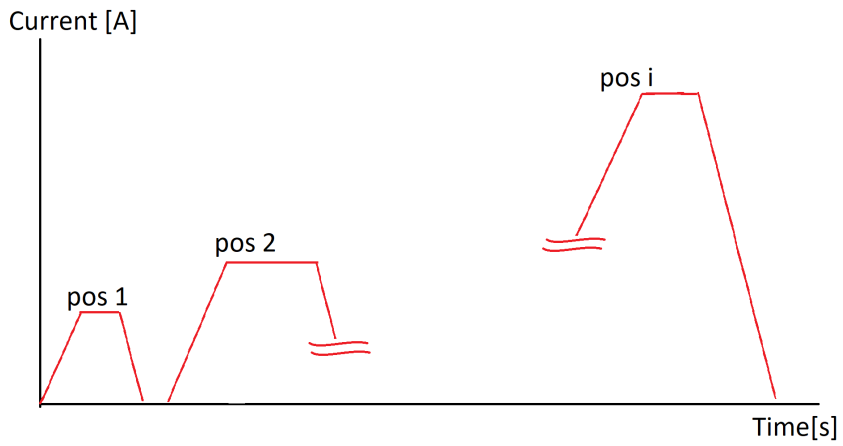

Figure 5.4: Current pattern achievable by using Escon studio

A certain current was chosen and supplied till the mechanic equilibrium was reached, then the current was stopped. A new current was analogically set, the test performed and so on until the final position was reached.
There are countless of issues with this method, that required numerous arrangements before the test, such as controlling manually the supplied current by potentiometer. Furthermore, it took long time to perform the same test and collected data would be very dispersive.
A new solution was mandatory, and it was achieved by using an additional microcontroller.

5.2.1 Arduino

A way to achieve a good control of analog parameters is to use a second hardware that enable the acquisition of external data, process them and produces real-time output. Thanks to its availability and simplicity, it was chosen an Arduino microcontroller.

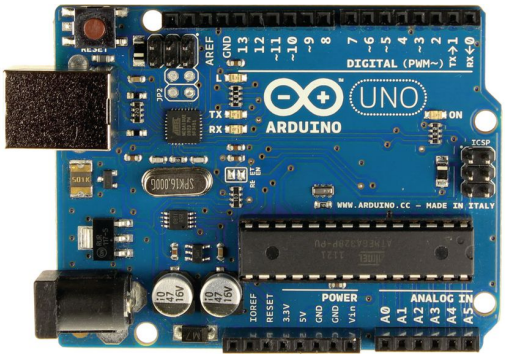

Figure 5.5: Arduino uno microcontroller

This solution was easy to implement thanks to its immediacy, and very cheap compared to other controllers.
As can be seen in the picture 5.5, Arduino can be connected to several devices thanks to its various pins, which can provide and acquire a small amount of current [17].

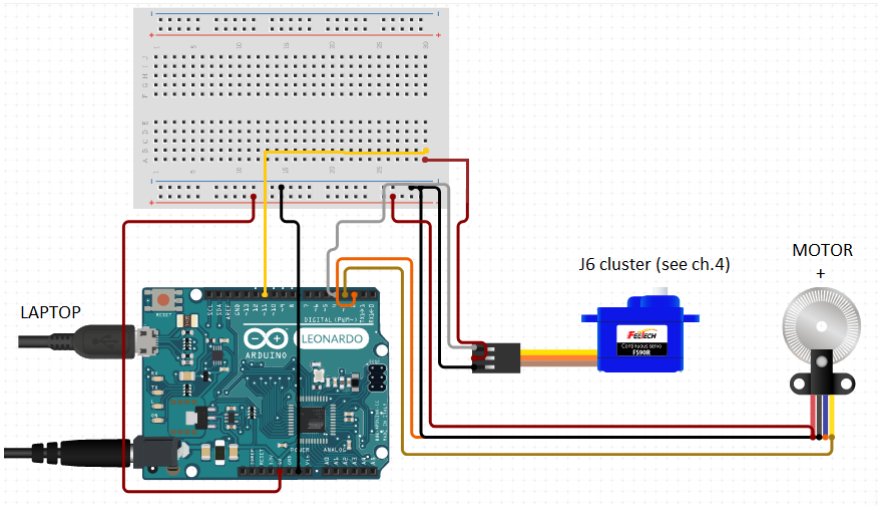

Figure 5.6: Arduino circuit

The picture shows the final configuration of the Arduino circuit. The microcontroller is not linked to the motor because the current is given by the power supplier, and Arduino only modulates analogue signal received by the servo. Meanwhile, the servo is linked to the switch, as described in chapter 4, and the encoder is attached to the RE65.

A proper text editor with its programming language had to be learned. Here it was possible to communicate with Arduino, creating the script (so-called sketch) to be run

during the tests. Thanks to its features, it was possible to follow the logic pattern previously described. Further information in annex 2, where it's available the final script used for the feedback control.
Also, the software provides a serial monitor to follow in real time the process while it's still working [18].

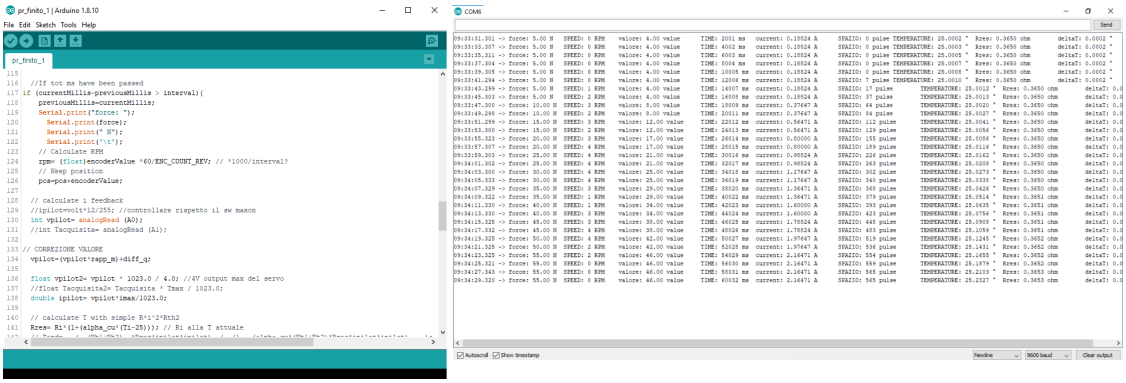

Figure 5.7: Example of Arduino sketch layout with the serial monitor

5.3 Stop condition

As previously said, it was necessary to stop the test when specific situation was reached to guarantee system safety. All the stop conditions were decided leaving a certain security interval. When the threshold is surpassed, the leg is escorted to its initial position.

5.3.1 Position

The first obvious parameter that needed attention was the position reached by the leg.
This data was also an information acquired for analysis purpose, so it just required to set a limit value and imposing it as end of the ride.
The number of pulse chosen as limit defined the final angular position that the tibia had to reach before the test ends and was estimated as follow.

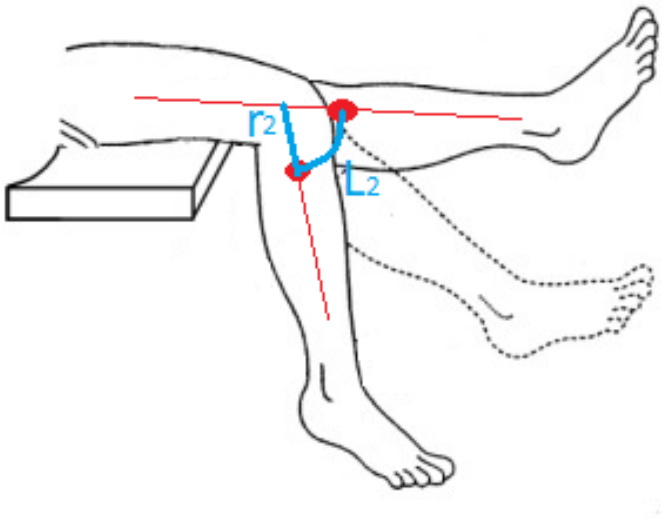

Figure 5.8: Insertion point and its pattern (myptcorner.com)

It was assumed that the knee behaved as a simple hinge joint, that is an acceptable approximation for this test.

$$L_2 = \frac{\pi r_2}{2} \tag{5.1}$$

$$L_1 = 2\pi r_1 \tag{5.2}$$

Where

- r_2 is an estimated distance between the center of rotation of the knee and the insertion point of the patellar tendon, that is about $70mm$;
- L_2 is the length crossed by the insertion point performing the complete movement;
- r_1 and L_1 are the radius and the circumference of the cap placed on the top of the shaft.

Since $L_2 = 110mm$ and $L_1 = 31.5mm$, the shaft performs 3.5 revolutions, that means about 1700 pulse of the encoder.
Thus, once the total counter reaches 1700 pulse, the rotation ends and the return phase begins.

5.3.2 Temperature

It was essential to monitor the temperature of the motor in order to avoid its overheating. As described in its data sheet, there was a critical temperature that, when reached, makes the motor unable to work again. It was necessary to not reach the limit value of $125°C$ detailed in the data sheet of the RE65. Talking about temperature, the motor can be thought in two main elements: the stator and the winding, that own two different thermal behaviour.

- the thermal constant of the winding, τ_w, is 123s;
- the thermal constant of the stator, τ_s, is 1060s;

It was the winding temperature that mostly deserved more attention because it overheats faster than the stator.
The winding is placed inside the case of the motor, so it was impossible to directly measure that parameter analogically. A function to estimate the actual temperature of the winding was found and it's widely discussed in the chapter 6. When the temperature reaches the chosen threshold, decided as $110°C$, the extension stops, and the leg returns to its initial position.

6 Motor calibration

Every measuring device requires a fine calibration phase before to acquire any value, in order to verify the reliability of the provided readings.
As discussed before, the motor works according to current provided and this is related to the applied forces. It's necessary to find out the relation between supplies and the actual forces generated by its activation.

6.1 Current and Force

6.1.1 Analog input

The force generated by shaft rotation depends on the radius of the cap design and the current supplied by the servo controller (4.2). The point was how to communicate with the servo-driver in order to control the supply step by step.
It was noticed that ArduinoUno is able to produce an analog output up to $5V$ from its pins. This fact was exploited to communicate with the Escon 70/10 by linking Arduino to analog input of the servo. This cluster was previously used with a potentiometer in order to modulate its output current.

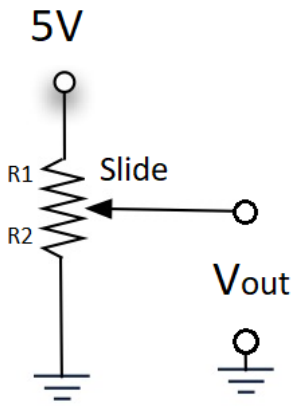

Figure 6.1: Schematic potentiometer

The potentiometer acts as voltage partitioner.

$$V_{out} = V_i \frac{R_2}{R_1 + R_2} \tag{6.1}$$

The servo provided $v_I = 5V$ to the potentiometer. If the slide was totally closed $R_2 = 0$ and the V_{out} resulted null. In the other hand, a fully opened slide meant $R_2 = R_1 + R_2$, the fraction was unitary so $V_{out} = 5V$. Once understood which was the output pin of the potentiometer, it was thought to connect the relative servo input port directly to the output pin from Arduino. The link to the ground was preserved. That idea proved successful: the message brought by the potentiometer was replaced by the Arduino voltage output and the servo was able to interpret the reading as well, producing the wanted supply to the motor. It was required to use a mapped function to convert a force request into a codified code for the voltage output. The Arduino function "map" allowed to properly transpose the wanted force magnitude to a different range, interpreted by the microprocessor to generate the wanted voltage output.

$$volt = map(force, 0, 300, 0, 255)$$

This way the wanted force is converted into a magnitude scale recognized by Arduino, which codify the voltage output according to that value. In this case, if the wanted force is $300N$, Arduino converts that value in 255, that is the max value reachable with map function and codify for $5V$ output from the designed output pin. Once the output pin was connected into the input analog pin of the servo, it was possible to modulate the current by script, following the flow chart described in chapter 5.
Last word must be spent about the talk between the two devices: it was said that Arduino provides a certain tension between $0V$ and $5V$ to the analog input of the servo-controller. It's now that picture 4.10 became absolutely important to keep in mind.

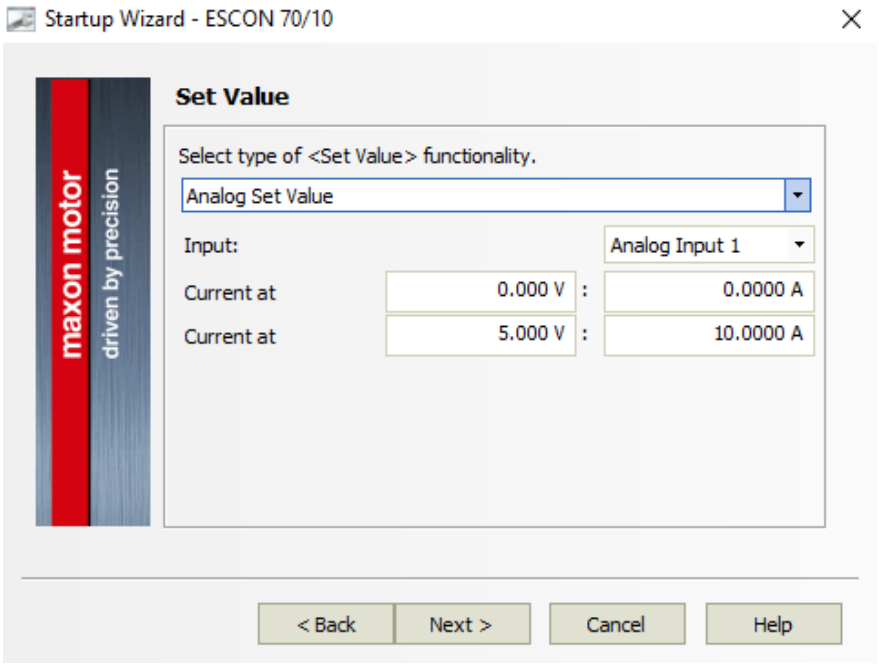

Figure 4.10: Set value example for current controlled motor

Here it was defined the relationship between the voltage read by the servo and the current that it must provide to the motor.
The picture, shown again to better follow the reasoning, indicate that Escon 70/10 will provide a supply of $10A$ to the motor when receives an input voltage of $5V$. According to the boundary condition, specimen investigated and task to be evaluated, the torque applied can be modified by properly adjusting this very dialogue box. According to the specimen, and thanks to the optimization of the shaft's cap, it was possible to set the current output from $0A$ to $5A$, increasing the sensitivity of the supplies.
Finally, it was possible to supply the DC motor with the wanted current, that meant apply the wanted force for the leg extension.

6.1.2 Dead weight calibration

The current makes the motor rotate, applying a certain torque, that was converted in a force thanks to its cap.
It was necessary to check if the actual force exerted was equal to the theoretically estimated (4.1). To acquire data, it was settled a workbench to perform a dead weight calibration.

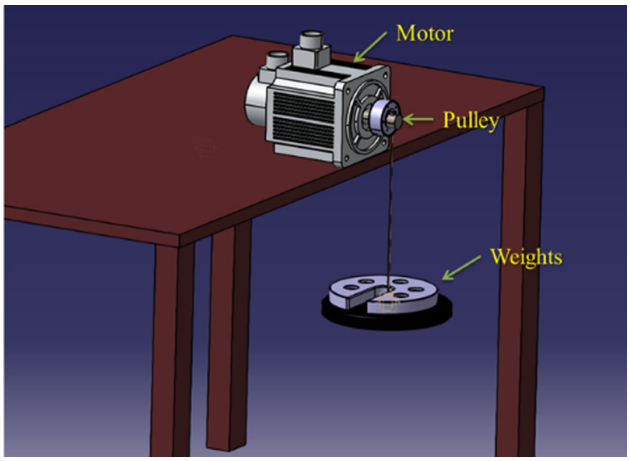

Figure 6.2: Workbench settled for calibration (instrumentationtools.com)

The motor was asked to lift a weight following the Arduino sketch. Due to low currents provided the first phase, it wasn't initially able to pull up the object. The supply increased until the motor could afford to lift the weight, the acquisition stopped and the value of current that comes right before the lift phase was stored from the Escon studio data recording. The process was repeated five times for each weight.
It was interesting to understand if it was possible to discriminate weights differences of $0.5kg$, so were used respectively 1, 1.5, 2, 2.5 and 3 kg.

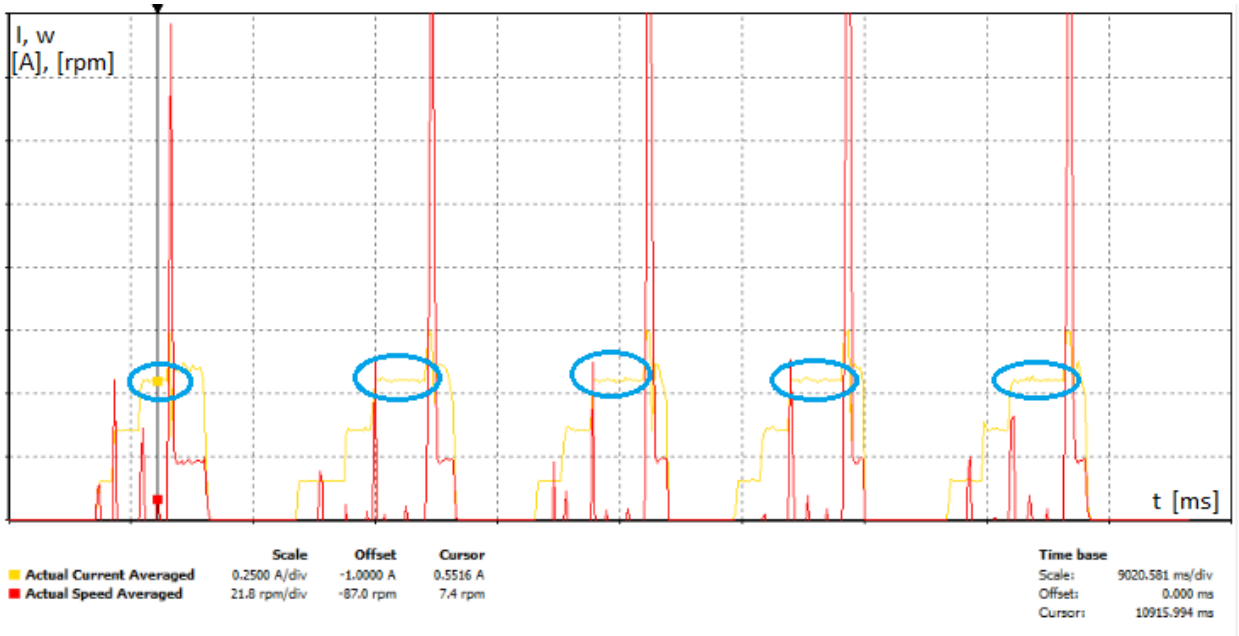

Figure 6.3: Data acquired lifting 1 kilo

The picture 6.3 shows the five test performed during the calibration of the motor for $1kg$. The blue circles identify the region of interest, and highlighted data were averaged in 5 main values that characterizes each try. Data were taken from an Excel table provided by Escon studio at the end of the test, which is available in annex 3.

Evaluation of data reliability

F_th [kgf]	I_th[A]	I_av [A]	Error %
0	0	0.15	
1	0.6380488	0.55	16.00887
1.5	0.9570732	0.95	0.744544
2	1.2760976	1.26	1.277584
2.5	1.595122	1.5	6.341463
3	1.9141463	1.88	1.816295

Figure 6.4: Theoretical and averaged currents

A check on the relative error was enough to verify that the actual supplied current was close enough to the theoretically expected, that meant that a specific weight was going to lift once the ideal current was furnished to the motor.
However, the calibration test was different from the wanted task because there aren't any torques involved during the lift. While the leg is extending, the weight of the tibia generates a torque to the joint that must be considered during the scale phase. The most important information acquired by the calibration, other than provide a general and standardized table to relate current and force, was the repeatability of force measurements.

The fact that emerged in these test was that, in order to make the motor to rotate freely, it was necessary to feed it with $0.15A$. Further investigation revealed a behaviour owned by the motor that it's essential to highlight by making a practical example to better visualize the matter:

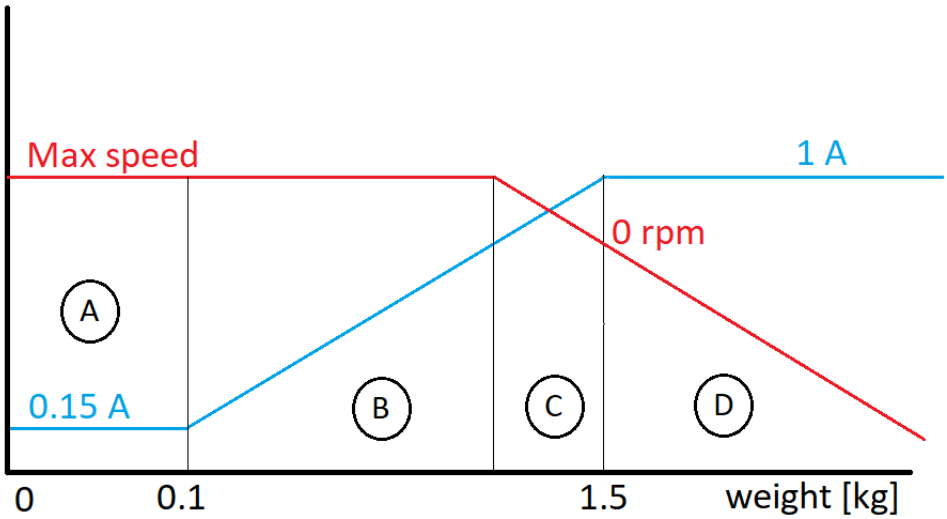

Figure 6.5: Motor behaviour

Imposing a supply of $1A$ for easiness and knowing that the motor is going to lift up to $1.5kg$ applying about $15N$, as shown in picture 6.4.

1. initially the motor is free to rotate, and the current required for this task is $0.15A$;

2. by rising the weight, the current increases in order to continue the rotation while lifting the weight, until supply gets closer to $1A$;

3. from this point, the current used for the rotation will be used instead to lift the weight. The speed rotation starts to decrease cause of the missing of supplies. When the load reaches $1.5kg$, the rotation stops and the current cannot increase anymore as it reached the max value imposed.

4. if the load is still increased, the rotation starts going backward and the more weight is applied, the higher will be the absolute value of the speed while spinning in the opposite direction.

However, it's about $0.15A$ that are used for maintaining the motor to spin for that kind of speeds, that **are fully employed for the balancing of the forces when the mechanical equilibrium is reached**, that is the region of interest for this study.
In the future, it can be implemented a linear function to evaluate the current used to spin and subtract it when the speed is higher than zero, but it won't be necessary because acquisition shows a variability of $0.2A$ during tests performed in the actual situation of leg extension. That is because it isn't a constant lifting, and the current required suffers the inertia of the motion which is ineffective during the calibration.
Comparison between theoretical and measured values

test	1	2	3	4	5
I_average	0.5561	0.5553	0.5586	0.5577	0.5513

average	stdev	stat.disp
0.5558	0.00283	0.00509

Figure 6.6: Main data collected for $1kg$

In picture 6.6 are displayed most important data:

- The averaged currents for each repetition;
- The average of the five currents;
- The standard deviation of the five currents was obtained as

$$\sigma = \sqrt{\frac{\sum_{i=1}^{N} |x - x_{av}|^2}{N}} \tag{6.2}$$

and it is a measure of the amount of dispersion of a set of values. A low standard deviation indicates that the values tend to be close to the expected value of the set, while a high standard deviation means that the acquisitions are spread out over a wider range.

- The relative standard deviation, obtained as

$$\sigma_r = \frac{\sigma}{\mu} \tag{6.3}$$

allows to evaluate the dispersion of a set values. Being related to its mean, it is a dimensionless number that is close to zero. It must be said that these values were collected using an $8mm$ radius cap that is going to be reduced to optimize the torque, but the acquisition is consistent as well. Clearly acquired values were different, and they are available in annex 3.

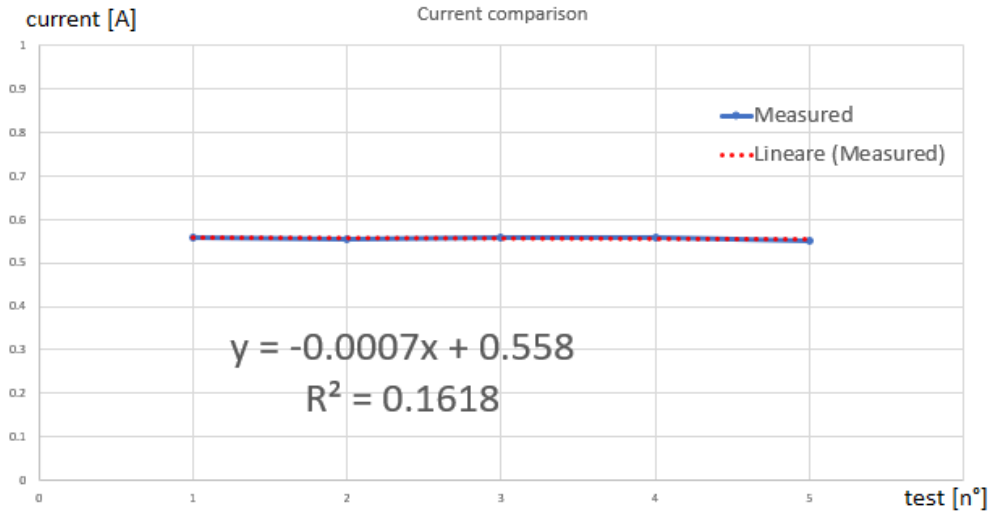

Figure 6.7: Measured current tendency

On the x axis there are the five tests, performed for the same weight, while on the y axis there's the current in Ampere. The blue line identifies the five averaged currents, and the red dots are the linear regression. The graph allows a better view of the accuracy of the calibration, proving the system had good consistence and repeatability, where the linear function is absolutely superimposable to the acquisitions. The parameter called R^2 is the *coefficient of determination*, that is a statistical parameter used to predict the future outcomes basing on acquired information and, being close to zero, means that the current acquired is not related to the try.

6.1.3 Feedback current calibration

As described before, the system worked by referring to feedback data. It was necessary to check if the current read by the micro controller was the real supplied to the motor.
By testing some different values, it appeared that there was an offset between read current and supplied that wasn't absolutely negligible.

A	* read	*supplied
1	78	103
2	160	205
3	242	307
4	324	410
5	405	512
6	489	614
7	571	717
8	655	819
9	736	921
10	817	1023
11	898	1126

* codified value

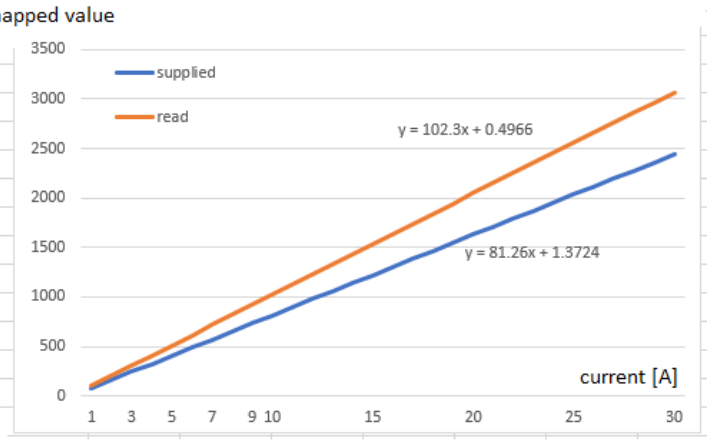

Figure 6.8: Data acquired and plot of the two trends

The columns "read" and "supplied" reports the values mapped by Arduino function, where the maximum output for $10V$ was 1024 because of it is described by an array of 10 bits (2^10). It could be noticed that the two line follows the same trends but the slope is quite different, causing high errors for big currents. However, the reading could be corrected by implementing a linear function

$$y = mx + q$$

where

- m is the slope, as the ratio of the two trend
- q is the intercept, as the difference between the two

The new equation

$$y = 1.26x - 0.87 \tag{6.4}$$

allowed to fix the problem (further info on annex 3).

A	read	supplied
1	103	100
2	205	203
3	307	306
4	410	409
5	512	511
6	614	617
7	717	720
8	819	826
9	921	928
10	1023	1030
11	1126	1132

Figure 6.9: Fixed acquired data

The good estimation of the effective current provided to the motor is also mandatory to obtain a reliable evaluation of internal winding temperature, in order to calculate the parameter with the actual current instead of the theoretical.

6.1.4 Mechanical scheme

As previously anticipated, the leg extension is actually a totally different matter and it's necessary to point out two main differences about the load and the muscle force. Of course, the weight of the leg doesn't change during a test, but what variate is the couple applied to the knee.
As always, it was assumed the joint as a hinge for easiness.

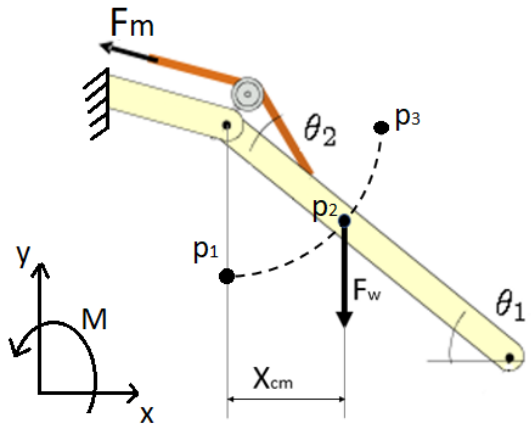

Figure 6.10: Free body diagram

The moment generated by the F_w related to the knee is

$$\tau_w = F_w X_c m \tag{6.5}$$

where F_w is the weight of the portion of the leg to be lifted, applied on its center of mass, while X_{cm} is the distance between the weight and the knee along the x axis .
The value of X_{cm} depends on the angle θ_1, in particular:

- X_{cm} is null for $\theta_1 = 90°$ (p_1);
- X_{cm} increases for θ_1 decreasing (p_2);
- X_{cm} is max for $\theta_1 = 0°$ (p_3);

Thus, the torque is not constant during the movement, and it's equal to zero for the relaxed leg up to its maximum for the complete extension position.
The reason why it was decided to perform a current step function was to analyze the position reached by the leg depending on the applied torque, that should be increased while the extension proceeds due to the resistance increase.

Free body diagram

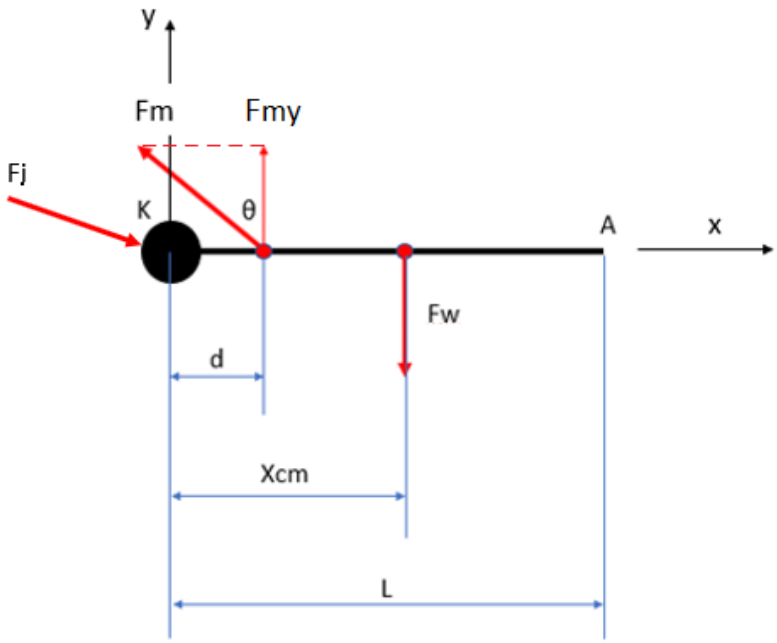

Figure 6.11: Analysis of the worst case possible, equilibrium reached in full extension

The theoretical quadriceps force required to keep the maximum extension was evaluated by hand and compared to the $300N$ from the literature [19].

Boundary conditions

- Weight of the patient $80kg \cong 800N$;
- Pull angle $\theta = 60°$;
- L total length of the tibia and d distance of insertion point from the hinge joint $= 50mm$. Notice that $50mm$ is worst case related the usual $70mm$, in order to keep a good safety interval;
- knee joint as hinge, blocking translation along x and y axis.
- F_j internal force of the knee. It doesn't affect the equilibrium because the joint cannot shift and the relative lever arm is null.

- Usually the tibia is cut, so the foot's weight would be negligible. However, in order to provide the most general solution, its weight was considered for the calculation of F_w.
- The length of the tibia was assumed as not cut, to study the worst case. The length of the foot wasn't considered for the position of the center of mass.

Anatomical references
X_{cm} was estimated from anatomical table references as positioned at 42% of the tibia, related to the proximal edge of the rigid body. $0.42 * 400mm = 180mm$. W_{shank} was evaluated as 4.6% of the total body weight
W_{foot} was evaluated as 1.4% of the total body weight
$F_w = (0.046 * 800)_s + (0.014 * 800)_f = 48N$
[20]

Static rotation equilibrium, related to K knee hinge joint

$$F_{my}d = F_w X_{cm} \tag{6.6}$$

$$F_{my} = 135N$$
$$F_{my} = F_m \cos(\theta)$$
$$F_m \cong 300N$$

Patella's role
It was said that the vertical component of the weight is constant during the movement. The vertical component of F_m instead, that is the force generated by quadriceps contraction, changes during the extension.

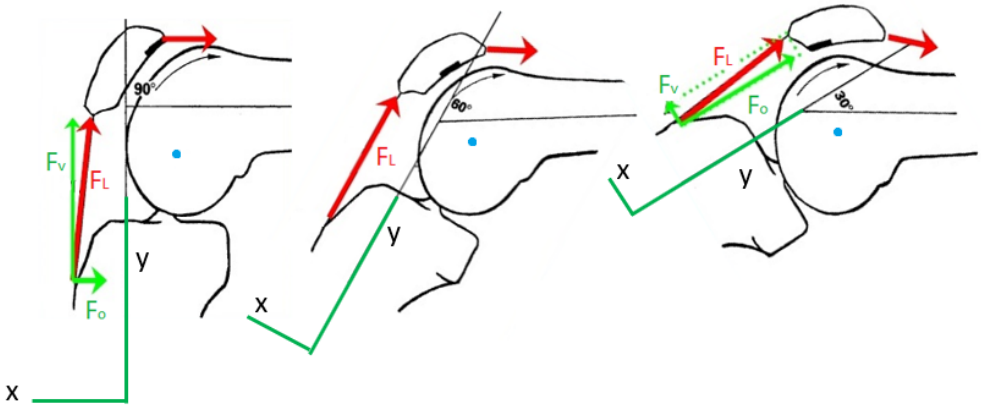

Figure 6.12: Patella effect on quadriceps force (orthobullet.com)

The picture 6.12 shows how the force is changing during extension of the knee. Patella allows to increase the distance between the virtual center of rotation and the pulling force provided by the quadriceps. It is useful to think about it with a relative reference, where the vertical axis is the anatomical axis of the tibia. Initially the vertical component of the force is much bigger than the horizontal but during the movement their magnitude changes significantly.
The little arm gained plays an important role, drastically reducing the force required to extend the leg.
The effectiveness of the patella cannot be negligible. Once the calibration was completed, it was necessary to add a new element to emulate the action of the floating bone for the sample used for the tests.

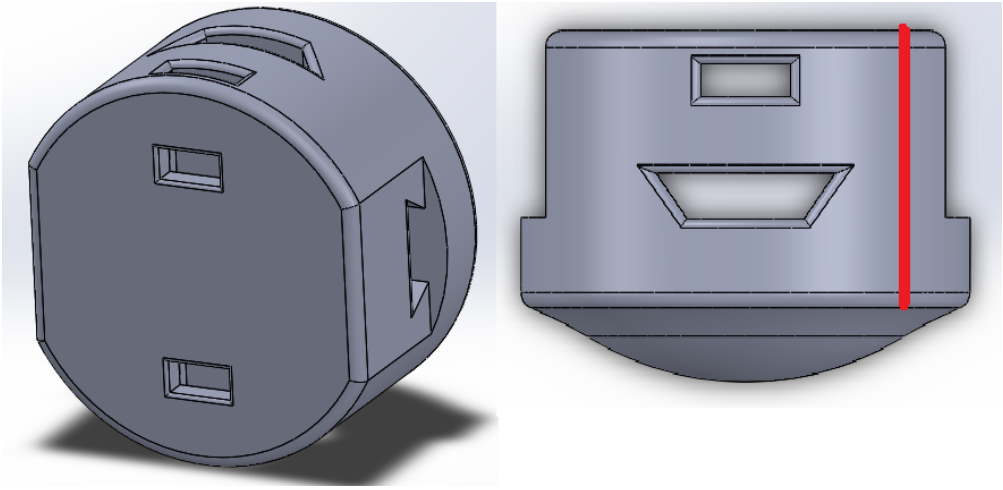

Figure 6.13: Patella element

That way it was possible to reproduce a structure functionally close to the natural kneecap. The most important parameter is the width of the element, identified by the red line, because it is the feature which increase the lever arm of the pulling force. It was settled as $10mm$ in order to perform a correct extension.
There are some through all pierces: they were made to insert a thread, fixed by friction, to reproduce the patellar tendon and the medial patello-femoral ligament. Finally, the rounded surface was designed to allow the patella slide on patellar surface (a region of the femur placed between the two condyles) during the movement, in order to better reproduce the physiologic kinematic of the joint.

6.2 Temperature analysis

The motor sees it's temperature increase while it is working, and it was necessary to monitor that value during the tests to avoid irrecoverable damages. The raise of temperature could be caused by different reasons like the internal friction and the Joule effect.

Maxon company provides manuals about their motor behaviour, where it's explained that most of the heat produced during the work is due the Joule effect. For further information about the friction negligible, check for Thermal Calculation in annex 2.

6.2.1 Motor parameters

The Joule effect is the event generated by a current flowing through a conductor.
Each body shows a certain endurance to be crossed by current, and this property is the electrical resistance. The more is this value, the more difficult will be for electrons to pass across that body.
When there's a flow, the resistance makes the voltage to fall, causing a Joule power losing that is

$$P \propto RI^2$$

where R is the electrical resistance of the wire and I is the current flowing on it.
The thermal behaviour of the motor can be related to a simple circuit to better evaluate the phenomena.

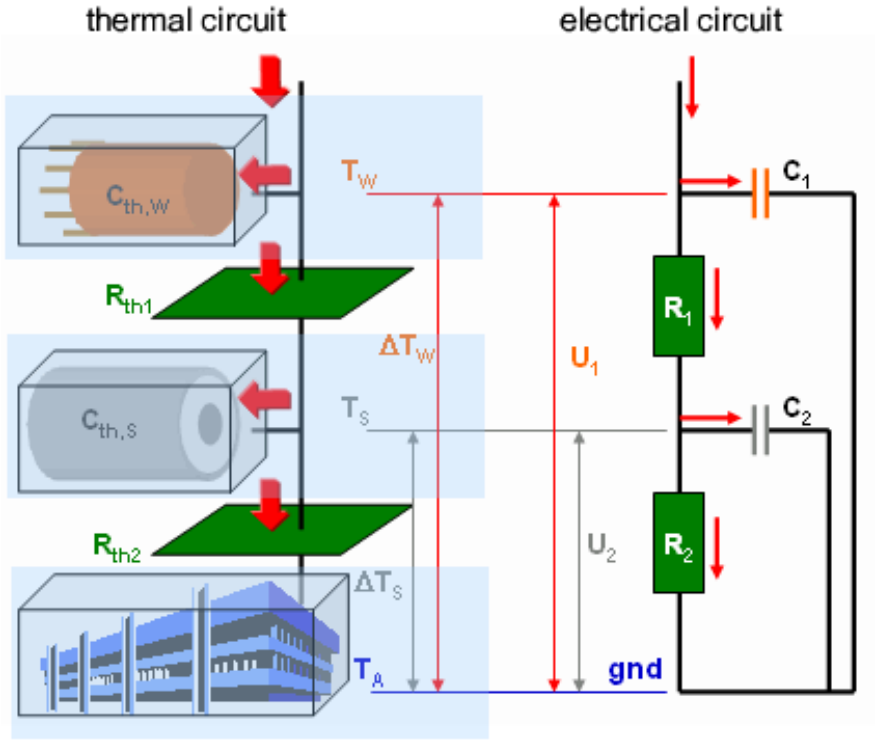

Figure 6.14: Analogy between thermal and electrical circuit

On the left, there is the thermal circuit of the motor, where:

1. The first block is the winding of the motor;
2. The second block is the stator of the motor;

3. The third block is the ambient.

The three of them are those that most characterizes the thermal behaviour of the motor. In fact, number one and number two are physical elements that get warmer during the work. The ambient instead continue to keep the same temperature independently from the other components. The heat produced by Joule effect starts to pass through the winding and the stator, reaching the external room that his colder. The two elements have different response to heating, cause of their different material and geometric properties.
That said, it was easy to reproduce this situation using an electrical circuit, where each element of the motor has both a resistance and a capacitor. The resistance depends on how much the body allows the flow to pass, while the capacity shows the tendency of the element to keep the thermal energy before dissipating it. The ambient is like a capacitor with infinite capacity, which means that for every heating phenomena its temperature will stay still, and it was considered as the electrical ground.

thermal	symbol	units	electrical	symbol	units
power losses			current source		
heat energy	Q	J	el. charge	Q	C
power	P_V	W = J/s	current	I	A = C/s
temperature diff.	ΔT	K	voltage diff.	U	V
ambient temp.	T_A	°C (K)	ground	gnd	V
therm. resistance	R_{th}	K/W	resistance	R	Ω
heat capacity	C_{th}	J/K	capacity	C	F

Figure 6.15: Analogy between thermal and electrical parameters

All the values were reported by the motor data sheet.

6.2.2 Main equations

It was necessary to find an equation to estimate the temperature inside the motor. Particular attention was paid for the winding, that owns a thermal time constant of $123s$ against $1060s$ of the stator, that means that the winding reaches a high temperature faster than the stator.
The flowing current generates a temperature increasing that could be associated to a step force, as described by the following laws provided by Maxon data sheets.

$$\Delta T = \frac{(R_{th1} + R_{th2})P}{1 - (\alpha_{cu}(R_{th1} + R_{th2})P)} \tag{6.7}$$

where

- ΔT_w is the difference between the temperature of the winding and the ambient;
- R_{th1} is the thermal resistance between housing and ambient, and it's $1.3\frac{K}{W}$;

- R_{th2} is the thermal resistance between winding and housing, and it's $1.85\frac{K}{W}$;
- α_{cu} is the temperature coefficient for the chopper, that is 0.0039 K^{-1};
- P is the Joule power dissipated, that is $R_i * I^2$

In order to give an idea of the thermal behaviour, if a current of $1A$ flows in the motor, ΔT_w is 1.15 $°C$, that means the temperature raises until about 26 $°C$ a regimen. For $10A$, the winding reaches 233 $°C$. Further information in testT.xls file in annex 3. Notice that temperature is expressed in $[K]$ but, being a difference between two temperatures, from now will be considered in $[°C]$.
It is necessary to discuss about the internal resistance of the power dissipated. In the data sheet of the motor it was defined as "internal resistance at $25°C$". Maxon motor discuss the internal resistance as a value strongly dependent on the actual temperature of the winding (annex 2). In fact, its resistance increases with the higher temperature reached by windings while the motor works.

$$R_i = R_{25}(1 + \alpha_{cu}(T - 25)) \tag{6.8}$$

The value of the resistance is the one at $25°C$ added for a certain value, that is related to the difference between the current temperature and $25°C$. If the temperature is higher than $25°C$, the resulting R_i will be bigger than R_{25} and vice versa.
A winding temperature of $75°C$ causes the winding resistance to increase by nearly 20%, and it's a not negligible effect.
The thermal behaviour of a system with both resistance and capacitor could be associated to a simple first order system. This is subjected to a step force defined by the Joule power. In particular it is the current supplied the only variable to be decided.

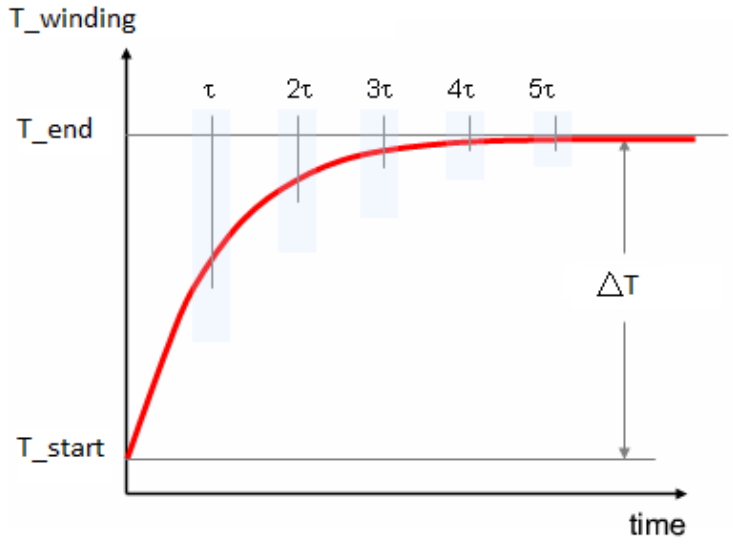

Figure 6.16: First order system response to a step force

The curve shows the behaviour of a first order system responding to a step input that is the temperature

$$T_{end} = T_{start}(1 - \exp^{\frac{-t}{\tau}}) \tag{6.9}$$

If the winding is at a certain temperature T_{start} and a temperature T_{end} is forcing it, the system tries to reach a new thermal equilibrium. This takes its time, depending on the $\tau_{winding}$ that is $123s$.
It is the same situation of an old thermometer filled with mercury: once it was put under the armpit, it takes about five minutes to reach the new thermal equilibrium, where the T_{start} was the ambient and T_{end} the body temperature to measure.
In this case, a τ_w of $123s$ means that, to reach about the 86% of the ΔT, it will take four minutes.
Notice that the motor was not supposed to work for such long periods in this tests, but the max temperature of the winding is reachable with relatively low currents. Thus, for high current supplied, a minute can be too much.

6.2.3 Calculation method

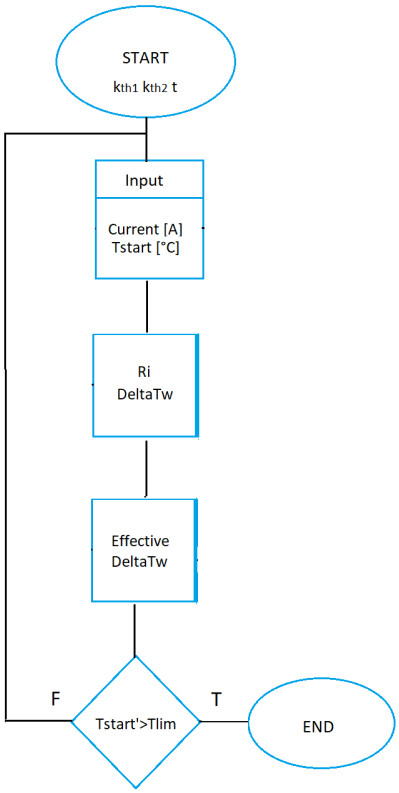

Figure 6.17: Flow chart for temperature evaluation

1. first, the script needed the thermal constants of the motor, that were detailed by data sheet. It was important to define a certain time interval, that is the time between two successive acquisition. That was because Arduino is able to collect data very fast, but for the test this was unnecessary. Once settled $2000ms$ as time interval, the software started the evaluation while working on the angular position.
   The temperature evaluation belonged to the security parameter check box of flow chart 5.1;

2. values of supply and actual temperature are acquired respectively from the analog data acquisition and the previous temperature reached. For the first cycle, T_{start} is the ambient;

3. the internal resistance is evaluated with 6.3, and then ΔT was calculated with equation 6.2.

4. the effective ΔT followed 6.4, where $t = 2000ms$ and $\tau = 123000ms$.

5. finally, the current temperature was calculated by adding the effective ΔT to the previous temperature, and it had to be compared to the limit temperature, settled as $110°C$ to be slightly below the critical temperature, to guarantee the safety of the motor.
   To double-check the script, it was used the excel calculation file called "testT.xls" in annex 2. Once the boundary conditions were specified, results showed after the current was settled demonstrated that the script worked correctly.

6.2.4 Equation issues

Before to perform any test, there were something to pay attention in the equation 6.2.

$$\Delta T = \frac{(R_{th1} + R_{th2})P}{1 - (\alpha_{cu}(R_{th1} + R_{th2})P)} \tag{6.7b}$$

As discussed, ΔT greatly increases by supplying bigger currents. During the calibration tests, a problem in that law appeared for current that were bigger than $14A$, that is about two times the nominal current of the very RE65.
It can be noticed that the denominator is basically composed by 1 minus a certain value. That value is

$$\alpha_{cu}(R_{th1} + R_{th2})P$$

$$\alpha_{cu}(R_{th1} + R_{th2})R_i I^2$$

the only parameter decided during the tests is the current I. For high values of current, it was easy to notice that the denominator became negative. That causes the inconsistency of the equation 6.2 for high supply, with a ΔT dropping to thousand degrees under the zero.

Thanks to the patella, it wasn't a problem for the project but it's necessary to mention that issue in order to avoid any problems for future improvements.
Furthermore, there was another issue shown by Maxon documentation.
As said, RE65 owned a nominal current of $I_n = 6.8A$.

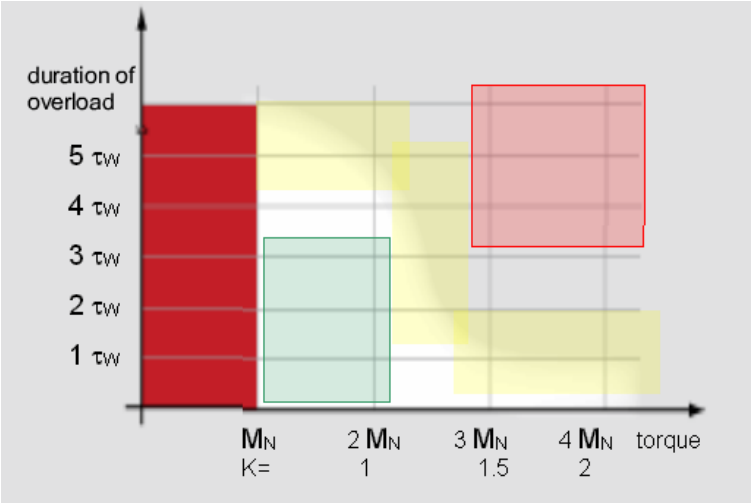

Figure 6.18: Motor overloading work

The figure 6.18, provided by Maxon company, show how one of their motor is supposed to work to avoid winding damages, depending on the current supplied.

- for no overload, that means a current (and a torque) inferior than the nominal, the motor can work for long period of time as identified by the brown region;
- once the supply increases, it's safe to work with shorter periods. The light blue region is safe, while the yellow one it's better to be avoided. For RE65 means that it's safe to work for $t < 3\tau = 369s$ using up to $2M_n = 2I_n = 13.6A$
- then, for higher current the motor work isn't safe, but again it's possible to use in yellow region, and strongly recommended to avoid the red one.

The matter in this documentation is that, as discussed in 6.2.2, for $10A$ the temperature reaches 233 $°C$ by working for $5\tau = 99.3\%$, and 222 $°C$ for $3\tau = 95\%$. The maximum temperature that can be reached without damaging the winding is actually 125 $°C$.
Further investigation brought to another check to perform, always from Maxon's Thermal Calculations. It was necessary to evaluate the overload factor K as

$$K = \frac{I}{I_n} * \sqrt{\frac{T_{max} - 25}{T_{max} - T_{start}} * \frac{R_{th1}}{R_{th1} + R_{th2}}} \tag{6.10}$$

For the usual values, and $T_{start} = 25°C$, it was obtained $K = 1.06$.
The period which the motor can work safely is

$$t_{on} = \tau_w * \ln\left(\frac{K^2}{K^2 - 1}\right) \tag{6.11}$$

Using coherent values, $t_{on} = 275s = 2.25\tau_w$.
This result is certainly more accurate than the general graph 6.17 but, for $I = 10A$ and $t = 2\tau_w$, the winding should actually reach 204 $°C$, widely bigger than the critical temperature of 125 $°C$.

It was necessary to contact an engineer from Maxon company to discuss these issues and, after a deep investigation, it was commonly agreed that the two laws aren't working with that kind of high currents. For this reason, the denominator shows incoherencies and the evaluation of the t_{on} isn't reliable.
It was developed a new formula that is less accurate but allowed to obtain trustable evaluation of the temperature even for high values of current.

$$T_{end} = R_i I^2 * R_{th2}; \tag{6.12}$$

The most important matter to pay attention with 6.12 is that, referring to picture 6.15 (first order response to a step external force), here it is evaluate the maximum temperature reached with a certain current and not the ΔT, as for the previous 6.7.
The ΔT was calculated as

$$\Delta T = T_{end} - T_{current} \tag{6.13}$$

Then, the Arduino script continue to follow the same logic chart described.

6.2.5 Internal resistance evaluation

In order to obtain the best accuracy possible, it was necessary to evaluate a parameter that was considerate as known until now.
The value of R_{th1} was, in fact, directly provided by the data sheet of the motor. R_{th1} is the thermal resistance housing-ambient, and it was equal to $1.3\frac{K}{W}$. However, this value strongly depends on the work conditions of the motor during the test, in particular on the motor support ability to dissipate heat, and on actual ambient temperature. It was necessary to make sure about the actual value of this parameter according to the working condition of the project.
The evaluation of this parameter was so organized:

1. set up the motor in its working condition and left for $5\tau_s$, that is the thermal constant for the stator, at ambient temperature to make sure about its initial condition;

2. power it at arbitrary current, the closest to its application. It was constantly supplied $1.9A$.

3. wait until the housing reaches the thermal equilibrium. That was obtained after waiting $5\tau_s$, that is the thermal constant of the stator.

4. after 90 minutes, measure the housing temperature. It was used an infra-red gun detector;

5. calculate the actual resistance as

$$R_{th1} = \Delta T_s * \frac{1 - \alpha_{cu} R_{th2} R_a I^2}{R_a I^2 (1 + \alpha_{cu} \Delta T_s)} \tag{6.13}$$

   where ΔT_s is the difference between the ambient and the housing temperature and R_a is the internal resistance at $25°C$, that is 0.365Ω.

It was obtained a value of $2.1\frac{K}{W}$, that means the actual thermal resistance is the 160% of the theoretical one. Higher internal resistance meant higher temperature reached for the same amount of time and supply.

6.2.6 Support optimization

To obtain lower values of R_{th1}, it was designed a new support for the motor.

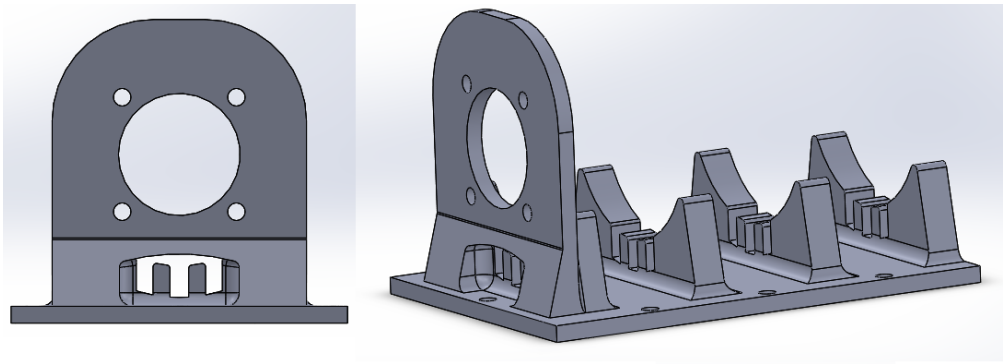

Figure 6.19: Final support for the motor

The previous structure was covering too much the motor, reducing the surface in contact with the ambient. The new version was sketched to let also the lower part of the case to be free from any covering, in order to have higher dissipation of the heat.
A new evaluation of R_{th1} was performed, obtaining a value of $1.5\frac{W}{K}$, that was lower than the previous one and close to the theoretical value reported in the data sheet.

It wasn't possible to obtain better values because the support was made by PLA, that has a thermal conductivity two order of magnitude lower than a classic steel support recommended for this purpose.

7 Velocity problems

7.1 Low velocity rotations

The wanted movement had to be performed slowly to avoid both visco-elasticity and inertia effects.
Unfortunately, Maxon RE65 wasn't able to perform low velocity rotation. The speed estimated to perform the pattern in about $30s$ was $5rpm$, and motor couldn't reach speeds below $15rpm$. Furthermore, the motor couldn't apply the wanted current at such low velocity, and that was well understood both in dead weight calibration and in leg extension tests. In fact, even in the current provided was higher, the effective supply was widely inferior.

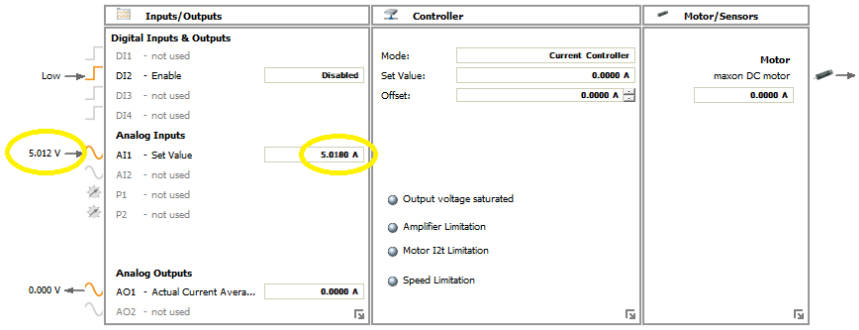

Figure 7.1: Control monitor (Escon Studio)

In picture 7.1 can be noticed how the servo is receiving an input signal of about $5V$ and it's supposed to provide $5A$ to the motor rotation, according to the Startup Wizard (described in chapter 4).

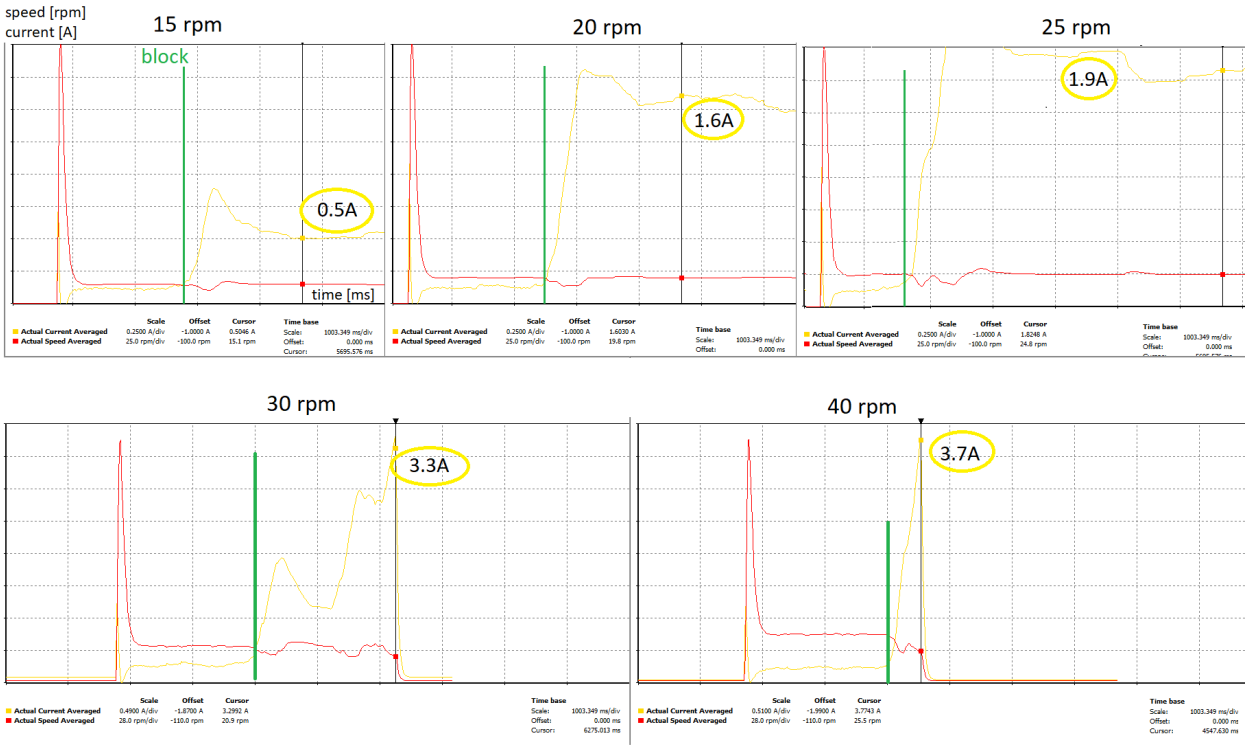

Figure 7.2: Comparison between five different acquisition

The five tests were performed in the same boundary conditions (same supplier, temperature and driver set up). The speed rotation is the only parameter that was changed, and it goes from $15rpm$ to $40rpm$.
The motor was kept free to rotate without any resistance till a certain moment, identified by the green vertical line, where it was forced to stop its movement. It can be noticed how the maximum current provided to the motor raise while the speed rotation is increased. However, even at $40rpm$, the maximum current (that means the maximum force applied by the muscle) is close to $4A$ but still far from the supposed $5A$.
Furthermore, the speed rotation should be about $5rpm$, a value that is not even achievable by the motor paired with its servo driver.

Another issue concerns about the initial burst in velocity that is also noticeable from the previous picture. It was thought that it can be due to the range of speed which the motor is supposed to act in between.

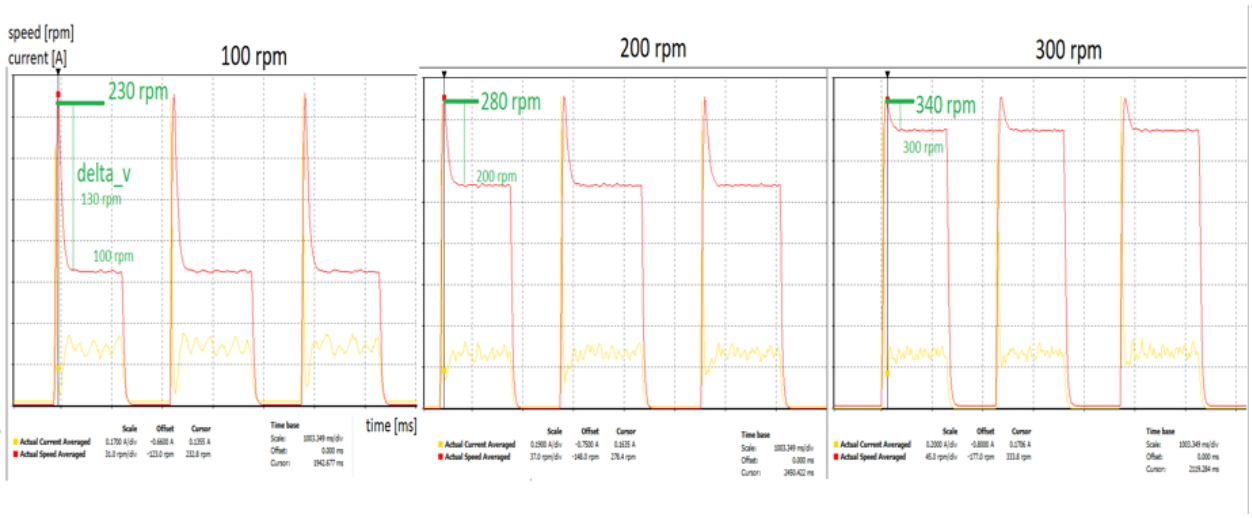

Figure 7.3: Speed burst evaluation

By testing the device, it was clear how the difference among the wanted value and the initial peak gets lower by increasing significantly the speed rotation. The motor is able to work up to $3500rpm$, and it would be interesting test the burst at $500 - 1000rpm$ but the supplier provided was not able to reach the required power.
Anyway, it was demonstrated the benefits achievable by using a speed reducer device. This way it is possible to work with higher velocity, obtaining a system able to deal with low rpm while supplying high currents, and without any initial burst (notice that also the speed difference is going to be divided by the device reduction rate, making the phenomenon basically drop to zero).

7.2 Solution: speed reducer

7.2.1 Comparisons

In order to achieve low speed rotation, it was thought to use a reduction mechanism. There were three main solutions:

1. cog set: using the same principle of the bicycle's transmission, it is possible to reduce the speed of the extension. This solution is easy to assemble and disassemble, can be directly bought at low price and allow even to modify the transmission rate. Thanks to the chain, there isn't any sliding during the spin. Unfortunately, the cog set is quite bulky and could be harmful if touched during the work.

2. gears: speed can be decreased using a system of gears. A gear substitutes the shaft's cap, and another in contact gear provides rotation to a new vertical shaft. It can be seen as a classical crossed configuration gear. The system is safe but it's more complicated to design, and most important it's not very general.

3. friction drive: the idea to use a pulley is because of its simplified design and manufacturing, using a chain to reduce the shift during the rotation. It allows to change a single wheel to adjust the reduction ratio, it's safe and not expansive.

Figure 7.4: Example of cog-set, crossed gears and pulley-belt (Wikipedia)

7.2.2 Best solution choice

At the end, it was a chosen to use a pulley system but, after some researches, it was discovered that Maxon provides motor gearheads at contained prices. The gearhead uses basically the same principle of a pulley but optimized to reach very high ratios.

Figure 7.5: Maxon gearhead

This solution sure is safe, not bulky, easy to attach and allows to obtain the wanted reduction at reasonable prices. In order to purchase a suitable element, the following calculations were made using real measures and granting a certain interval of security.

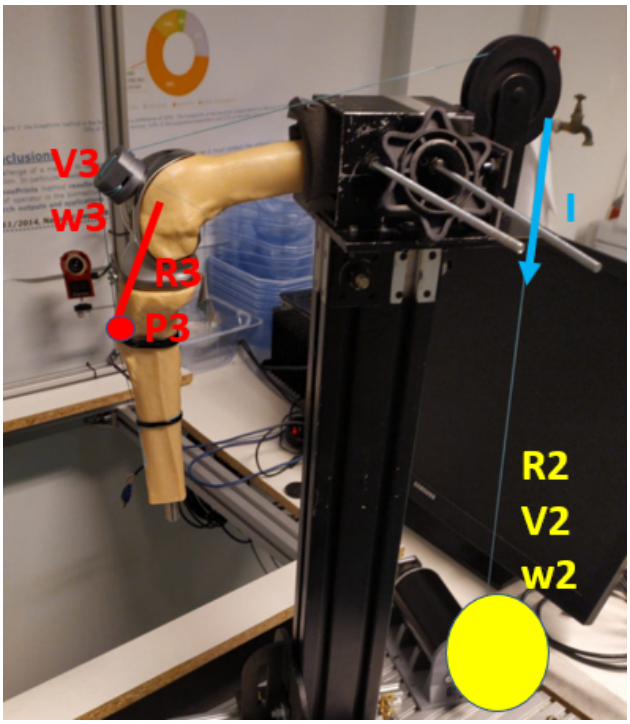

Figure 7.6: Test bench references

Where

- P3: insertion point of the patellar tendon on tibia tubercle;
- R3: radius of the pattern made by the point =50mm. The lower it is, the lower will be V3 (linear velocity of P3), the higher transmission ratio I need;
- w3: to perform $\frac{1}{4}$ of the total circumference in about $30s$, the speed would be $0.5rpm$;

$$V3 = w3 * R3 = 25mm/min \tag{7.1}$$

- R2: radius of the cap put on the output shaft of the hypothetic mechanical reductor, =5mm;

$$V2 = V3 \tag{7.2}$$

$$w2 = V2/R2 = 5rpm \tag{7.3}$$

- I: current used to perform the test $0.7A$

The angular velocity of the motor shaft was thought as $200rpm$ at least. That way, the reduction ratio was

$$RR = w_{motor}/w2 = 300rpm/5rpm = 60 \tag{7.4}$$

Using $0.7A$ with a torque constant of $123\frac{mN*m}{A}$ means a torque of $90mN * m$.
In order to be safe in a good range of different boundary conditions, $300mN * m$ as max torque is sufficient. In that way it is possible to reach about $2.4A$ and perform the movement even using a leg with doubled weight.

7.3 Gearhead test

In order to demonstrate the effectiveness of adding a speed reducer, it was arranged a pulley system between the motor and the frame pulley.

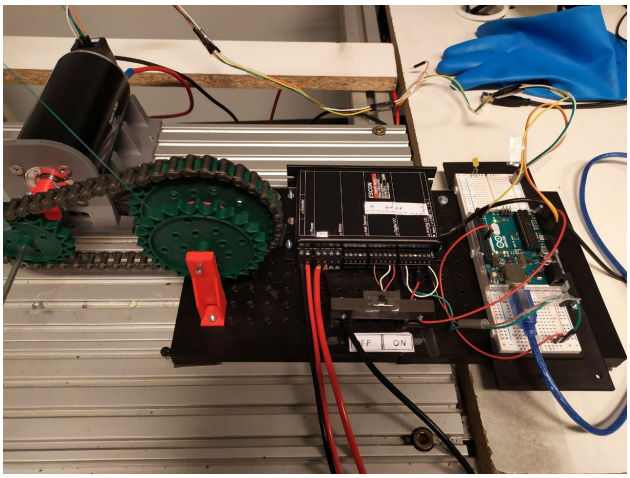

Figure 7.7: Two-pulley speed reducer system

The simple structure provided a gear ratio equal to two, which means a reduction of the speed from $25rpm$ to about $13rpm$. The test was performed and the achieved extension resulted slower.However, a ratio equal to 2 wasn't enough to obtain very low speed and sizable burst reduction, but proof that a gearhead should be purchased in order to get a slower ride and the benefits explained in chapter 7.1.

8 Motion Capture

Motor data acquired let to obtain motion parameters such as position, angular velocity and quadriceps force. The estimated angular position of the tibia doesn't enable to evaluate detailed information about joint relative mobilization.
To follow the pattern of precise point of the joint, like the patella contact point or the shift between the two bones during the roll-back, it was necessary to trust on a new device.

Motion capture allow to follow also the other movements come into play during knee extension by marking them and following their pattern in a 3D space.

8.1 Acquisition system

Motion capture is a technology that allow to estimate the motion of bodies by filming the shift of single main points. This method is widely used in fields like entertainment, military and bio-medics.

Figure 8.1: Optitrack camera, markers and software

That kind of systems are mainly composed by three elements:

1. a marker set, that is composed by a certain number of spheres fixed on the body. More markers mean a more reliable movement reconstruction, but also more preparation and post-processing. For this study, passive markers were used.

2. infra-red cameras allow to acquire markers position during the movement. Each camera is able to acquire only 2D informations, so it was necessary to use multiple camera to obtain a 3D reconstruction.

3. the software, generally provided by the very company owner of the two previous elements. It allows to estimate the position of each marker in a 3D space by processing 2D data from each camera. It also enables to visualize each camera acquisitions, to label differently groups of markers and evaluate cinematic features.

8.2 Optitrack

Optitrack is a company that provides high quality motion capture toolsets, easy to set up and to use. A system, equipped with ten cameras, was already available and ready to be used. The company provides also a dedicated software to process data and perform post processing.

8.2.1 Marker position

In order to identify a rigid body by describing an orthogonal triad, three markers must be attached to the body segment and follow its movement during all the test without relative motions.

Figure 8.2: Marker base for rigid body

The company provided a component to be fixed on the segment and where the three markers could be placed. Once this element has been positioned, the cameras were able to discriminate a single rigid body.
It was useful to have two rigid bodies at least, one fixed and the other free to move, to obtain a relative motion between the two of them. To test the system, it was decided to describe the movement of three rigid bodies: the tibia, the patella and the femur. Thus, three marker sets were placed on the sample.

8.2.2 Motive

The software provided by Optitrack is named "Motive". The ten cameras recognize spatial point according to their reflectance.

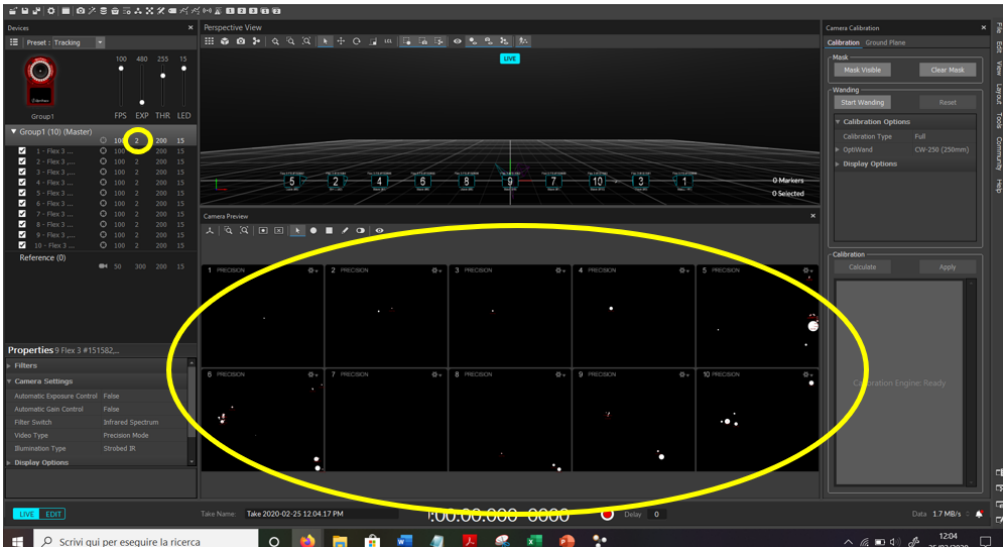

Figure 8.3: 2D camera view

The ten windows highlighted show what are the cameras detecting as points of interest. It depends of the light reflection of the body, and can be tuned with the EXP (exposition) value in order to let the system recognize only the real markers.
However, it was necessary to mask some detected points because generated by sources with optical properties that are close to the markers.

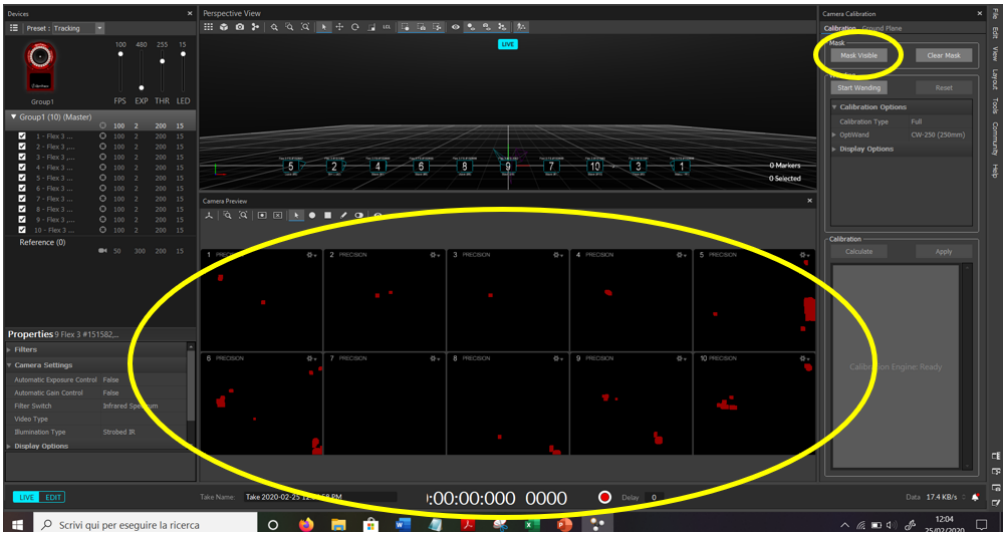

Figure 8.4: Masking the false positive detection

The command button "Mask visible" allowed to hide the unwanted points that were detected as marker by the motion capture system. This way, all false positive were deleted and the calibration phase could start.

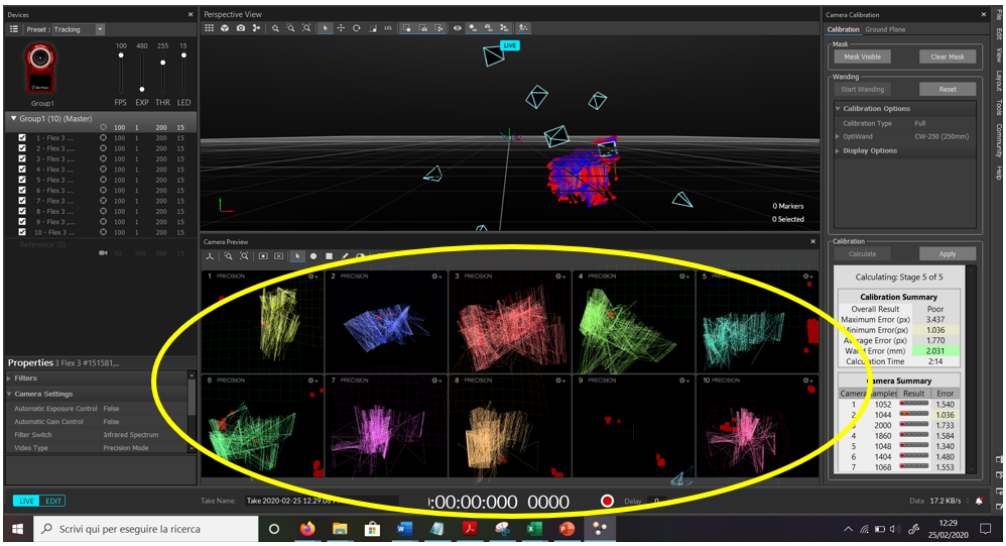

Figure 8.5: Calibration phase

The software needs information about the camera orientation, which is provided during the calibration phase. Thanks to a calibration wand, that is a support device with known standard dimension, Motive could evaluate the position and the orientation of all the ten devices.
Once the software has re-built the camera disposition, the configuration of the system appears in the upper box. It can be noticed the orientation of the numbered cameras, and the detected markers as orange points.

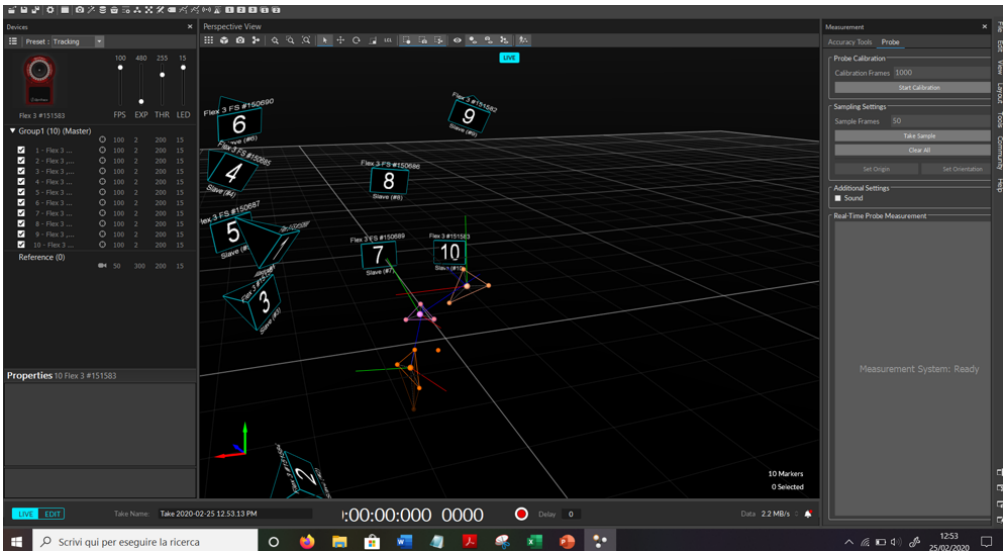

Figure 8.6: Rigid body definition

When the three markers positioned on the same body segment are acquired, it's necessary to define them as part of the same rigid body. This way the software recognizes the body segment and evaluate marker position related to the global system of reference. Now, the software can calculate relative motion and provide detailed reports of body displacement.

Another interesting feature of the system is the possibility to add a virtual marker on the rigid body. Thanks to a special wand with four marker placed in known position and a tip, the software can add a virtual point in correspondence of the wanted position after a short estimation of wand's tip position. This way it's possible to relate more than three point to a single rigid body, obtaining a better visualization of the movement. This feature was exploited for the tibia, making the segment more like the natural bone.

9 Results and discussion

The first test performed was the constant speed leg extension imposed equal to $25rpm$. The current provided for the task was acquired by Escon studio.

Figure 9.1: Constant speed extension, five repetitions

The task was repeated five times to reduce variable error. It can be noticed the red line, which is the actual speed averaged in a time interval of $117.5ms$, is constant for all the during of the task, with the initial burst discussed in chapter 7. The yellow line shows instead the current, averaged for the same time step.

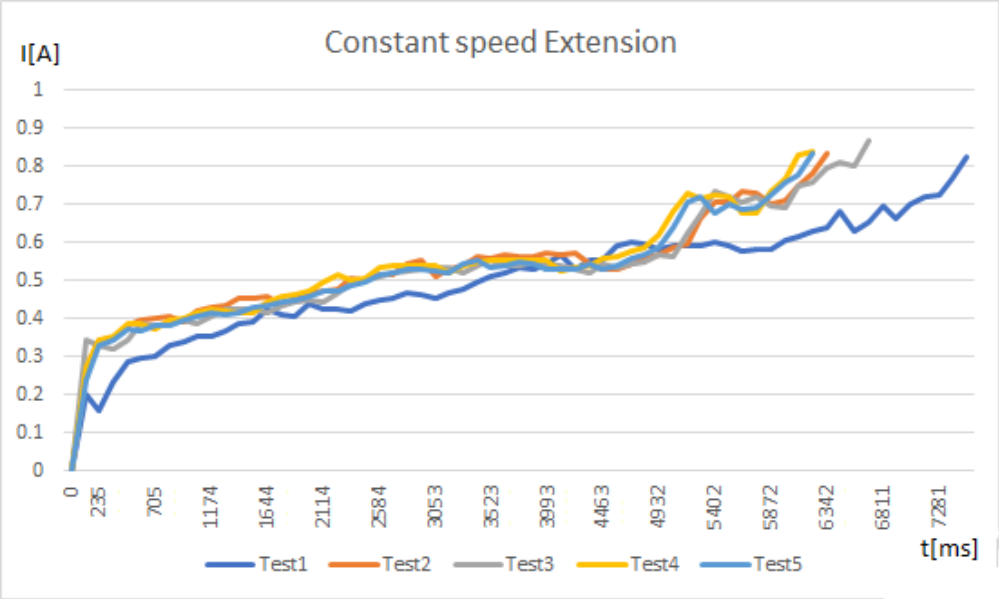

Figure 9.2: Constant speed extension, current acquired

The picture shows the trend of the current supplied for the task: after a first step required to start the movement, the force necessary to perform the extension increases until the very end of the ride. This is coherent with the theory, where the muscle activity increases while the angular position decreases (as described in chapter 6.1.4). Except for test1, data are

consistent for all the duration, with an average of $0.84A$ and a standard deviation of 0.017 for the moment of maximum extension.
The fluctuation of the pattern is due the high velocity imposed for the test, that was settled to guarantee an appropriate supply. Low speed rotation should be able to remove the inertia contribute. Test number 1 is considerable an outlier: it's notable how the current fell significantly during the very beginning of the test, around $235ms$. Thus, considering that it was the first test of the row, allows to consider test1 statistically negligible.
The system is able to acquire consistent data about the quadriceps activation during constant speed leg extension.

The second task was to apply different forces sequentially and observe the behaviour of the leg. In particular, nine tests were performed in order to reduce data variability and provide consistent results.

Figure 9.3: First cluster, four tests

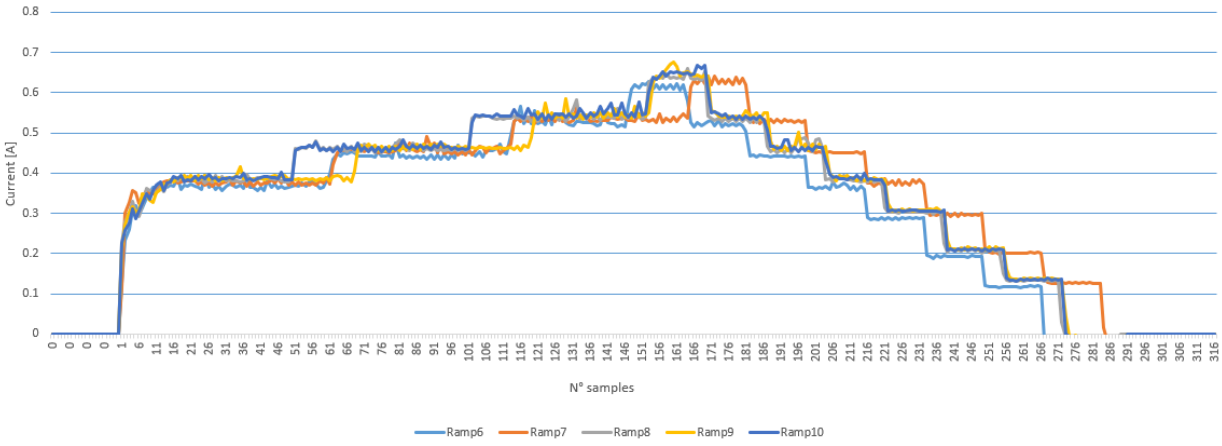

Figure 9.4: Second cluster, five tests

It can be seen how different tests returned the same pattern of activation. The wanted function is achieved by increasing the supply each time the rotation stops, until the total extension is reached.

The only difference between the tests was a time shift, but it isn't a real matter since current and position are reliable. In fact, the pattern between plateaus has not quantitative impact on acquisition, and the shift can be widely reduced by imposing a time step of few ms instead of $2000ms$.

Data plot allowed a good visualization of the performance by showing the force behaviour during the tests, but it was needed a statistic study to investigate their coherence.

	Plateau A	PlB	PlC	PlD		Pl2	Pl3	Pl4	Pl5	Pl6	Pl7	Pl8
average												
Test1	0.388107	0.464739	0.544573	0.651914		0.540912	0.462806	0.383971	0.310271	0.213835	0.138747	-0.00518
Test3	0.387089	0.468871	0.547579	0.637665		0.538388	0.469906	0.386365	0.30775	0.211031	0.137131	-0.00647
Test4	0.376497	0.458394	0.536238	0.6387		0.545135	0.453112	0.376076	0.300018	0.202624	0.127959	-0.01733
Test5	0.382347	0.465808	0.542891	0.642918		0.546141	0.461594	0.385081	0.307831	0.208841	0.134418	-0.01268
Test6	0.368106	0.446516	0.529779	0.616344		0.52205	0.442171	0.3655	0.287582	0.192876	0.117688	-0.02808
Test7	0.374675	0.458606	0.5346	0.629294		0.529912	0.451912	0.376094	0.297218	0.202135	0.126625	-0.01905
Test8	0.384463	0.461502	0.5398	0.639431		0.533624	0.466959	0.382624	0.302794	0.208069	0.132825	-0.01233
Test9	0.388027	0.464216	0.546044	0.649688		0.544412	0.466941	0.387665	0.308369	0.2125	0.137181	-0.00736
Test10	0.387248	0.463076	0.546856	0.649763		0.540638	0.46465	0.386835	0.306612	0.210071	0.135356	-0.01168
stdev	0.007159	0.006475	0.006228	0.011288		0.008006	0.009066	0.007278	0.00725	0.006608	0.006769	0.007241

Figure 9.5: Averaged data and standard deviation

According to the previous graphs, data from each plateau were averaged in order to get a value to be analyzed. It was interesting to compare averages from the same step for all the tests: it was chosen to calculate the standard deviation for each plateau, obtaining the highlighted values. These values are close to zero, in particular they are always below 1%, demonstrating high reliability of measurements.
It's important to mention that the standard deviation proved coherence for all the steps, both in the increasing phase and during the passive return. That values are associable to the force applied by the quadriceps muscles to accompany the knee flexion.
These data are interesting to argue because the forces used to extend the leg are higher than the ones required to escort the return to the initial position, how should it be due to the weight action while the leg has reached the mechanical equilibrium.
The current pattern, that is the quadriceps force after applying equations 4.1 and 4.2, can be filtered to obtain a fine pattern activation of leg extensors.

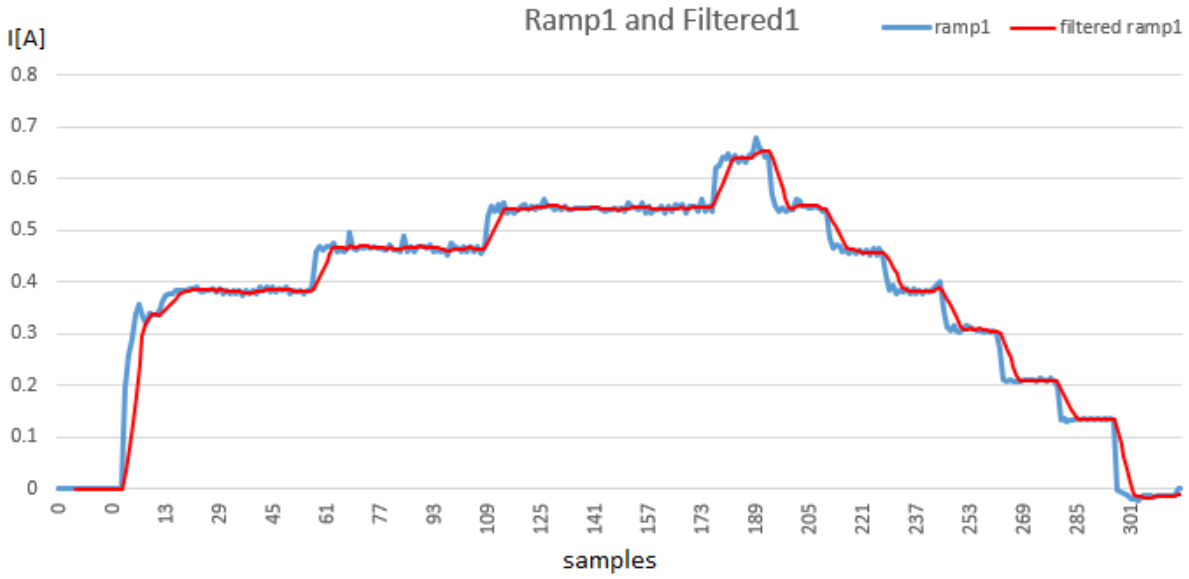

Figure 9.6: Smoother current pattern of ramp1, obtained by low-pass filter (moving average)

The pulse counter allowed to follow the pattern of the body segment, constantly monitored by the feedback system.
Once it is known the starting point, which was about 100° for the pulse number 0, the position is obtained by using

$$D_p = 360/P_r = 0.72dpp \tag{9.1}$$

where D_p is the degrees-per-pulse and P_r is the number of pulse acquired for each revolution, that is 500 given by encoder data sheet. Notice that the D_p is of course related to the motor shaft.
The pattern of the tibial insertion point was considered as circular, with a radius of $R = 70mm$. The ratio between the radius of the ride and the shaft cap of the motor is

$$ratio = R/r = 0.0714 \tag{9.2}$$

Thus, the degree-per-pulse related to the tibia position is

$$D'_p = ratio * D_p = 0.051dpp \tag{9.3}$$

Once a change of direction is detected by the encoder, number of pulse are subtracted instead, and the position returns to 100 degrees.

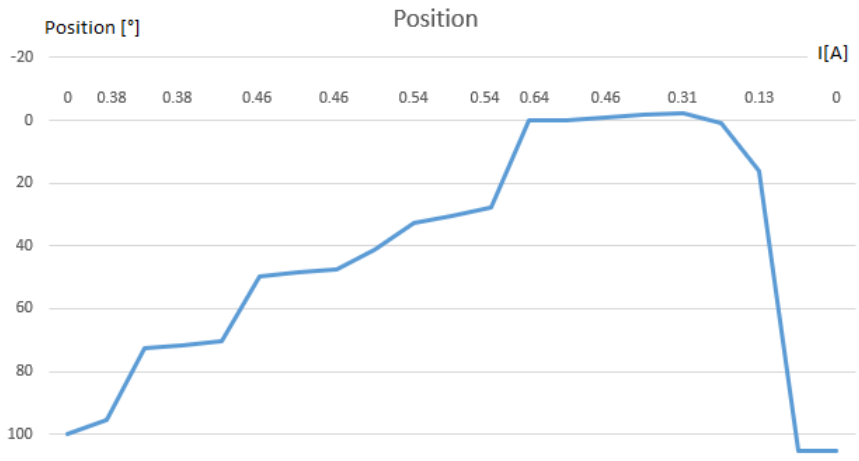

Figure 9.7: Angular position during leg extension and return

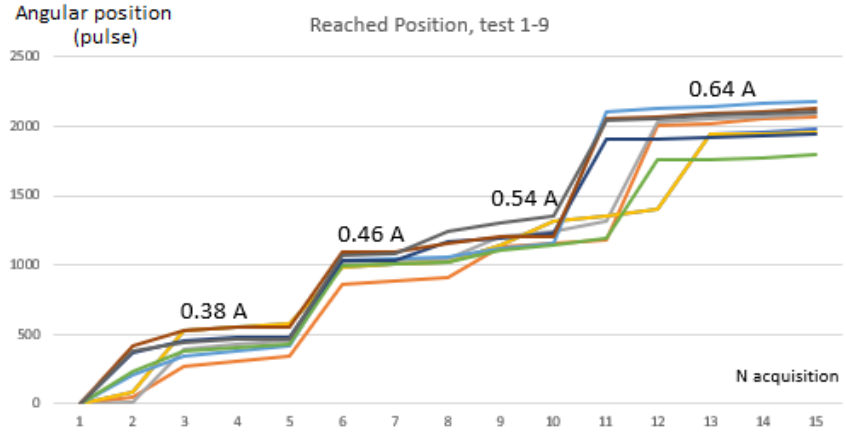

Figure 9.8: Pulse counted during extension phases

Is it possible to obtain better analysis by reducing the time step but it'd mean to multiply the size of data. It's advisable to switch between $500ms$ to $2000ms$ according to the main topic that is going to be investigated. However, the angle detection strongly depends on the speed problem discussed in chapter 7 and on the light weight of the subject used for the tests, both of which makes inertia alter the pattern of the leg. Due to these issues, the acquired data demonstrated how necessary is to purchase of the gearhead in order to reduce the speed burst, obtaining a finer evaluation of reached position. Figure 9.8 shows how variable the pattern is, with a normalized standard deviation of 16% in worst case, that means an error of about 12° on the estimated angular position.

Motion capture

The task was acquired by the Optitrack system.

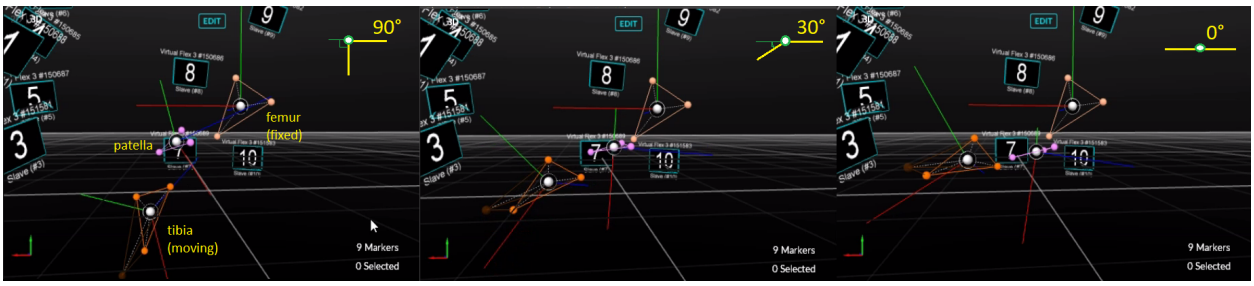

Figure 9.9: Leg extension reconstructed by Motive

The picture shows the position of the leg in three different instants. The lower rigid body, which identifies the tibia, go from the initial position to its maximum extension following the natural pattern lead by surfaces interaction. The patella is a floating bone and is sliding between the two condyles while getting closer to the fixed third rigid body, that is the femur. With an accuracy of $2 - 3mm$, the acquisition was considered good enough to be used on synergistically with the workbench to obtain detailed position data but, in order to perform deeper investigation, a finer calibration should be performed to reduce the accuracy to less than $1mm$. More information about video taped in annex 5.

10 Conclusion and Future development

The final system is perfectly able to keep the specimen steady and achieve the wanted motion, recording coherent data with a good sensitivity and reliability.

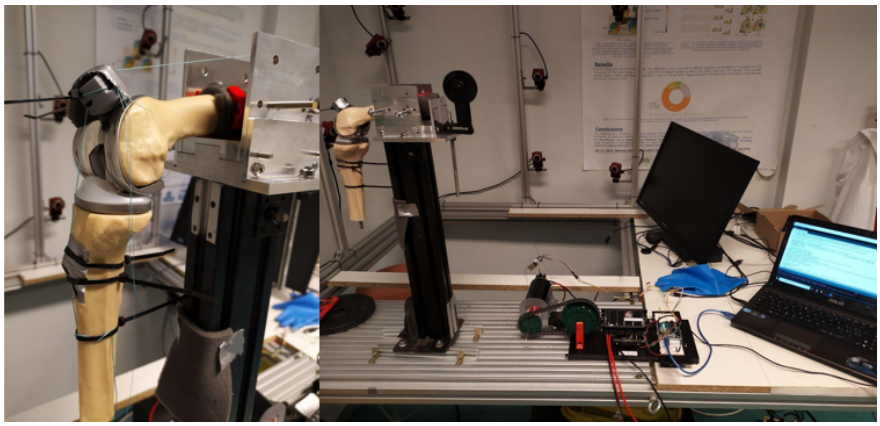

Definitive workbench setup

The system allows to perform in vitro studies about the open chain kinematic of knee extension, with a good emulation and estimation of quadriceps action and forces, accomplishing the main requirement. Thanks to motion capture cameras, all forces can be

also related to a position in a 3D space, obtaining a good visualization of leg movement during the task.
It's important to highlight if and how the initial requirements have been fulfilled at the end of the project.

TOPIC	TASK	DETAILS AND MOTIVATIONS
Frame	Modular Design	Both idea and CAD were made
	Assembling	The pieces are currently on manufactory phase. They will be ready to be assembled as soon as possible.
Extension	Mechanism	The motor is ready to perform the leg extension. Gearhead is required
	Control	The system is able to adapt to different samples
	Safety	The mechanism is completely safe for both itself and the operator
Data	Calibration	Magnitudes and measurements were properly calibrated
	Validation	Acquisition tests demonstrate good reliability
	Motion Capture	Segment record and visualization was performed

Recap of the accomplished tasks

Frame

- the designed frame allows an easy positioning and a steady bearing of the specimen thanks to the rotating bases and the modularity of the upper part;
- the two missing bases are required to ultimate the structure. However, the upper part was manufactured and its work was tested.

Extension

- the motor well emulates the presence of the quadriceps muscles, applying coherent forces along the anatomical axis and providing an accurate estimation of physiological activities. The indicated motor gearhead will be purchased to reduce speed issues, as proved in chapter 7;
- the feedback control of the motor allows to perform the same test independently from the boundary condition of the specimen. It's possible to achieve the wanted tasks, acquire data and investigate behaviours that are coherent to the specimen investigated;
- all tasks can be performed in complete safety thanks to the feedback-controlled system, avoiding any risks for both the prosthesis and the motor. The mechanism is safe for the user, that is the most important matter that must be always guaranteed.

Data collect

- motor torque and current readings were double-checked to ensure acquisition reliability;

- data acquired showed good repeatability on each test, and values are coherent with theoretical expectation and literature informations;
- a 3D model of the extension was achieved and can provide more accurate information about joint behaviour.

Future development
There are some implementations that can be done to increase the usefulness of the system. First of all, it would be interesting to improve the motor controlling by new patterns of motion. For example, a newsworthy implementation would be to provide Arduino an Excel file containing experimental data like electrogoniometer or EMG acquisitions. This way, it'd be possible to emulate muscle behaviour and perform an inverse analysis by replicating the same pattern. Note that each time the task is performed, it will be reasonably the same, allowing to analyse the same movement in different situation such as different specimen or prosthesis. Once the software update is ready, it'll be possible to reproduce common task like doing squats or climbing stairs, and so on.

Another idea is to add a second motor to also evaluate the action of the hamstrings during all the cited task.
That way, it'd be feasible to emulate also active flexion and taking into account the antagonist contribute while analysing kinematic parameters like pressures on joint behaviours.

The system can be enhanced by other real time evaluation and visualization. An example could be to plot wanted data directly on the screen instead of using the Arduino virtual monitor. Furthermore, it would be interesting to coordinate motion capture reconstruction and kinematic data to relate micro-movement of the joint to specific load condition and obtain a more detailed investigation of the open chain knee extension.

It'd be interesting to investigate displacement of specific point of interest taking advantage of virtual markers to obtain more detailed data, which could be used to perform FEM analysis. That way a more complete investigation could follow the in vitro tests. It'd be

possible to add more sensors to obtain additional data. For instance, a piezoelectric sensor as the Tekscan could be placed between condyles and menisci to evaluate contact area and local pressure. Another idea can be to apply an electrogoniometer to directly read the end of the ride and link this information with the Arduino sketch.

Last optimization could be on the clamping system, blocking the distal region of the specimen's femur by an additional small component, hinged on the fixed clamp, which covers the anterior region when a dedicated screw is turned during the set-up phase.

References

[1] Lynn S. Lippert. Knee, clinical kinesiology and anatomy. *F.A. Davis Company.*

[2] M.D. Kenneth A. Krackow and Davis S. Anatomy and kinematics of the normal knee. *Hungerford, M.D.*

[3] Innocenti B. Orthopaedic biomechanics. *Knee Biomechanics Lesson*, 2019.

[4] PhD corresponding author1 Prashant Komdeur, 1 Fabian E. Pollo and MD1 Robert W. Jackson. Dynamic knee motion in anterior cruciate impairment: a report and case study. *Baylor University medical center*, 2002.

[5] Richard T. Keller and Andrew A. Amis. Anatomy and biomechanics of the natural knee and after tkr. *Book: The Unhappy Total Knee Replacement*, 2015.

[6] 2 Matheus Braga Jacques Gonçalves 2 Leonardo Lanziotti Costa 3 Lincoln Paiva Costa 3 Rodrigo Rosa Lessa 3 Lúcio Honório de Carvalho Júnior, 1 Luiz Fernando Machado Soares and * Marcelo Lobo Pereira3. Femoral roll back in total knee arthroplasty: Comparison between prostheses that preserve and sacrifice the posterior cruciate ligament. *Revista brasileira de ortopedia*, 2015.

[7] Soudry M Mestriner LA Insall JN, Binazzi R. Total knee arthroplasty. clinical orthopaedics and related research. *Clinical Orthopaedics and Related Research*, 1985.

[8] Type of total knee implants, bonesmart.

[9] Geert Pagenstert Victor Valderrabano Andrej M. Nowakowski, Patrick Vavken. Design, shape and materials of total knee replacement. *Book: The Unhappy Total Knee Replacement*, 2015.

[10] Innocenti B. Medical device, orthopaedic biomechanics. 2014.

[11] Okazaki k. Kawahara S., Matsuda S. Asymmetric femoral component design is preferable for the patellofemoral contact configuration in total knee arthroplasty.

[12] John C. Richmond John P. Goldblatt. Anatomy and biomechamics of the knee. *Elsevier Inc.*, 2003.

[13] Stan L. Lindstedt. Skeletal muscle tissue in movement and health: positives and negatives. *Journal of Experimental Biology*, 2016.

[14] How a dc motor works from https://community.nxp.com/docs/doc-1067.

[15] How a stepper motor works https://cdn-learn.adafruit.com/downloads/pdf/all-about-stepper-motors.pdf.

[16] How to control an encoder https://howtomechatronics.com/tutorials/arduino/rotary-encoder-works-use-arduino/.

[17] What is arduino https://www.mauroalfieri.it/informatica/programmare-con-arduino-le-basi.html.

[18] How to control a motor with arduino https://www.allaboutcircuits.com/projects/control-a-motor-with-an-arduino/.

[19] Simone Bersini, Valerio Sansone, and Carlo Frigo. A dynamic multibody model of the physiological knee to predict internal loads during movement in gravitational field. *Computer methods in biomechanics and biomedical engineering*, 19:1–9, 06 2015.

[20] Anthropometric table, https://people.unica.it/brunoleban/files/2012/04/fmb-esame2013-01-16-tabelle-antropometriche.pdf.